University of Nairobi

School of Engineering

CHARACTERIZATION OF MICROSTRUCTURE AND MECHANICAL PROPERTIES IN THE HAZ OF EN24 STEEL AFTER POST WELD HEAT TREATMENT

BY

KELLY MUTONGA

F56/74556/2014

BSc HONS. (U.o.N)

A thesis submitted in partial fulfillment of the requirements for the degree of Master of Science in Mechanical Engineering, in the Department Mechanical and Manufacturing Engineering of the University of Nairobi

2018

DECLARATION

Except where otherwise stated, this thesis contains my own work. This work has not been submitted in whole or in part at this university or any other institution of higher learning for examination or other purposes.

Mr. Kelly Mutonga…….Date…….

This thesis has been submitted for examination with our knowledge and approval as university supervisors.

Prof. J.K. Musuva ……..……...Date…….

University of Nairobi

Dr. T.O. Mbuya……..……Date……

University of Nairobi

Prof. F.P.L. Kavishe ……...Date……...……

University of Namibia

DEDICATION

This work is dedicated to my wife Loice Nashipae and children: Mutheu, Sision, Muuo and Mosyani.

ACKNOWLEDGEMENTS

First and foremost, I would like to express my profound gratitude to Prof. J.K. Musuva for his unrelenting support, guidance and patience throughout the course of this project. I am sincerely grateful to Prof. F.P.L. Kavishe for his guidance and valuable insights. I am also immensely grateful to Dr. T.O. Mbuya for his guidance and fruitful discussions.

I am thankful to the University of Nairobi for sponsorship and to African Material Science and Engineering Network (AMSEN-A Carnegie-RISE Network), through Prof. G.O. Rading, for providing partial financial support. Thanks are due to the entire AMSEN fraternity for their friendship. I am greatly indebted to Dr. Mbuya and Mr. Pius Koech for availing some reference materials to me.

I acknowledge the technical support of the following persons:-

- Mr. Agik for his assistance in welding and heat treatment
- Mr. Njue and Mr. Waribu for their assistance in Metallography
- Mr. Ndeti and Mr. Kariithi for their assistance in Non-Destructive tests
- Mr. Mwendwa for his assistance in machining test specimens
- Mr. Mwarsame and Mr. Waribu for their assistance in mechanical tests

Finally, I thank my family, relatives, friends and colleagues for their unfailing support, patience and encouragement throughout this project.

Kelly Mutonga

Anti – Plagiarism Statement

This research thesis has been written by me and in my own words, except for quotations from published and unpublished sources which have clearly been indicated and acknowledged. I am aware that the incorporation of material from other works or paraphrase of such material without acknowledgment will be treated as plagiarism, subject to the custom and usage of the subject, according to the University Regulations on Conduct of Examination.

Name	Signature	Date
Kelly Mutonga	……	……

ABSTRACT

EN24 steel is widely used to fabricate components for power transmission in industry due to its high strength to weight ratio. The hardness of this steel in tempered (T) condition, EN24T, is between 265 HV_{10} and 320HV_{10} and tensile strength between 850MPa and 1000MPa. On request, some manufacturers can supply the material in annealed condition, EN24A, with a hardness value of approximately 220HV_{10} and slightly lower strength. This steel can be fusion welded using a wide range of filler materials. However, no data has been provided for microstructure and property changes when EN24 steel is welded with austenitic electrodes in its Annealed and in Tempered condition in the presence of preheat and Post Weld Heat Treatment (PWHT).

In this work, comparative mechanical properties and microstructural features of the weldment and the Heat Affected Zone (HAZ) in EN24T and EN24A steel have been investigated. EN24T steel and EN24A steel bars were first preheated to 288℃, arc welded with austenitic filler rods (A5.4 E312-16) then subjected to PWHT at 350℃, 620℃ and 675℃. Ultrasonic tests and X-Ray radiography were done to rule out discontinuities in weldment. Mechanical properties of resultant welded joint were considered to be a function of the filler rod material, base metal microstructure prior to welding and PWHT. The morphological features of microstructure in the Coarse Grained Heat Affected Zone (CGHAZ) and their evolution during PWHT were examined.

Charpy impact energies of the CGHAZ, microstructure and tensile properties of welded materials in relation to PWHT were evaluated.

Hardness of EN24T steel bought from local market was found to be 328 HV_{10} and it softened to 233 HV_{10} after annealing. Hardness of as bought EN24T steel reduced with increase in PWHT temperature. Hardness of EN24A steel was not affected by PWHT. The hardest location in welded specimens was found to be in the HAZ at approximately 0.6 mm from the fusion line. Multi-pass welding was found to temper the previous HAZ and to increase the band of the hardest region from CGHAZ to the Fine Grained HAZ. The same effect was found to occur during PWHT. PWHT at 620℃ and 675℃ was found to temper all specimens to hardness below 300HV and a minimum difference in hardness levels between base metal and HAZ was found during PWHT at 675℃. The tensile test specimens failed with a brittle fracture as no significant necking was observed on all welded specimens at all the PWHT conditions in this study. Generally, PWHT had no effect on the Ultimate Tensile Strength (UTS) of all specimens. Temper embrittlement in the CGHAZ was observed from results of hardness level and impact energy from EN24A steel subjected to PWHT at 350℃. The same was not observed on EN24T steel specimens. The CGHAZ of single-pass welded specimens of EN24A and EN24T steel presented a martensitic structure. The CGHAZ microstructure of specimens that were subjected to PWHT at 620℃ and 675℃ comprised of carbide precipitates in ferrite. The microstructure of EN24A steel was not altered by PWHT but that of EN24T steel was transformed from tempered martensite to ferrite and cementite at 675℃. PWHT had no effect on the microstructure and hardness of austenitic filler material comprising the weld metal.

At the PWHT temperature of 675℃ the room temperature - impact energy of CGHAZ in EN24A steel was higher than that of CGHAZ in EN24T steel by 22%.

TABLE OF CONTENTS

LIST OF FIGURES

LIST OF TABLES

LIST OF SYMBOLS

α	Allotriomorphic ferrite
α'	Martensite
α^b	Bainite
A1	Lower critical temperature line (eutectoid temperature)
A3	Upper Critical Temperature
AISI	American Iron and Steel Institute
APT	Atom Probe Tomography
ASTM	American Society for Testing and Materials
AWS	American Welding Society
BM	Base Metal
CE	Carbon Equivalent
C_{ppt}	Carbon Precipitate in Ferrite
CCT	Continuous Cooling Transformation
CGHAZ	Coarse Grained Heat Affected Zone
CVN	Charpy-V-Notch
DIN	Deutsches Institut für Normung (German National Standard)
EN24A	Annealed EN24 Steel
EN24T	Quenched and tempered EN24 steel.
EN24A-M0	Annealed EN24 steel, multi-pass welded and no PWHT
EN24A-M350	Annealed EN24 steel, multi-pass welded, PWHT at 350℃ for half hour
EN24A-M620	Annealed EN24 steel, multi-pass welded, PWHT at 620℃ for half hour
EN24A-M675	Annealed EN24 steel, multi-pass welded, PWHT at 675℃ for half hour

EN24A-S0	Annealed EN24 steel, single-pass welded and no PWHT
EN24A-S350	Annealed EN24 steel, single-pass welded, PWHT at 350℃ for half hour
EN24A-S620	Annealed EN24 steel, single-pass welded, PWHT at 620℃ for half hour
EN24A-S675	Annealed EN24 steel, single-pass welded, PWHT at 675℃ for half hour
EN24T-M0	EN24T steel, multi-pass welded and no PWHT
EN24T-M350	EN24Tsteel, multi-pass welded, PWHT at 350℃ for half hour
EN24T-M620	EN24Tsteel, multi-pass welded, PWHT at 620℃ for half hour
EN24T-M675	EN24T steel, multi-pass welded, PWHT at 675℃ for half
EN24T-S0	EN24Tsteel, single-pass welded and no PWHT
EN24T-S350	EN24T steel, single-pass welded, PWHT at 350℃ for half hour
EN24T-S620	EN24Tsteel, single-pass welded, PWHT at 620℃ for half hour
EN24T-S675	EN24T steel, single-pass welded, PWHT at 675℃ for half hour
FGHAZ	Fine Grained Heat Affected Zone
FL	Fusion Line
HAZ	Heat Affected Zone
HSLA	High Strength Low Alloy steel
HTLA	Heat Treatable Low Alloy steel
HV	Vicker’s hardness number
ICHAZ	Inter-Critical Heat Affected Zone
KIRDI	Kenya Industrial Research and Development Institute
Mf	Martensite Finish temperature
MS	Martensite Start temperature
NDT	Non-Destructive Testing

NMC	Numerical Machining Complex Ltd
PWHT	Post Weld Heat Treatment
PAGB	Prior Austenite Grain Boundaries
Q&T	Quenched and Tempered
SEM	Scanning Electron Microscope
TEM	Transmission Electron Microscope
TME	Tempered Martensite Embrittlement
UIT	Ultra Sonic Impact Treatment
UTS	Ultimate Tensile Strength
WM	Weld Metal

CHAPTER ONE

INTRODUCTION

1.1 BACKGROUND

EN24 steel is a hardenable medium carbon low alloy steel. Low alloy steels contain Nickel, Chromium and Molybdenum which maximize their strength after heat treatment [1]. They are classified into three major categories: High Strength Low Alloy Steels (HSLA Steels), Quench and Tempered Low Alloy Steels (Q&T steels) and Heat Treatable Low Alloy Steels (HTLA Steels).

HSLA steels are composed of less than 0.2% C and less than 2% alloy content. Their yield strength ranges from 275 to 550 MPa [1]. Carbides and nitrides in HSLA steels make grain growth difficult by preventing movement of grain boundaries. The resultant reduction in grain size improves their mechanical properties. They have weldability similar to mild steels [1].

Q&T steels contain a maximum of 0.25% C and less than 5% alloying content and their yield strength ranges from 345 to 895MPa [1]. Q&T steels are often strengthened by quenching and tempering to produce martensitic and bainitic microstructures. They have a low 'Martensite start' (MS) temperature brought about by their high alloy content. Thick sections of Q&T steels are usually preheated before welding [1, 2].

HTLA Steels contain carbon content between 0.25 to 0.5% and up to 5% alloy content [1]. EN24 steel falls in this category. EN24 Steel has a low MS temperature and can be strengthened by same processes as Q&T steels. The martensite formed in the HAZ of En24 steel is usually very

hard and susceptible to cold cracking. Like all HTLA steels, cracking tendency in EN24 steel is reduced by preheating the steel prior to welding [3]. EN24 steel is often welded successfully by using lower strength, low hydrogen filler materials [4, 5]. Several different covered electrodes are used for welding EN24 steel; for instance, electrode types E10016 and E15016 can be heat treated to strengths of between 1380 to 1550 MPa [6]. Inert gas welding technology is commonly used with Filler rods of the same composition as the base metal. In contrast, filler rods of the same composition as base metal have been reported to produce troublesome weld metal cracks [6]. Filler rods of mismatched compositions such as austenitic filler materials are therefore commonly employed in welding structures made from HTLA steels including EN24 steel since they are known for good resistance to cold and hot cracking [7] and meet requirements of good impact properties along with strength.

1.2 Problem statement

Austenitic electrodes are often used to weld a wide range of low alloy steels including dissimilar steels and steels of unknown composition [8]. This study will investigate Manual Arc Welding of EN24 steel with austenitic electrodes. Welding of EN24 steel is preferred to be carried out in annealed condition [9] except this is not always possible. Researchers [10, 11] have established that technical problems in regard to welding of steels can be eliminated by employing specific welding procedures and consumables. However, no comparative data has been provided for microstructure and property changes when EN24 steel is welded with austenitic electrodes in its annealed (EN24A) and Tempered (EN24T) condition in the presence of preheat and Post Weld Heat Treatment (PWHT).

Components restoration by welding is often quicker and cheaper than replacing them entirely. Components made from low alloy hardenable steels can be restored by welding provided special

precautions are observed. Tempered steels usually retain some hardness, become tougher and weld better than in their 'as quenched' condition. EN24T is a product of tempering quench-hardened EN24steel. When EN24T is welded with austenitic electrodes and post-heated, the mechanical properties of the weld joint are expected to be different from that of same material processed from an annealed condition (EN24A). This is because of the differences in microstructure of baseplate prior to welding [12]. Investigations will determine whether annealing of EN24T is necessary before welding with austenitic filler materials. The annealing process represents an increase in cost of production.

1.3 Objective of the Study

To characterize the effects of PWHT on the microstructure and mechanical properties of the weldment and the HAZ of EN24A and EN24T steel welded using austenitic electrodes.

Specific objectives

i. To survey the hardness of weldment in order to find the hardest and most brittle location of the HAZ in single and multi-pass welded joints.

ii. To characterize and compare microstructure of the hardest region of HAZ in welded EN24T and EN24A steel before and after PWHT.

iii. To determine and compare the fracture energy from impact tests on the hardest region of HAZ in multi-pass welded EN24A and EN24T steel before and after PWHT.

iv. To determine and compare tensile properties of multi-pass welded EN24A and EN24Tsteel in relation to microstructural changes caused by PWHT.

CHAPTER TWO

LITERATURE REVIEW

2.1 EN24 steel

EN24 steel is a heat treatable low alloy (HTLA) steel widely used due to its high strength to weight ratio. It is a low alloy martensitic steel popularly described as a $1\frac{1}{2}$per cent Nickel Chromium Molybdenum Steel. The EN24 steel designation is a British standard specification equivalent to AISI 4340 steel and DIN 17200-34CrNiMo6 steel [13].

Aircraft-quality AISI 4340 (designated E4340) has been used in the manufacture of aircraft landing gear, missiles and main rotor yoke for commercial and military helicopters for many years. Strong light-weight materials have been responsible for the ever increasing efficiency of airborne vehicles. Commercial quality EN24 steel is used in production of shaft - power transmission components, high tensile bolts, mandrels for tube manufacture, gun barrels, breech mechanisms, components for dies, plastic and rubber molds, hydraulic rams and pistons and various parts of machine tools. EN24 steel is commonly supplied in quenched and tempered condition, with hardness values between 265 HV and 320HV and ultimate tensile stress (UTS) between 850 MPa and 1000 MPa [14, 17]. Induction or flame hardening of EN24 steel can give high case hardness of approximately 510 HV [15]. It has a high ability to strain-harden making it slightly difficult to machine with high speed tools but it is readily machinable with carbide tools. In the annealed condition, the machinability of EN24 steel is 53% slower compared to mild steel [13].

The weight percentage of carbon in EN24 steel ranges from 0.35% to 0.45% and total alloying content is between 2.99% and 4.69 % (Table 2.1).

Table 2.1: Typical chemical composition of EN24 steel [9, 16, 18]

Element	C	Ni	Cr	V	Mo	Si	Mn	S	P
% by weight	0.35-0.45	1.3-1.8	0.9-1.4	0.09	0.2-0.35	0.1-0.35	0.4-0.7	0.04 Max	0.04 Max

2.1.1 Role of alloying elements.

Hardenability tests on EN24 steel reveal that untempered martensite with hardness more than 550HV can be maintained to a depth of 15 mm from the quenched end of a Jominy specimen [19]. Nosov et al [20] states that hardenability of low alloy steels is depended on alloy content and accurate hardenability values can be calculated directly from their alloy chemistry. However, Grange et al [21] found that for AISI grade steels, including EN24 steel, carbon has the sole influence in the hardness of untempered martensite. All the other alloy elements tend to retard softening of the 'as quenched' martensite especially when tempering is done at temperatures above 204℃ [21].

The specific roles played by major alloying elements in EN24 Steel are briefly outlined:-

Carbon

Carbon has the greatest influence on hardness of 'as quenched' martensite [21]. The higher the carbon content, in steel, the higher the 'as quenched' hardness.

Silicon

Silicon is used as a powerful deoxidizing agent during production of steel. It improves fluidity during casting of steels. In heat treatable steels, silicon increases strength of tempered martensite by solid solution strengthening. It inhibits conversion of ε- carbides ($Fe_{2.4}C$) to cementite (Fe_3C)

when tempering is carried out at 316℃. Silicon content greater than 0.3% reduces notch toughness and weldability [21].

Manganese

Manganese is used as a deoxidizing agent during production of steel but it is not as powerful as aluminum and silicon. It has affinity for sulphur and therefore combines with it to form manganese sulphide which is insoluble in steel. If manganese sulphide is not completely removed as slag during steel making, then, the amount that remains exists as insoluble non-metallic inclusions. In heat treatable steels, manganese increases hardness of tempered martensite by retarding coalescence of carbides. It behaves like a mild solid solution strengthener in ferrite [21].

Phosphorous

For heat treatable steels, phosphorous tends to decrease fracture toughness. Phosphorous levels less than 0.05% can cause embrittlement by segregating to the prior austenite grain boundaries (PAGB) during tempering [21]. Phosphorous at higher levels has high potency for promoting hardenability by strengthening ferrite through substitutional solid solution strengthening; but due to undesirability of tempered martensite embrittlement (TME), phosphorous levels are held at no more than 0.04% in heat treatable steels [2]. Phosphorous has little effect on carbides size. At tempering temperature above 204℃, phosphorous increases strength of tempered martensite by solution hardening of the ferrite matrix.

Nickel

It is a weak solid solution strengthener. It has a small effect on the hardness of tempered martensite [21]. Nickel is often added in combination with chromium. It improves fracture toughness in high strength steels. Nickel as an alloy addition causes no difficulty in welding [2].

Chromium

It is responsible for the good atmospheric corrosion resistance of EN24 steel. It easily forms chromium carbides and improves hardenability. Chromium retards softening of martensite at all tempering temperatures and its maximum effect is achieved at 427℃. At higher tempering temperatures its carbides retards coalescence of cementite [21]. In heat treatable steels such as EN24 steel, controlled amounts of chromium are added to avoid excessive hardening or cold cracking of the heat affected zone during welding [2].

Molybdenum

Molybdenum is often added to reduce susceptibility to temper embrittlement. It retards softening of martensite at all tempering temperatures. At higher tempering temperature, it partitions the carbide phase thereby producing a distribution of large quantities of small carbide particles [21]. The typical content of molybdenum existing in hardenable steels such as EN24 steel is often supplemented by elevated manganese content and small amounts of nickel. The reason is to suppress formation of pearlite in the microstructure or to reduce the size of pearlite areas and to produce cementite lamellae. At higher amounts it improves creep resistance and strength [2]

Vanadium

Vanadium has a great influence on the hardness of tempered martensite. It improves hardenability even when added in low amounts. Effect of vanadium is probably due to precipitation of vanadium carbides (V_4C_3 or VC), which replaces cementite at high tempering temperatures and exists as a fine dispersion up to the lower eutectoid (A1) temperature [21].

The other noteworthy effect of alloying elements is their influence on upper critical temperature (A3), eutectoid temperature (A1) and martensite start (MS) temperature in low alloy steels [2]. When MS temperature is reached during cooling of austenite, martensite begins to form and this continues until martensite finish (Mf) temperature is reached. Equations 2.1 to 2.3 show relationships between transformation temperatures and alloy content [22].

$$A3\ (℃) = 0.56\{1570-323(\%C)-25(\%Mn)+80(\%Si)-32(\%Ni)-3(\%Cr)-32\} \quad (2.1)$$

$$A1\ (℃) = 0.56\{1333-25(\%Mn)+40(\%Si)-26(\%Ni)+42(\%Cr)-32\} \quad (2.2)$$

$$MS\ (℃) = 0.56\{1042-833(\%C)-60(\%Mn)-30(\%Ni)-38(\%Mo)-32\} \quad (2.3)$$

2.1.2 Continuous Cooling Transformations diagram

Continuous Cooling Transformations (CCT) diagram depend on alloy chemistry of steel and its cooling rate from austenite phase to determine its final microstructure. Figure 2.1 shows the CCT for AISI 4340 steel (EN24 steel). A critical cooling rate of 8.3 ℃ / s is necessary to transform austenite to martensite in this steel [23]. MS at 300℃ and Mf at 80℃ were observed [13] during Continuous Cooling Transformations of a round bar Ø25 mm of EN24 steel which had been water quenched from 830℃ . Same MS and Mf were observed when bars of Ø20 mm or less were cooled in air from the same austenitizing temperature. Slower rates of cooling, Figure 2.1,

result in formation of a bainitic microstructure which has a lower hardness than a martensitic microstructure [13, 23].

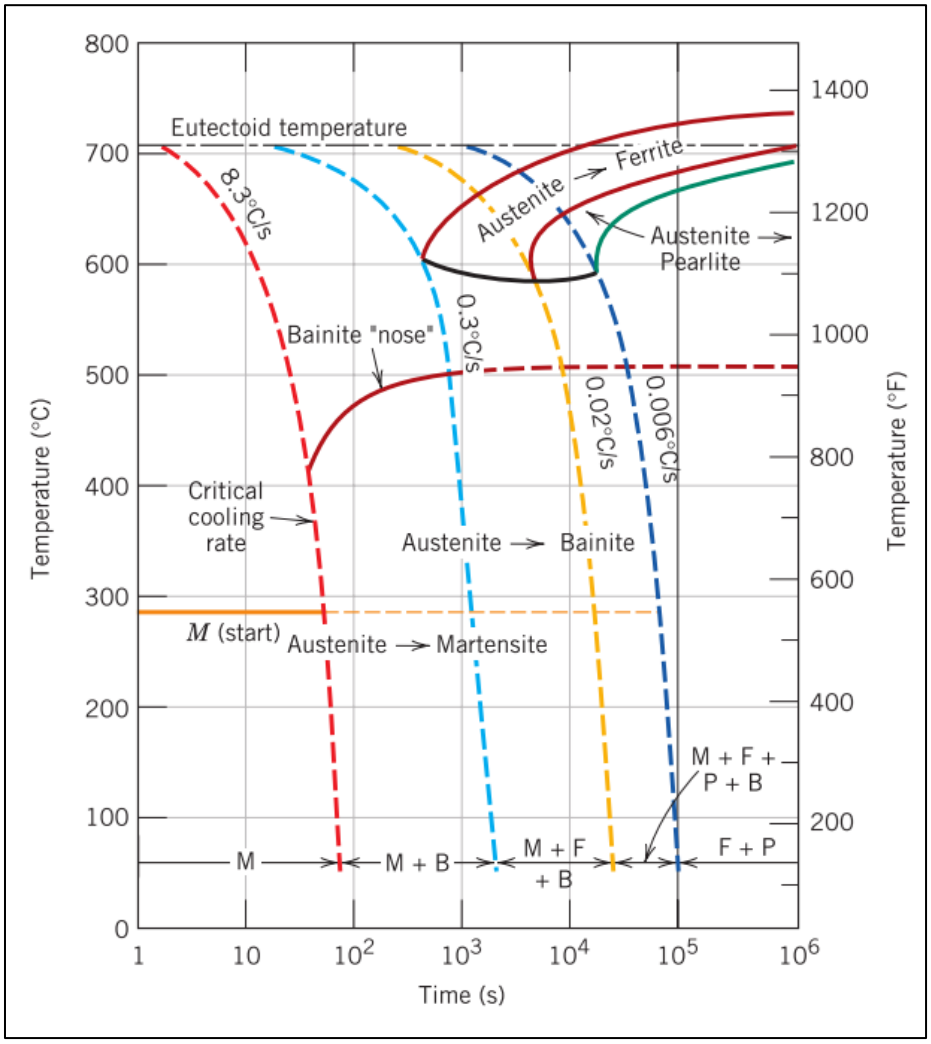

Figure 2.1: CCT diagram for EN24 steel [23]

2.1.3 Heat treatment.

The aim of heat treating steel is to achieve desirable microstructure and physical properties. By virtue of its carbon content, EN24 steel is a hypo-eutectoid steel. Hypo-eutectoid steels are usually heated 25℃ to 50℃ above the A3 temperature (Figure 2.2) during annealing, normalizing and quench hardening heat treatment. Research has revealed the desirable austenitizing temperature for EN24 steel to be 844℃ [24]. Austenitizing at higher temperatures is expensive as more energy is required and does not lead to any significant changes in 'as quenched' hardness [16].

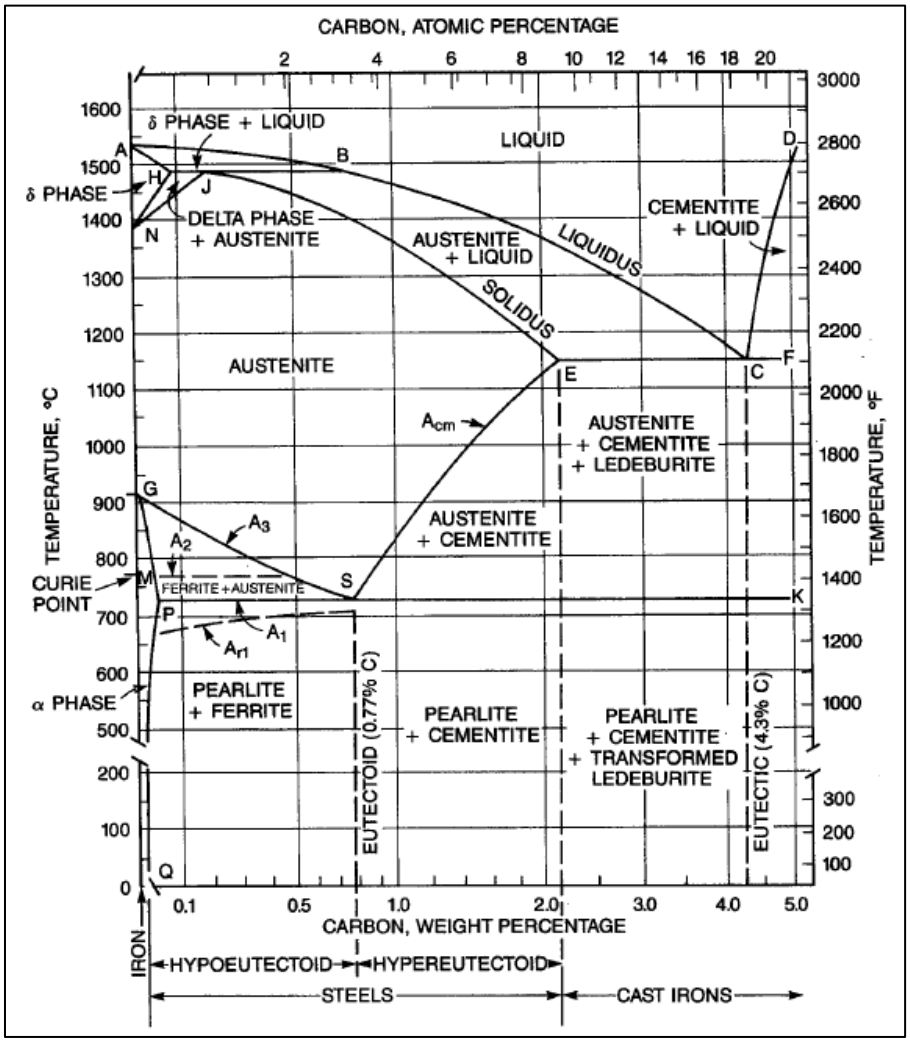

Figure 2.2: Iron-Iron Carbide Phase diagram [2]

2.1.3.1 Annealing

This is achieved by allowing a uniformly austenitized EN24 steel to cool down in the furnace to room temperature [25] or to cool to its MS temperature in furnace before withdrawing to cool in air to room temperature. The 'as annealed' hardness for EN24 steel lies between 16-22 HRc (≈ 200HV) [16]. Welding of EN24 steels in the hardened and tempered condition is not recommended and should be avoided if possible, as the mechanical properties will be altered within the weld heat affected zone. It is preferred that welding be carried out on EN24 steel while in the annealed condition prior to hardening and tempering. If welding in the hardened and tempered condition must be carried out, then the work piece, immediately on cooling down to room temperature should be stress relieved at 15 ℃ below the original tempering temperature (if known)[5].

2.1.3.2 Quench Hardening

Higher hardness of EN24 steel is achieved by quickly quenching a uniformly austenitized material in oil [5, 25]. Tempering on quench-hardened EN24 steel is usually carried out to the desired strength and toughness levels [26] as soon as it cools to room temperature. Induction hardened EN24 steel has very good fatigue and wear resistance and maintains good strength at service temperatures below 315℃ [17]. Induction hardening is mostly preferred during manufacture of gears, splines and power transmission shafts.

2.1.3.3 Tempering

Tempering is carried out on martensitic steels in order to reduce the hardness and brittleness of martensite after quench hardening. This process relieves the internal stresses introduced during quench hardening and reduces hardness of martensite thus leading to increase in ductility and

toughness. Tempered En24 steel finds applications in heavy duty shafts, high tensile bolts and couplings [5].

The effect of tempering temperature and time on tempering parameter (hardness) of steel with carbon content ranging from 0.31 to 1.15% can be expressed by the Holloman and Jaffe expression [27].

$$\text{Tempering parameter} = T(c + \log t) \tag{2.4}$$

Where 'T' is the temperature in Kelvin, t is the tempering time in seconds and 'c' is a constant that depends on the type of steel. Bryson [28] observed that it made little difference if tool steels are soaked for 6 hours or 6 days during tempering. This implies that tempering temperature has more influence on the outcome than time and as such tempering tool steel beyond 6 hours is unnecessary.

For high strength and toughness, such as in gears and cutting dies, tempering of EN24 steel is performed for 2 hours at temperatures between 180℃ and 250℃ and for other purposes, such as power transmission shafting, tempering is carried out between 550℃ and 660℃ [6, 13, 19]. Effects of tempering on hardness and impact properties of EN24 steel are shown in Figures 2.3 and 2.4. Figure 2.3 shows an almost linear decrease in hardness with tempering temperature. Low impact energy values in EN24 steel (Figure 2.4) are obtained at low tempering temperature (100 to 200℃). A further reduction in toughness occurs at tempering temperatures between 200 and 450℃. However, tempering at higher temperatures between 450 and 700℃ causes almost linear increase in toughness.

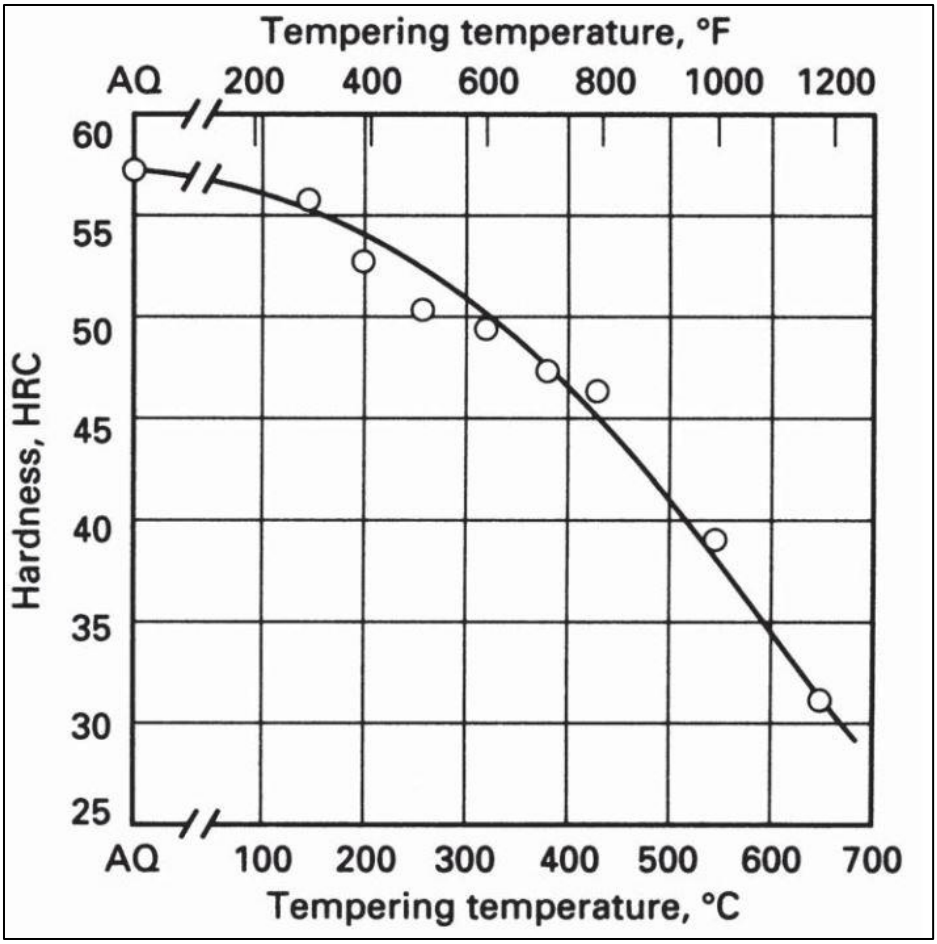

Figure 2.3: Tempering curve for AISI 4340 Steel (EN24 steel) [26]

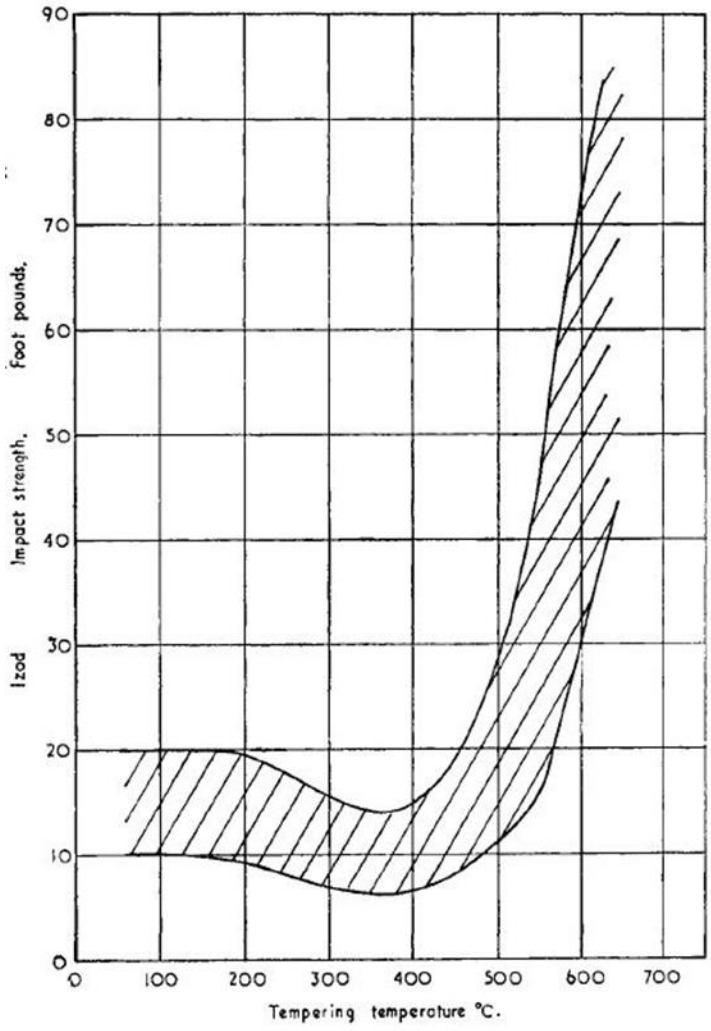

Figure 2.4: Room temperature Charpy V-Notch (CVN) energy of EN24 Steel at various tempering temperatures [13]

2.1.3.4 Normalizing

This treatment may be carried out on hot or cold worked EN24 steel products to refine their microstructure prior to final heat treatment. The nominal normalizing temperature for EN24 steel is 815 ° C followed by cooling in air to room temperature. Soaking time at the normalizing

temperature depends on the thickness of the product and it is approximated to be 1 hour per 25 mm of thickness. Production experience may necessitate a temperature either 10 º C above or below the normalizing temperature. As a rule of thumb, when forgings are normalized before, say, carburizing or hardening and tempering, the upper range of normalizing temperatures is used. When normalizing is the final heat treatment, the lower temperature range is used [15]

2.1.4 Microstructures

The major microstructures in low alloy steel and EN24 steel are reviewed in sections 2.1.4.1 to 2.1.4.5.

2.1.4.1 Austenitic microstructure

Growth of austenite grains is enhanced by the length of time at elevated temperatures above A3 [23]. Dilatometric and calorimetric analysis of tempered martensite in 1.13% C steel has shown that diffusion of carbon into austenite during austenization is the rate controlling mechanism of an austenite microstructure [29]. Not all austenite transforms to martensite during quenching. Retained austenite is the amount that remains untransformed. Medium carbon steels of 0.4% C like EN24 steel can have approximately 5% retained austenite [30]. The quantity of carbon in retained austenite is usually significantly higher than the general carbon content of the alloy [31].

2.1.4.2 Annealed microstructure

The microstructure of as quenched EN24 steel consists of martensite, Figure 2.5 (a), compared to the annealed microstructure that consists of lamellar pearlite colonies in ferrite, Figure 2.5 (b). Figure 2.5 (c) shows a microstructure of tempered martensite and numerous carbides precipitates coexists with tempered martensite after tempering, Figure 2.5 (d).

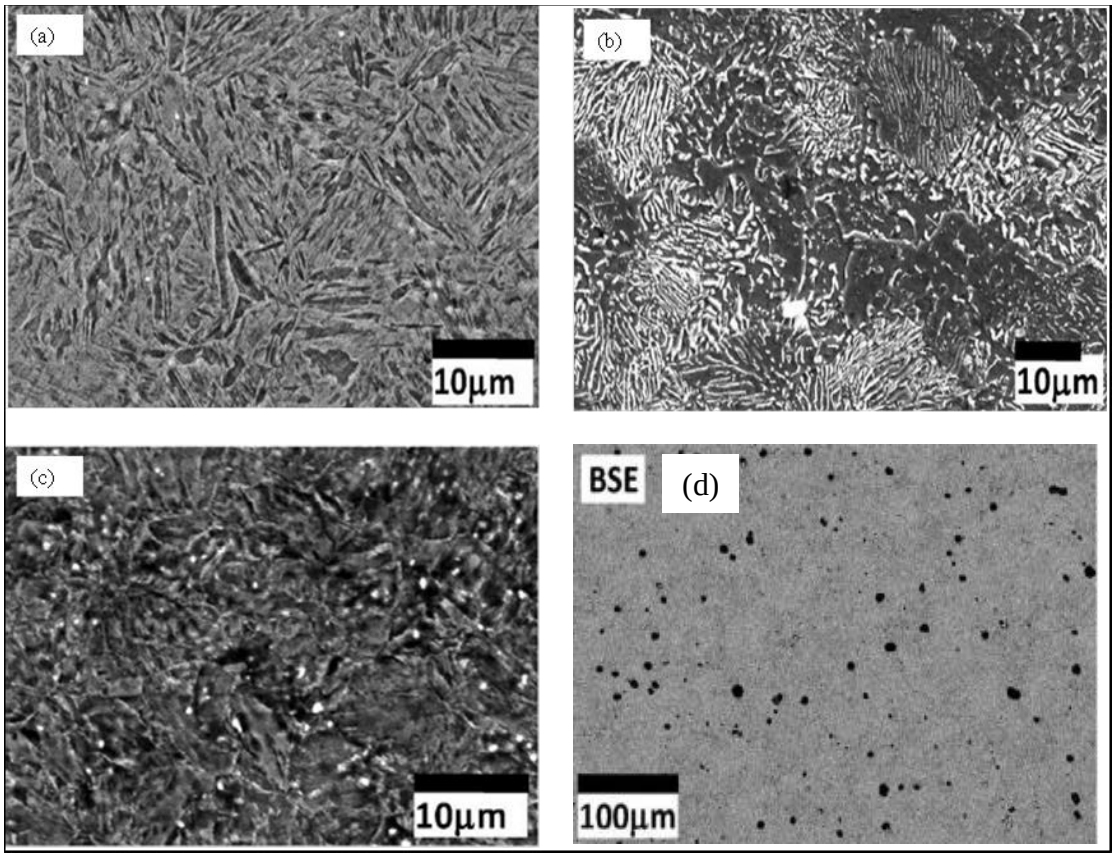

Figure 2.5: SEM Images of EN24 steel after austenitizing at 850℃ and (a) quenching in oil, (b) cooling in furnace to room temperature, (c) quenching in oil and tempering for 1 hour at 550℃ and (d) Back Scattered Electron image of (c) showing distribution of carbides after tempering [16]

2.1.4.3 Bainitic microstructure

Bainitic microstructure is composed of alpha ferrite and a dispersion of iron carbide. Two types of bainite namely upper and lower bainite are documented [32]. Lower bainite consists of non-lamellar aggregate of ferrite and carbides. Upper bainite consists of cementite and bainitic ferrite without carbide precipitates. Upper and lower bainite exists with retained austenite or constituents such as martensite or cementite which form after growth of bainitic ferrite. The

decrease in strength on tempering bainite is smaller because unlike martensite there is hardly any carbon in solid solution [32, 33]. Figure 2.6 shows optical microstructure of bainite and martensite in medium carbon steel 0.38% C micro-alloyed with 1.01% Cr and 0.12 % V. At this resolution, it is difficult to distinguish between upper, lower and coalesced bainite without having prior knowledge at higher resolution through transmission electron microscopy [34]. Bainite is dark etched relative to martensite [35] because it consists of a dispersion of carbides in ferrite.

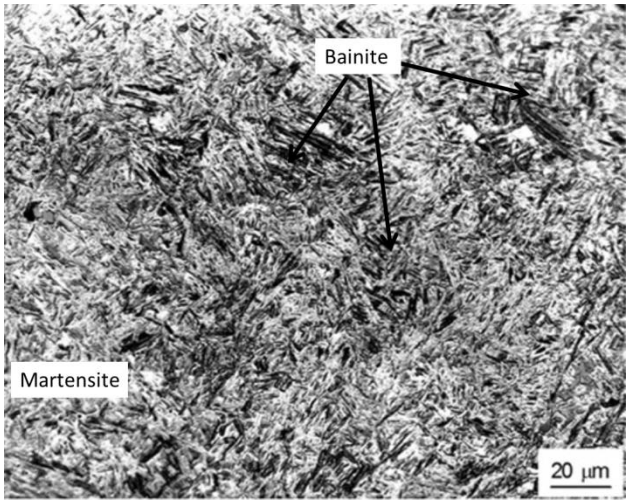

Figure 2.6: Bainite and Martensite in a quench hardened 0.38% C steel closely conforming to EN24 steel [35]

2.1.4.4 Martensitic microstructure

Martensite is the hardest and strongest microstructure produced by medium and high carbon steels (0.3-1.5% C). It is well known that 100% martensite represents the highest level of hardness achieved by any steel. However, the volume fraction of martensite in steel can be controlled by a heat treatment procedure [21]. Saeidi et al [36] carried out controlled heat

treatment of EN24 steel and produced dual structured steel composed of martensite/ferrite and bainite/ferrite with 34% ferrite in both cases.

Martensitic microstructures can comprise mixtures of retained austenite, carbides and martensite crystals of several morphologies [37]. Observations using Atom Probe Tomography (APT) have shown segregation of carbon atoms at lath boundaries and intra-lath boundaries in auto-tempered 0.1-0.5% C steels [38]. Martensite exists in a matrix of martensitic crystals in lath morphology depending on Carbon content (Figure 2.7) [37, 39].

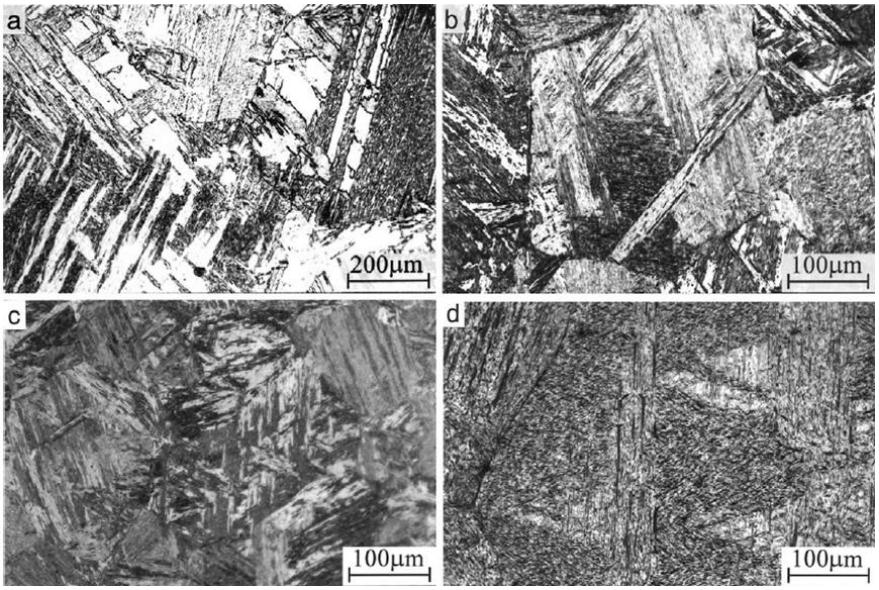

Figure 2.7: Optical micrographs for lath martensite in (a) 0.0026% C (b) 0.18% C (c) 0.38% C and (d) 0.61% C Steel. Etching solution was 3% nital [40]

Martensite packets formed within austenite grains are controlled by the size of the grain. The packets subdivide further into blocks [41]. It has been found that the block size of lath martensite is a parameter that influences strength in hardenable steels. Typical width of lath as found through TEM imaging is approximately 1micron. High Dislocation density within martensite laths is also evident (Figure 2.8) A decrease in lath width or packet diameter in lath martensitic –

bainitic steels leads to an increase in yield strength [42, 43]. Recent reviews [37, 43] have established that the yield strength of lath martensite can be expressed by the equation:

$$\sigma_y = \sigma_o + \sigma_p + \sigma_s + k_{HP} d^{-0.5} \quad (2.5)$$

where:

σ_o=friction stress of pure iron, σ_p= precipitation hardening component catering for hardening of dislocations within laths and in low angle boundaries, σ_s=component for solid solution hardening, k_{HP}= Hall-Petch slope and d= the effective grain size or the spacing of high angle boundaries.

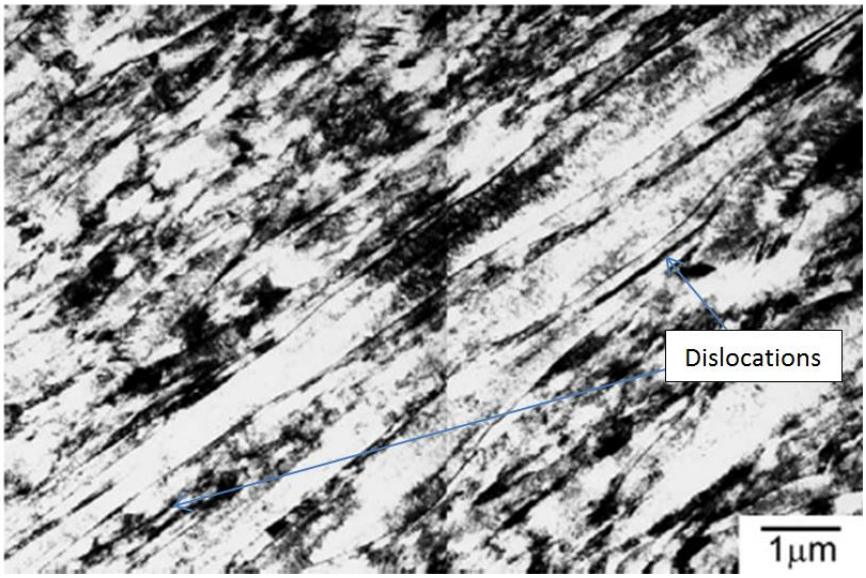

Figure 2.8:T.E.M image of lath martensite in 0.2 % C steel [44].

2.1.4.5 Tempered EN24 steel

High tempering temperature transforms the microstructure in 0.42% C steel from martensite to carbide precipitate in alpha-iron matrix (Figure 2.9 b). Tempering EN24 steel at temperatures ranging from 580-650℃ was found to be characterized by a microstructure of lower bainite with numerous precipitates of carbides [45]. At low tempering temperature (200℃) the carbide

precipitates in EN24 steel have a plate like structure [46] and a spheroidal one at high tempering temperature (650℃). Parker et al [47] carried out studies on fracture toughness of quenched and tempered EN24 steel, AISI 4130 and 300M and found blocky ferrite, twinned martensite plates and upper bainite to be deleterious to fracture toughness. On the other hand autotempered martensite, lower bainite and retained austenite were found to enhance toughness [47]. Auto-tempering is a phenomenon in which the first formed martensite near MS temperature is tempered during the remaining process of quenching or cooling.

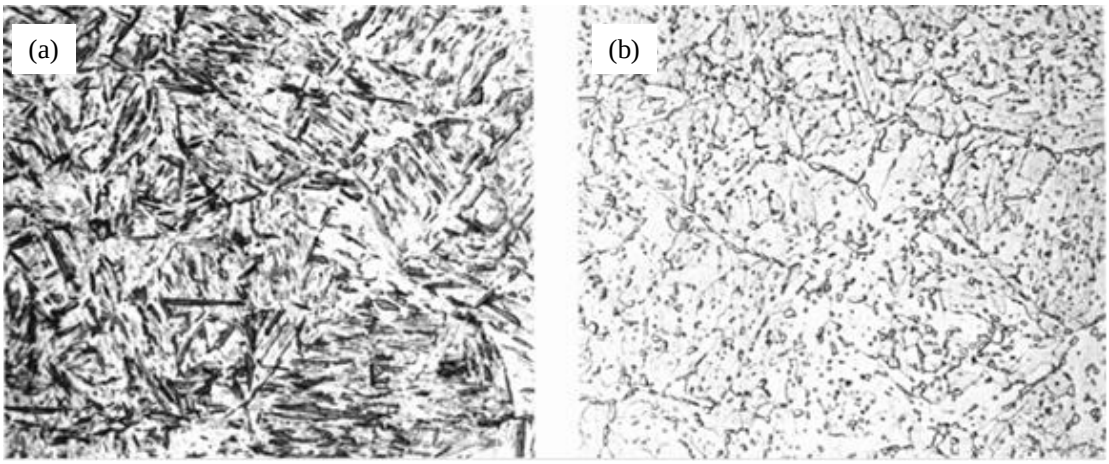

Figure 2.9: Optical micrograph for (a) As quenched martensite (b) tempered martensite in a 0.42% C steel tempered at 704℃(Magnification 500) [21].

2.1.4.5 Tempered Martensite embrittlement

The lowest Charpy impact energy (Figure 2.4) for EN24 steel is obtained at around 350℃ and it is caused by Tempered Martensite Embrittlement (TME) [48]. The embrittlement is caused by the presence of fine carbides and retained austenite [49, 50] and when $Fe_{2.4}C$ (ε- carbide) is replaced with interlath cementite during tempering. Lim et al [51] carried out APT to measure amounts of carbides and impurities in EN24 steel tempered at 400℃. The results clearly showed

that formation of film-like carbides and phosphorous segregation was the main cause TME. Horn et al [52] found fracture in embrittled structures in EN24 steel was caused by interlath cleavage. No evidence of intergranular cracking was observed but they also noted segregation of residual impurities of manganese sulphide along grain boundaries and interlath/intralath carbides (Figure 2.10). Bhadeshia et al [30] found TME in Fe-C-Mo steel to be depended on the relatively coarser intralath cementite rather than the interlath cementite resulting from the decomposition of less than 2% retained austenite present as films between the martensite laths. In a Fe-C-Mn-Si Steel containing fine carbides and negligible retained austenite, TME was not found.

Eliaz et al [48] found fractography to be a reliable tool in determining which, under similar conditions, between hydrogen cracking, stress corrosion cracking and TME is responsible for failure in EN24 steel structures.

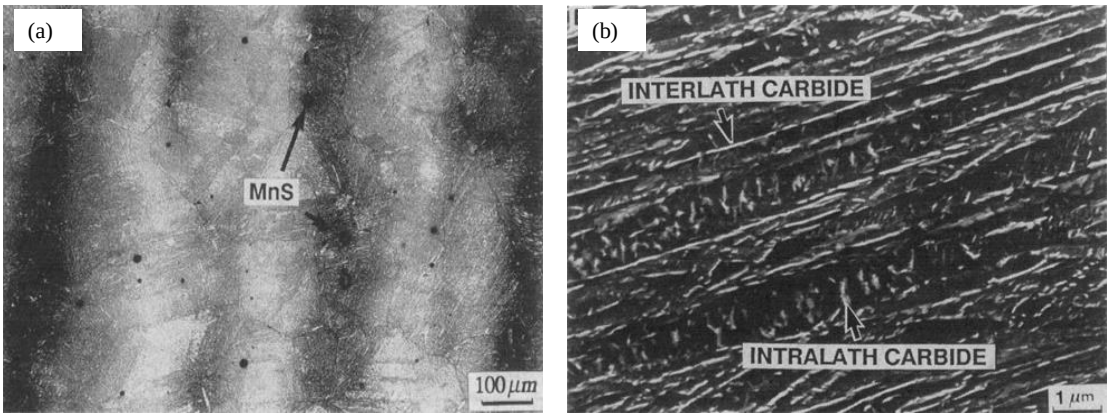

Figure 2.10: (a) Optical Micrograph for EN24 steel austenitized at 1150℃ followed by quenching and tempering at 350℃ and (b) SEM image under the same heat treatment conditions[49]

2.2 Manual Metal Arc Welding

Manual Metal arc welding is the most common and cost effective fusion welding process employed in welding of low alloy steels including EN24 steel. It is generally used to join

components and materials in an assembly during production, repair and maintenance [53, 54]. Welding can be executed quickly and leak proof joints can be produced cost effectively. However, welding can create harmful HAZ, residual stresses, discontinuities and distortions. Inherent and invisible flaws can cause catastrophic failures in welded structures. A welding power source is usually used to convert utility energy to proper levels of heat input required to melt the filler metal and base materials [55-58]. Welding parameters determine the generated heat input and affect welded joints in terms of quality, grain size and structural phases [59]. The type of filler materials, heat flow characteristics and weld quality are considered when welding low alloy steels [60-62].

2.2.1 Composition of filler rod

A wide range of filler materials are used in welding low alloy steels. The austenitic weld metal used in this study comprises about 30% ferrite in an austenite matrix. The structure is resistant to solidification cracking and has good wear/corrosion resistance. The weld metal is capable of withstanding heavy impacts or shocks in service [63].

2.2.2 Energy generated during welding

The heat input and conductivity of base metal (BM) influences the width of the HAZ and cooling rate of weldment and therefore impacts on the mechanical and microstructural properties of welded joints [59, 64]. Heat input is directly proportional to voltage (V) in volts, current (I) in Amperes and it is inversely related to the welding speed (v) in mm per second as shown in equation 2.6. The typical heat input during arc welding ranges from 0.5 to 3.0 kJ/ mm [64, 65].

$$\text{Heat Input} = \frac{60VI}{1000v} \tag{2.6}$$

2.2.3 Cooling time from 800-500℃

Cooling time varies depending on the gross heat input, initial BM temperature and thickness [12, 66]. Slow cooling rates of the order of 5℃ / s are typical of high heat input with moderate preheat. Faster cooling rates (60℃ / s) are typical of lower heat input with no preheat [67]. The cooling time from 800℃-500℃, $\Delta t_{8/5}$,or simply Δt , determines cooling rate of the HAZ and influences austenite transformation during welding of steel [68].

In case of 3-Dimensional heat flow, like welding of thick steel plates, considered in this study: Δt is approximately proportional to E.

$$\Delta t \approx 5\eta E \tag{2.7}$$

where η = arc efficiency and E = gross heat input in kJ/ mm.

Arc efficiency for metal arc welding ranges between 65-85% [68].

The temperature T at time t (s) in a welding cycle can be fully characterized by equation 2.8 [69].

$$T\text{-}T_0 = \theta_1 \frac{\Delta t}{t} \exp - \left[\frac{\Delta t}{et}\left(\frac{\theta_1}{T_p - T_0}\right)\right] \tag{2.8}$$

where:-

$$\frac{1}{\theta_1} = \left(\frac{1}{773 - T_0} - \frac{1}{1073 - T_0}\right) \tag{2.9}$$

θ_1 = reference temperature interval for thick steel plates

T = Temperature (K)

T_0= Initial or Preheat Temperature (K)

T_P= Peak Temperature (K)

2.2.4 Preheat and interpass temperatures

Controlled preheat is recommended for medium and high carbon steels in order to reduce the cooling rate of the HAZ. Preheat temperature is calculated from the Carbon Equivalent (CE) of steel. The value of CE for steel with carbon content greater than 0.18 % is represented by equation 2.10 [70-72].

$$CE = C + \frac{(Mn+Si)}{6} + \frac{(Cr+Mo+V)}{5} + \frac{(Ni+Cu)}{15} \quad (2.10)$$

Preheat and inter-pass temperature for CE between 0.47 and 1.0 can be calculated using equation 2.11 [62, 73]:

$$\text{Preheat Temperature (℃)} = 450\sqrt{CE - 4.2} \quad (2.11)$$

It is important to note that Inter-pass temperature in arc welding can safely exceed preheat temperature by between 40℃ and 95℃ [74] but it is not allowed to fall below the calculated preheat temperature [3]. Both preheat and PWHT are necessary when the CE is greater than 0.55 to avoid cold cracking and other metallurgical complications inherent in welded high strength steels [10, 75].

2.2.5 Post Weld Heat Treatment (PWHT)

PWHT is carried out at temperatures below A1 because PWHT above the A1 results in reformation of austenite. Before commencement of PWHT, the HAZ should be allowed to cool to a temperature below Mf, as shown in Figure 2.11 (a). If not, there can be undesirable retained austenite left in the HAZ. The retained austenite may transform into ferrite and pearlite during PWHT or to untempered martensite upon cooling to room temperature [76, 77]. PWHT relaxes ferrite by facilitating grain boundary sliding and tempers any martensite in the weldment by changing it into discrete carbides leading to a decrease in dislocation density and therefore greater toughness [78]

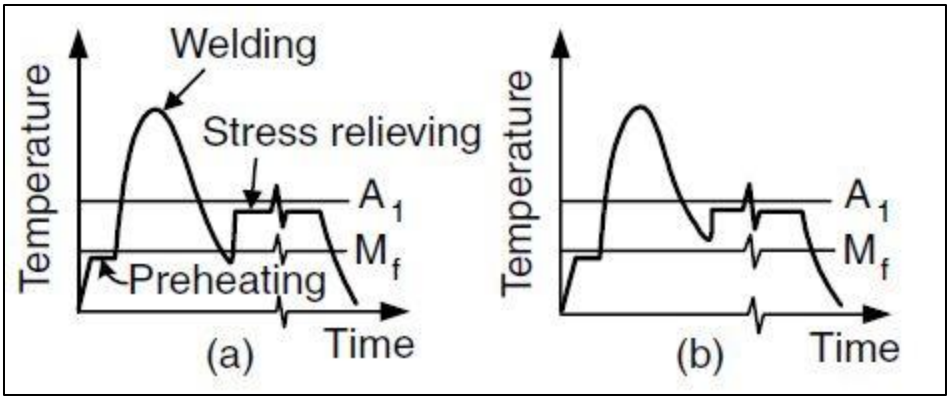

Figure 2.11: Thermal history during welding and PWHT of HTLA steel: (a) desired; (b) undesired [1]

2.2.6 Quality control in welding

Welding quality depends on the degree of compliance of base materials, consumables and weld discontinuities with established requirements [79, 80]. It is practically impossible to fabricate a completely defect free structure. The task is usually to ensure a minimum number of tolerable flaws [72, 81]. Visual inspection is commonly used in flaw detection. Detailed Non Destructive Test methods include Radiography and Ultrasonic tests [80, 81].

2.3 Welding of EN24 steel

EN24 Steel can be welded by all types of fusion processes, flash butt welding and resistance welding [6, 82]. Welding the steel in Q&T condition should be followed by tempering at a temperature 15℃ lower than the last known tempering temperature [5, 14]. Due to thermal stresses and metallurgical conditions of the welded joint, it is recommended that the welding operation should be preceded by preheating to avoid cold cracking [5, 10, 16]. Calculation of preheat temperature from Equations 2.10 and 2.11 (section 2.2.4) and composition of EN24 steel (Table 2.1) gives a preheat temperature range between 262℃ and 374℃. In practice [4, 74], preheat and inter-pass temperature of 288℃ is recommended when welding EN24 steel with a

low hydrogen filler material and 315℃ for other filler materials. Since the CE of EN24 steel is above 0.55, as calculated from its alloy composition (section 2.2.4), PWHT is recommended to be carried out after the welding operation [10, 75]. PWHT for EN24 steel is usually carried out at temperatures between 593℃ and 677℃, holding it for a length of time (typically one hour per 25 millimeters of thickness) and allowing it to cool in air to room temperature [74].

EN24 steel can be welded with matching and non-matching filler materials. Generally, stainless steel filler materials forms joints of lower strength except in thin sheets of EN24 steel where the weld metal is dilute and stronger [6]. Austenitic (or American Standard AWS A5.4 E312-16) electrodes are recommended for welding medium carbon, low alloy steels [8, 63]. These filler materials have lower carbon content than EN24 steel and have UTS of approximately 700MPa. Bend tests on welded EN24 steel have demonstrated that welding with filler material of lower carbon content reduces risk of crack formation [83].

2.3.1 Effect of Peak temperatures on microstructure

Peak temperature in a weldment affects the cooling rate of microstructure and changes the structure of the base metal and the prior austenite grain size in the immediate neighborhood of the weld metal as depicted in Figures 2.12 and 2.13. High peak temperature has significant effects on prior austenite grain size. The cooling rate of austenite, as deduced from Figure 2.12, has insignificant effect on prior austenite grain size.

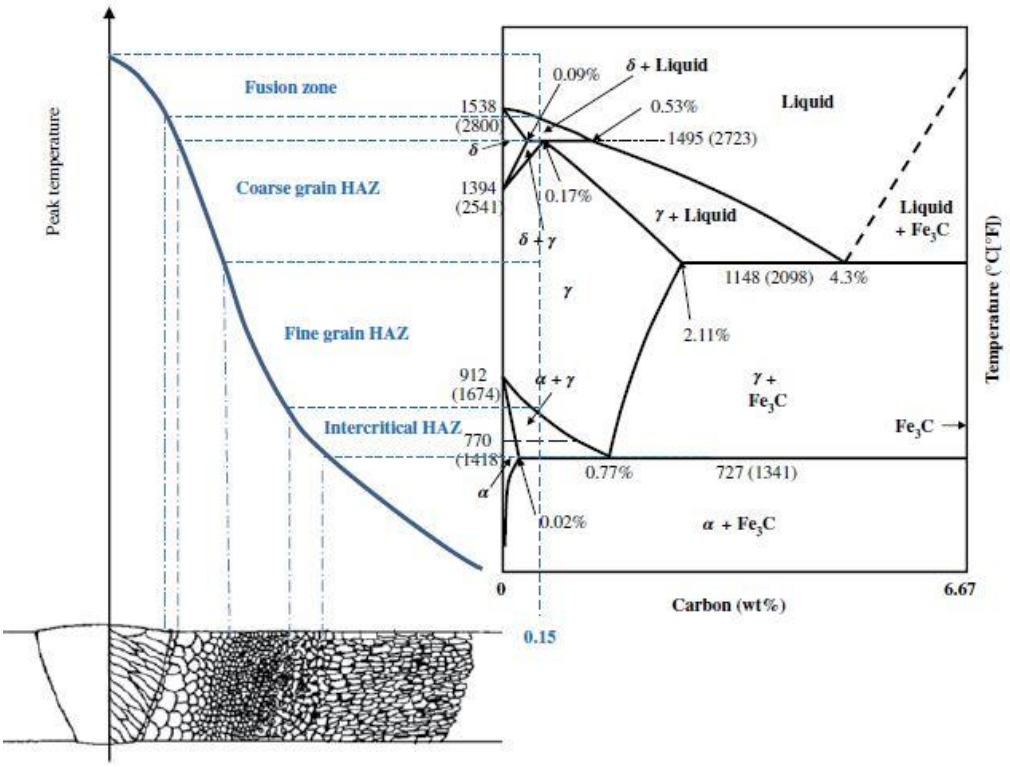

Figure 2.12: Peak temperatures and HAZ during welding for a 0.15%C steel [56]

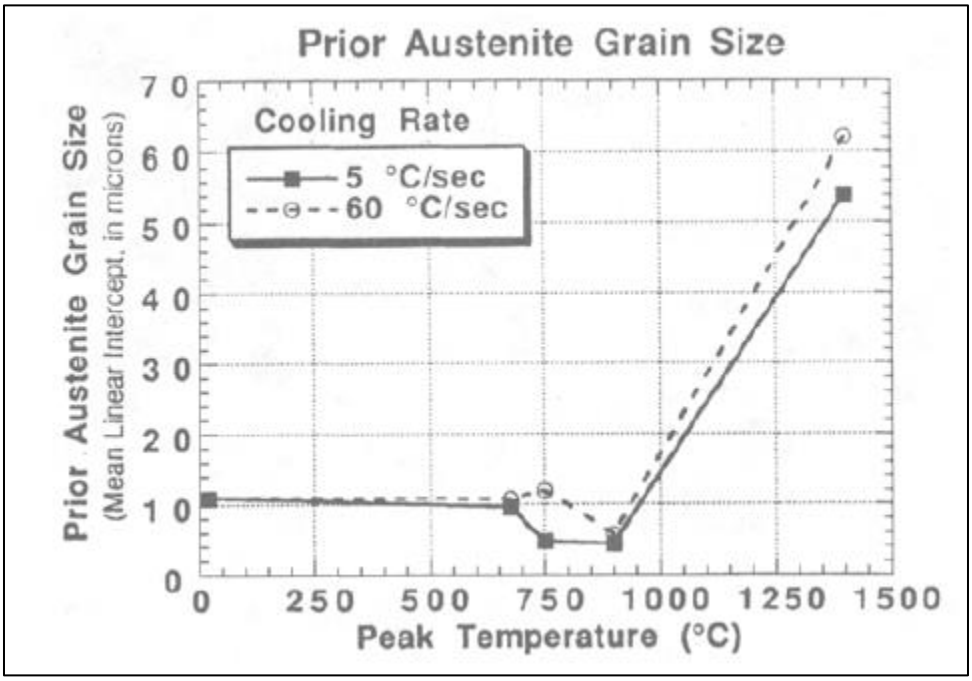

Figure 2.13: Prior Austenite Grain Size as a function of peak temperature and cooling rate [67]

Besides the sustained thermal cycle, the HAZ microstructure, grain size and texture are influenced by the original BM microstructure [12, 84, 85]. The HAZ in single-pass welds comprises three distinct regions namely coarse grained heat affected zone (CGHAZ), fine grained heat affected zone (FGHAZ) and inter-critical heat affected zone (ICHAZ) (Figure 2.12). Austenite grain growth in EN24 steel occurs in the CGHAZ and the martensite formed in this region can be very hard and brittle [22]. Simulations at varied peak temperatures on low carbon, 11.5% Cr- steels [86] revealed that the CGHAZ is a thin zone adjacent to the fusion line and it varied in thickness from 0.2 to 1.0 mm depending on the heat input. In the FGHAZ, the attained peak temperature is above A3 but below the grain coarsening temperature. A combination of smaller pre-austenite grain sizes and subsequent ferrite nucleation and growth reduce the grain sizes further [22]. A mixture of the original base plate austenite and ferrite is found in ICHAZ since re-austenization does not occur in this region [75].

Successive passes during multi-pass welding produce changes in the fusion and heat-affected zones of earlier passes resulting in reheated zones comprised of recrystallized CGHAZ and FGHAZ. In welds containing 0.68-1.36 % Mn the most brittle region was found to be in the CGHAZ reheated to a peak temperature of 1350℃ [87]. The reheat energy input increased the austenite grain size in the region. This, however, was not the case when high strength bainitic/martensitic steel containing 0.12% C, 0.6% Mn, 2.4% Cr, 0.99% Mo (and 8 ppm Boron) was reheated during multi-pass welding. Strunk et al [88] found that properties of the initial CGHAZ microstructure of the steel were not altered by thermal cycling of subsequent passes. Therefore, depending on the type of steel, multi-pass welding may or may not alter the CGHAZ microstructure significantly.

2.3.2 Weld Metal Microstructure

Savage et al [89] while studying the fusion boundary of HY-80 Low alloy steel (0.18% C, 2.99% Ni, 1.68% Cr) weldment found strands of melted but unmixed base metal in the bulk of weld metal. They found wide spread segregation of alloying and impurity elements in the inter-dendritic spaces. In austenitic steel weld metal (16% Cr, 12% Ni and 0.015% C) a form of martensite designated α_m and ε_m martensite is reported to form at very low temperature owing to its low MS (-59℃) temperature [90].

2.3.3 Discontinuities in Weld Metal and HAZ.

With all other parameters such as welding characteristics and filler materials constant, cracks are a major cause of failure of welded components. Discontinuities listed in order of decreasing severity are undercuts, slag inclusions, lack of penetration and porosity. Solidification cracks may be caused by low melting point eutectics or impurities at the grain boundaries or simply, by plain grain boundary weakness in weld metal [22, 79]. Reheat cracks may occur during PWHT or when EN24 steel is subjected to high temperature (350℃-550℃) service [91]. The cracks can occur in EN24 steel because it contains secondary carbide formers such as Cr, Mo, and V. These carbides normally dissolved in the CGHAZ during welding precipitate again during PWHT and may cause inter-granular fracture along prior austenite grain boundaries PAGB [91, 92].

EN24 steel may be susceptible to hydrogen cracking. A hard HAZ easily cracks if hydrogen dissolved in the weld metal diffuses into its microstructure [93]. In EN24 steel it has been found that hydrogen entrapment occurs along martensite lath intersection with PABG [94]. This causes micro-cracks along intergranular facets which grow to visible cracks as the hydrogen pressure increases. This is often remedied by post heating; more time at elevated temperatures allows the

dissolved hydrogen to escape from the HAZ [50, 95] without causing damage. Kinsey [96] found that hydrogen cracking on some high strength steels can be avoided if filler materials with less than 5ml H_2/100g of deposited weld are used. In austenitic weld deposits, Cr, Mo, Si and Nb promote formation of delta ferrite which greatly reduces the cracking tendency [97, 98]. Generally, when low carbon electrodes are used to weld high carbon BM, there may be Carbon pick up in the weld pool due to dilution and solid state diffusion from the BM [99]. However, highly alloyed structure of low carbon austenitic weld metal is extremely tolerant to dilution from hardenable steels [8].

2.3.4 Residual stress

Contraction of the weld metal during solidification is known to cause residual stresses, distortion or cracking of welded components. Residual stresses in weldment can be as high as the yield strength of the base metals [95, 100, 101]. They are remedied by means of mechanical shock (hammering, blasting, shot peening) or by post heating. Such treatments cause metal to undergo local plastic strain which leads to a reduction of the stress [102, 103]. Residual stress can also be reduced by the Ultra Sonic Impact Treatment (UIT). Simulations have been carried out on effects of overloads on fatigue life of welded joints and fatigue strength improvements due to UIT. Results from simulations have been found to match with those obtained in practice [104]. If residual tensile stresses are not removed, they tend to shorten the life a part by lowering its fatigue resistance and reducing its load carrying capability [105,106].

2.4 Mechanical properties

In practice, butt weld tests must include at least one transverse tensile test, CVN impact tests, hardness tests and micrographs of weld cross-section [65]. For a given metal, welding tests (whether actual or simulated) can only provide data to compare different welding procedures or processes [107]. Tensile test for weld metal is normally performed on an all weld metal tensile test specimen [4, 108]. On the other hand, transverse welded tensile test specimen is used to test the base metal and the weld joint. Therefore, tensile tests results on welded materials are usually limited to UTS since the specimens are non-homogeneous [83, 107]. It is important to note that the tensile strength of steel can be deduced from its hardness since the two properties are correlated [109-111]. Hard martensite responsible for hardness of steel presents with low notch ductility during a Charpy impact test [112]. Discontinuities in weldments can reduce mechanical properties significantly because they act like local stress risers.

2.4.1 Effect of welding on Hardness of HAZ

Hardness of HAZ increases with carbon content and rate of cooling due to increased solution hardening and formation of the martensite phase [113]. Studies on metal arc welding on industrial low carbon steel (0.19 %C) [114] showed maximum hardness values in the HAZ. Ramirez et al [115] while studying CGHAZ in V-micro-alloyed X60 steel pipe determined that the maximum hardness of the CGHAZ increased from 233 to 392 HV as the cooling rate from 800℃ to 500℃ changed from 5 to 80℃/s.

Investigations on hardness gradients in HAZ of welded Q&T steels (UTS 690Mpa) [108] showed they were different from those of lower Carbon equivalent steels. The peak HAZ hardness was found to be displaced from the CGHAZ to the FGHAZ. This phenomenon is considered to be caused by austenite grain size hardening effect and bainitic hardenability that is

high enough to result in the same microstructure in the GCHAZ and FGHAZ except for significant refinement of the microstructure of the FGHAZ [116].

2.4.2 Effect of PWHT

PWHT may have beneficial, harmful or have minor effects on the properties of a weldment depending on alloy chemistry of steel, welding procedure and the PWHT parameters employed [117, 118]. PWHT on low carbon structural steels can improve toughness without making any significant difference in UTS and hardness. PWHT has been found to reduce residual stresses in welded low carbon structural steel by about 70% [119].

PWHT for EN24 steel is usually carried out at temperatures between 593℃ and 677℃ for a period of time governed by the thickness of the material (normally 1 hour for 25mm of thickness) and after cooling down to room temperature. If filler rods other than the low hydrogen types are used then PWHT may be carried out one hour after completing the welding operation [71, 74].

The effect of PWHT in the HAZ of EN24 steel is similar to that of tempering the 'as quenched' steel at an equivalent tempering temperature. As PWHT or tempering temperature increase, the strength and hardness of the HAZ or the material decreases. Prabhavalkar et al found a good combination of strength (UTS 1108 MPa) and hardness (330HV) in EN24 steel at a tempering temperature of 580℃ [45]. Studies on the effect of PWHT on microstructure and mechanical properties of arc welded reactor pressure vessel steel SA 508 GR 4N (0.23 % C) [120] showed astounding improvements in toughness. The microstructure of the HAZ in the pressure vessel was found to be fully tempered. Similar effects were found by Silwal et al [121] after they investigated impact toughness of HAZ in Grade P- 91 steel after a 760^{o}C, 2hour PWHT. Roberti et al [122] investigated the fracture toughness of ASME SA 542M (0.15 %C) steel used under

severe conditions in the petrochemical industry. PWHT was carried out on samples at 750℃ and holding time of 1hr for each 25mm of thickness. Evaluation of the fracture toughness demonstrated that heat treatment for a short time at temperatures higher than the recommended PWHT had no significant effect on microstructures of BM, weld metal and HAZ. Stress relieving at 580℃ on multi-run submerged arc welded deposits containing 0.05 – 0.15% C and 0.6-1.8% Mn was investigated by Evans [123]. He found PWHT spheroidised the pearlite and cementite films that were present before the PWHT treatment. The overall hardness and tensile strength reduced while toughness improved.

An alternative to PWHT process was investigated by Peddle et al [124]. They reported elimination of PWHT in creep resistant 2.25Cr-1Mo steel by employing the temper bead and conventional weaving multi-pass welding.

PWHT in HSLA steels was found to enhance fatigue performance of the welded joint irrespective of the weld metal strength mismatch [118] and caused precipitation of fine carbides in the dissimilar super-martensitic stainless steel (AISI 410 steel) weld metal.

2.5 Summary of literature review

1. Tempered martensite embrittlement occurs after tempering of Q&T martensitic steels such as EN24 steel at temperatures within the range of 250 to 400℃. It presents as reduced room temperature notched bar impact energy.
2. During fusion welding of high strength heat treatable steels, avoidance of pre-heat and PWHT may result in cold cracking of the weld joint and other metallurgical complications.

3. For AISI 4340 steel (EN24 steel) preheat and inter-pass temperature of 288℃ is recommended when welding with low hydrogen filler materials and 315℃ for other filler materials.

4. PWHT for EN24 steel is usually carried out at temperatures between 593℃ and 677℃ for a period of time governed by the thickness of the material.

5. Researchers have established that conventional steel materials can be welded successfully by applying specific welding procedures and consumables. In austenitic weld deposits, Cr, Mo, Si and Nb promote formation of delta-ferrite which greatly reduces the cracking tendency. In some steels, cracking can be avoided without preheat provided filler materials with hydrogen less than 5ml per 100g of deposited weld are used.

Experimental parameters have been drawn from this summary to come up with a methodology to study effects of PWHT on the microstructure and mechanical properties of En 24T and EN24A steel welded with low hydrogen austenitic electrodes.

CHAPTER 3

EXPERIMENTAL METHODOLOGY`

3.1 Introduction

The aim of this study was to characterize and compare the effects of PWHT on microstructure of HAZ in EN24A steel and EN24T steel after welding with low hydrogen austenitic electrodes. Additionally the effect of PWHT on impact properties of HAZ and tensile properties of multi-pass welded EN24T and EN24A steel were investigated. Experiments were carried out to collect data for UTS, elongation, hardness and Microstructure in multi-pass welded specimens before and after PWHT. Charpy V- Notch (CVN) Impact energies of the CGHAZ in EN24T steel and annealed EN24 steel were compared and their response to PWHT was investigated. In addition, single pass welding was carried out to fully understand the effect of welding and PWHT on hardness and microstructure of EN24 steel in the two conditions. Special emphasis was laid on effect of PWHT on the morphology of microstructures in the CGHAZ. The details of experimental methodology are presented below:

3.2 Test materials

Low hydrogen austenitic welding electrodes (Type AWS A5.4 E312-17 and of diameter 3.25 mm) used in this study were purchased from the local market. Round stocks of EN24T steel material of diameter 30 mm were also bought from the local market in Nairobi.

Chemical analysis of a sample cut from the EN24T material was carried out on a mass spectrometer MAXx LMF06 located at Numerical Machining Complex Ltd (NMC) metallurgy laboratory. This was done to verify composition against the one cited in literature and product data sheets. Chemical analysis of the weld metal was also carried out on the mass spectrometer.

The round EN24T steel material was milled, in preparation for subsequent operations, into rectangular bars of 15 mm X 20 mm X 153mm on a MAHO 1000 CNC milling machine located in NMC workshops.

The bars were then divided into 2 groups namely group 'T' and group 'A'. Group T materials were welded in as bought (Tempered) condition. Group A materials were annealed and welded in their annealed condition. Further, welded samples from both groups were subjected to post weld heat treatment. For the sake of identification, the samples were coded as follows:

EN24T-S0 EN24Tsteel, single-pass welded and no PWHT

EN24T-S350 EN24T steel, single-pass welded and PWHT at 350℃ for half hour

EN24T-S620 EN24Tsteel, single-pass welded and PWHT at 620℃ for half hour

EN24T-S675 EN24T steel, single-pass welded and PWHT at 675℃ for half hour

EN24T-M0 EN24T steel, multi-pass welded and no PWHT

EN24T-M350 EN24Tsteel, multi-pass welded and PWHT at 350℃ for half hour

EN24T-M620 EN24Tsteel, multi-pass welded and PWHT at 620℃ for half hour

EN24T-M675 EN24T steel, multi-pass welded and PWHT at 675℃ for half hour.

EN24A-S0 EN24A steel, single-pass welded and no PWHT

EN24A-S350 EN24A steel, single-pass welded and PWHT at 350℃ for half hour

EN24A-S620 EN24A steel, single-pass welded and PWHT at 620℃ for half hour

EN24A-S675 EN24A steel, single-pass welded and PWHT at 675℃ for half hour

EN24A-M0 EN24A steel, multi-pass welded and no PWHT

EN24A-M350 EN24A steel, multi-pass welded and PWHT at 350℃ for half hour

EN24A-M620 EN24A steel, multi-pass welded and PWHT at 620℃ for half hour

EN24A-M675 EN24A steel, multi-pass welded and PWHT at 675℃ for half hour

3.2.1 Joint design for multi-pass welding

Sets of three or four bars (20 mm X 15 mm X 153 mm) from each group were tack welded together. The sets were then clamped on a power saw and split midway into two halves. A 45 degree beveling was carried out on one half so that when the two halves are assembled together they form a beveled geometry as shown in Figure 3.1(a). The beveled joint was filled with weld metal (WM) during subsequent multi-pass welding.

3.2.2 Groove for single-pass welding

One bar (20 mm X 15 mm X 153 mm) was selected from group A and another from group T. A 3mm deep groove was milled along the length of each bar using a ball nosed milling cutter as shown in Figure 3.1(b). The groove was filled with WM during subsequent single-pass welding.

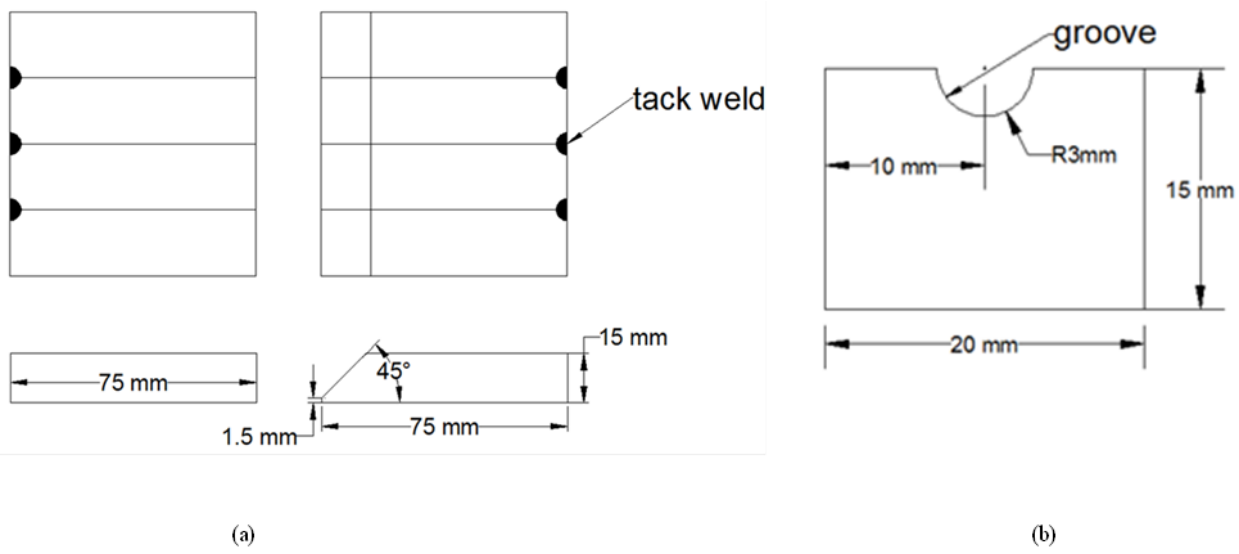

Figure 3.1: (a) Split and beveled bars for multi-pass welding (b) Grooved bar dimensions for single bead welding

3.3 Welding Fixture design

There was need to produce weldments of approximately same level of restraint on all multi-pass welded samples. Therefore, a welding fixture to hold the tacked bars together was designed and fabricated. Welding fixtures are used for holding workpiece in a given position with consistent accuracy during execution of welding. Dimensions of the workpiece played a major role in overall size of the fixture. The sizes of materials used to make the fixture were such that they could withstand the heat generated during welding without being distorted or damaged. Mild steel was the material of choice because it is relatively cheap and electrically conductive to accommodate the welding process [125]. The area of contact between the workpiece and the fixture was designed to be the minimum possible to discourage workpiece distortion while also minimizing loss of heat needed for welding. The other design consideration was the weight of the fixture. The weight was designed to be comfortable for the operator to manipulate it as desired during welding. Figure 3.2 and 3.3 shows the top plate and bottom plate of the fixture. A 3D-rendered drawing of the complete fixture is shown in Figure 3.4.

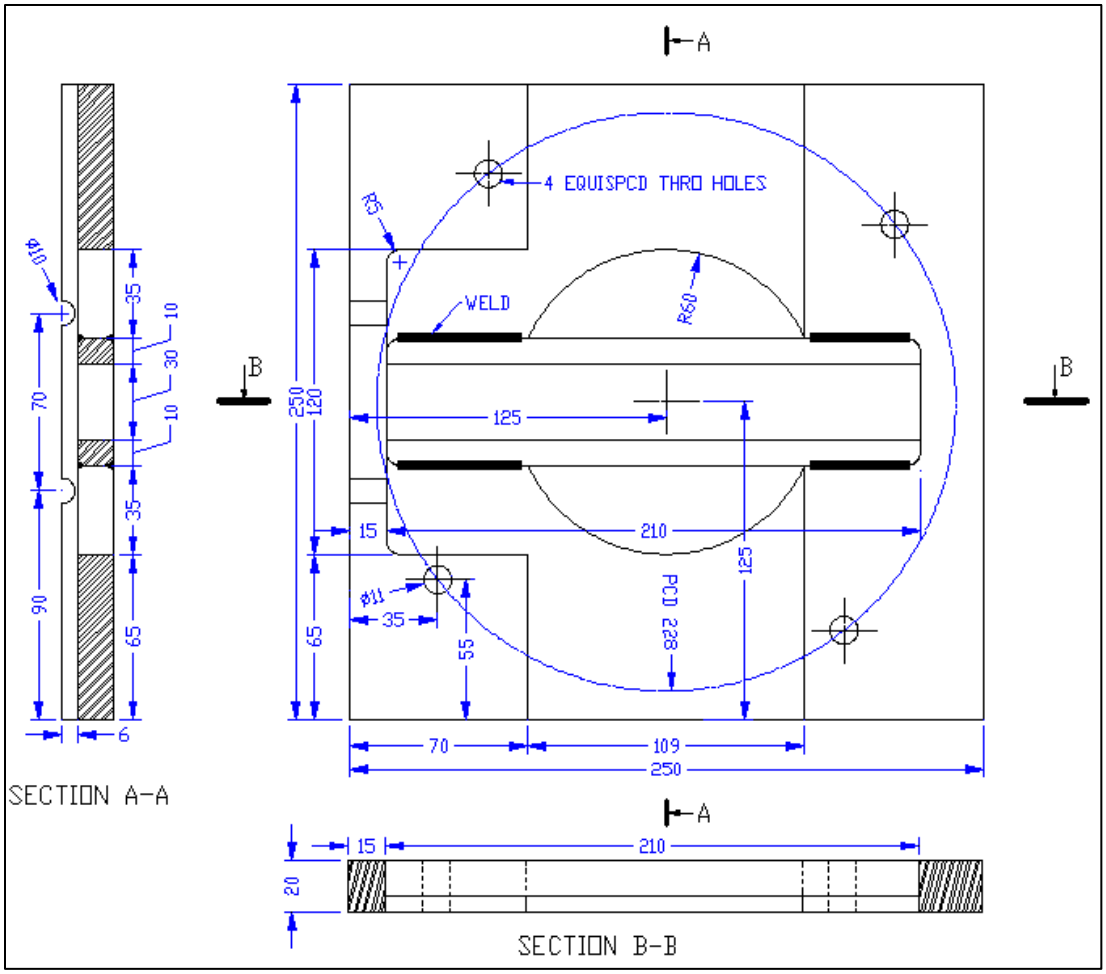

Figure 3.2: Top plate for welding fixture (Dimensions in mm)

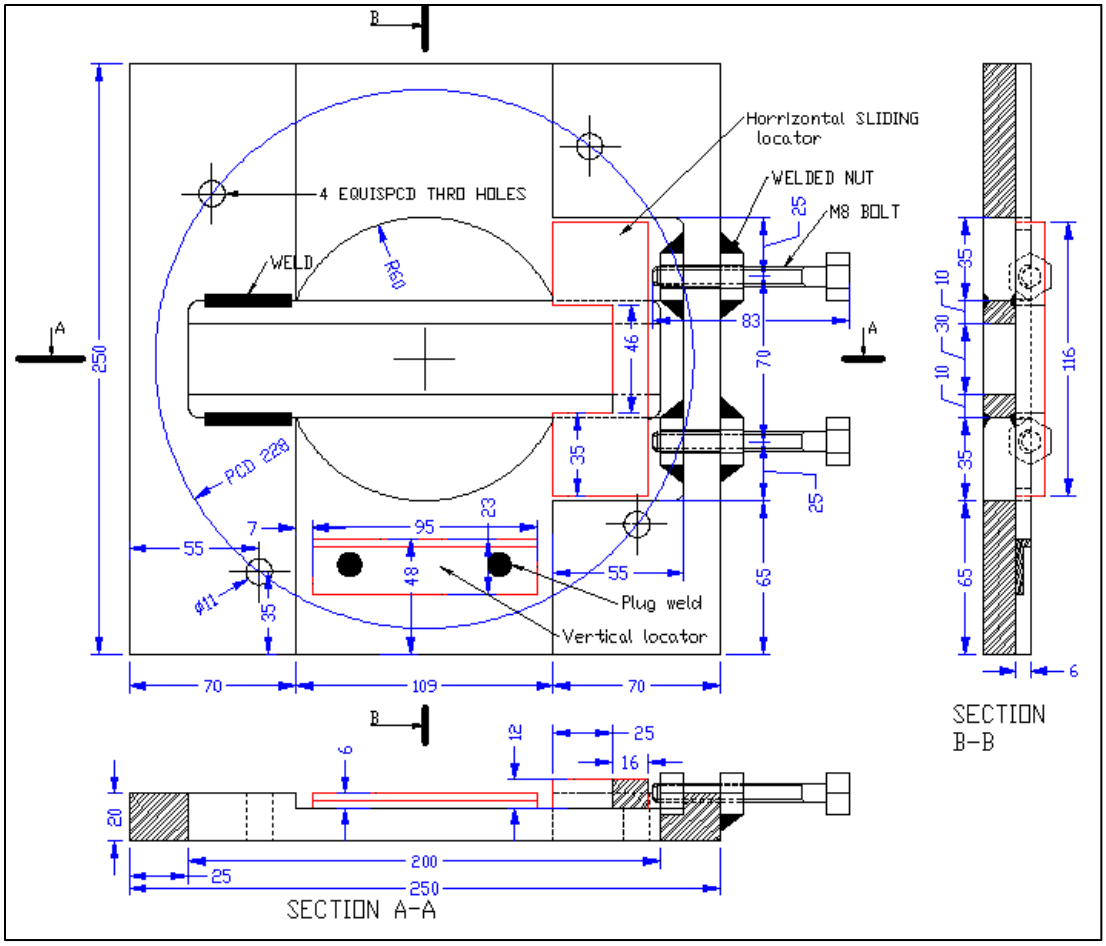

Figure 3.3: Bottom plate assembly (All dimensions in mm)

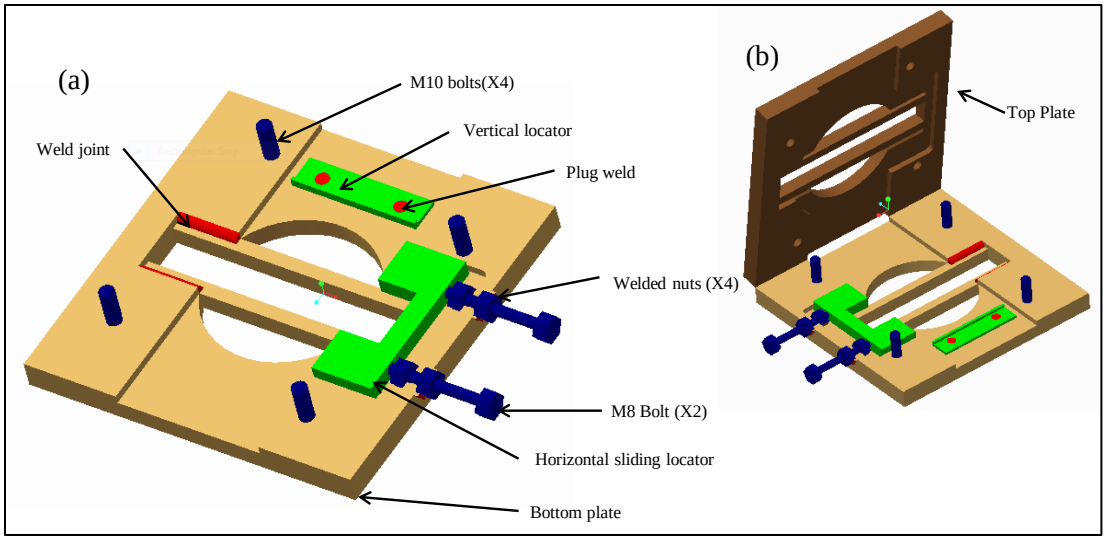

Figure 3.4: 3D-Rendering of welding fixture (a) bottom plate assembly and (b) The complete fixture with top plate opened

3.4 **Fabrication of welding fixture**

The fixture shown in Figure 3.5 was fabricated at Kenya Industrial Research and Development Institute (KIRDI) according to design drawings. Plates for its construction were cut from standard mild steel stock size of 25 mm thick. The plates were machined on a milling machine. Round features on the fixture were drilled and the center hole was bored on a four jaw chuck lathe. Sideway stoppers were welded at predetermined locations. Standard bolts were fitted on nuts welded on bottom plate. Clamping bolts were designed to exert horizontal pressure on the workpiece to ensure they remained in a fixed horizontal location during welding. The top plate was designed to apply pressure on workpiece and ensure they remained in a fixed position during welding and also ensure minimum distortion. The central hole was made large to ensure minimum loss of welding heat.

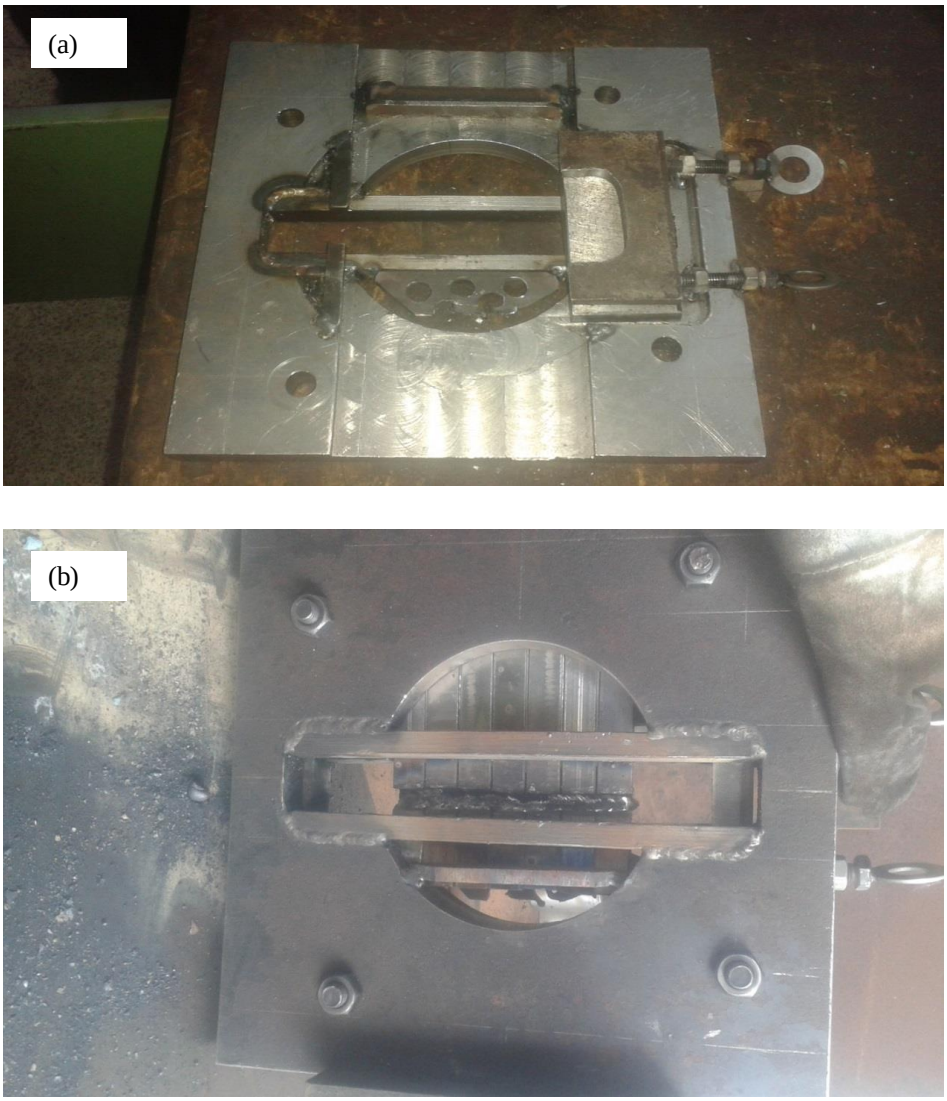

Figure 3.5: (a) Bottom plate of welding fixture and (b) welded bars clamped in fixture

3.5 Annealing procedure

Annealing was carried out on Group 'A' steel bars using Carbolite furnace type ELF 11/6B located in KIRDI laboratories. The furnace was switched on and temperature set to 400℃. Time was allowed for the furnace to attain the set temperature and then group 'A' steel bars were placed inside the heating chamber. The bars were allowed to soak heat at that temperature for half an hour in order to homogenize their temperature. Temperature was then raised to 844℃.

The temperature of the bars gradually increased and they were allowed to soak heat at 844℃ for another half hour. This was done to ensure a uniform austenite phase throughout the materials. The furnace was then switched off and the bars were allowed to cool down in the furnace to room temperature. The room temperature throughout this study was approximately 27℃.

3.6 Preheat and Welding

Since low hydrogen austenitic welding rods were used in this study, a pre-heat of 288℃ was chosen [74]. Preheating was carried out on Carbolite furnace type ELF 11/6B. All bars were preheated for 30 minutes (since they are approximately half inch thick) prior to welding them.

3.6.1 Energy generated during welding

The welding current (I) on arc welding machine Model No.BX1-400F-3 was adjusted to 150 Amperes. Other welding parameters were as follows:

- Welding voltage (V) = 32V
- Welding speed (v) = 160mm per minute
- Electrode feed rate = 4.9mm per second

In manual welding, the welding speed and electrode feed rate depends on experience of the welder [64]. Based on the welding parameters, the calculated heat input during the welding operation was found to be 1.08 kJ/ mm (calculated from equation 2.6 in section 2.2.2).

3.6.2 Single-pass welding

A continuous single bead of weld was carried out on grooved bars. The bars were left to cool down in air to room temperature before subjecting them to PWHT. After PWHT and on cooling down to room temperature, samples for hardness and microstructure analysis were extracted from the middle region shown in Figure3.6

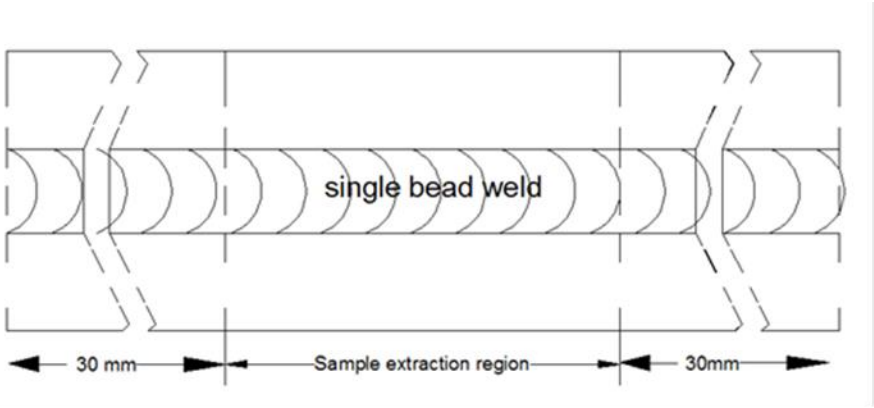

Figure 3.6: Single pass weld on grooved bar

3.6.3 Multi-pass welding

Tacked bars from group A and group T were successively inserted between two fixture plates shown in Figure 3.5. A root gap of approximately 3 mm was set on the beveled joint and bolt clamping pressure was applied to ensure that no movement of the bars occurred during welding. The beveled joint was then filled with weld metal in five welding passes. Slag was removed and weld metal surface thoroughly cleaned with wire brush between passes. Inter-pass temperature of 288 ℃ (+40℃) [74] was maintained by appropriately delaying the welding between passes. The inter-pass weld metal temperature was monitored using infra-red thermometer model MAJORTECH MT695.

After multi-pass welding, the bars were allowed to cool down to approximately 150℃ while still clamped on fixture. The bars were then removed from the fixture and left to cool down to room temperature before Post weld Heat Treatment. The uniform restraint on all multi-pass welded samples resulted in significant elimination of warping of welded bars (Figure 3.7).

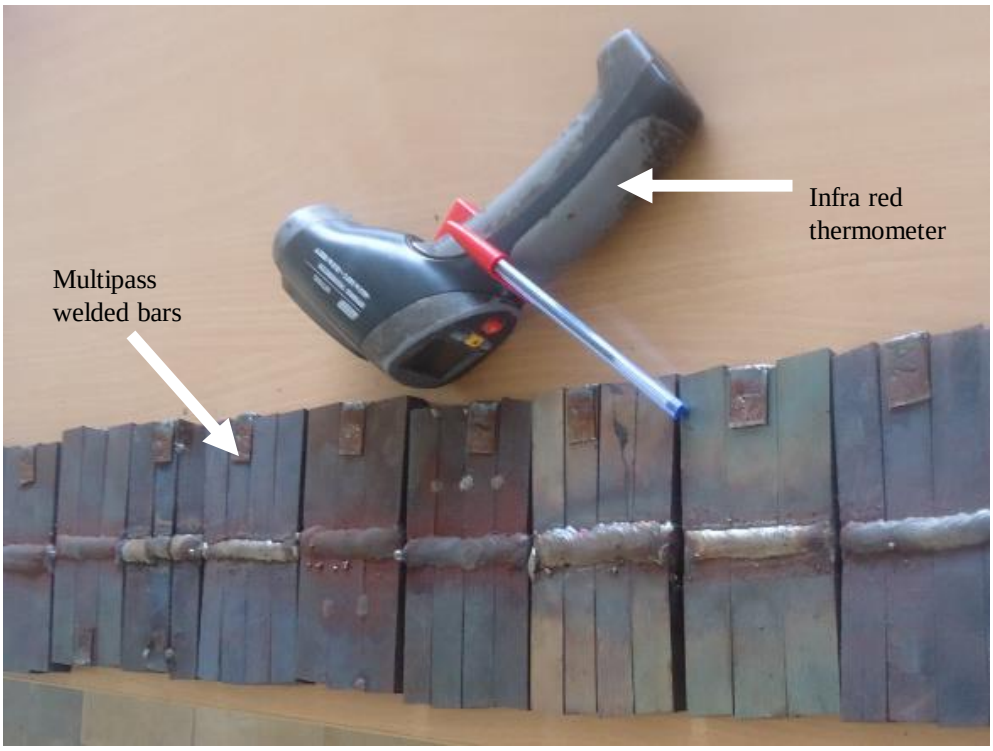

Figure 3.7: Multi-pass welded bars

3.6.4 Post Weld Heat Treatment (PWHT) parameters

Welded bars were subjected to PWHT after the last welding pass and on cooling down to room temperature. PWHT was carried out in a Carbolite furnace type ELF 11/6B. The bars were allowed to soak heat for half an hour at designated PWHT temperature and then removed to cool in air to room temperature. The PWHT temperatures selected for this study were 350℃, 620℃ and 675℃. Tempering at 350℃ is known to cause embrittlement of EN24 steel and this PWHT temperature was selected solely to find its effect on welded EN24A and EN24T steel. 620℃ lie within the recommended PWHT temperature and 675℃ is about the maximum recommended PWHT temperature for EN24 steel.

3.7 Non-Destructive Testing

The welded joints were inspected for flaws using ultrasonic test according to ASME V Standard and X- Ray radiography according to ASME V and IX or ISO 17636-1. Ultrasonic tests were carried out on welded coupons in the Non Destructive Testing (NDT) laboratory of the Institute of Nuclear Science, University of Nairobi. The same coupons were again inspected with X-ray at the NDT laboratory of Kenya Bureau of Standards.

Figure 3.8 (a) shows the ultrasonic equipment and Figure 3.8(b) shows the X ray tube used for Non-Destructive tests on multi-pass welded EN24 steel bars.

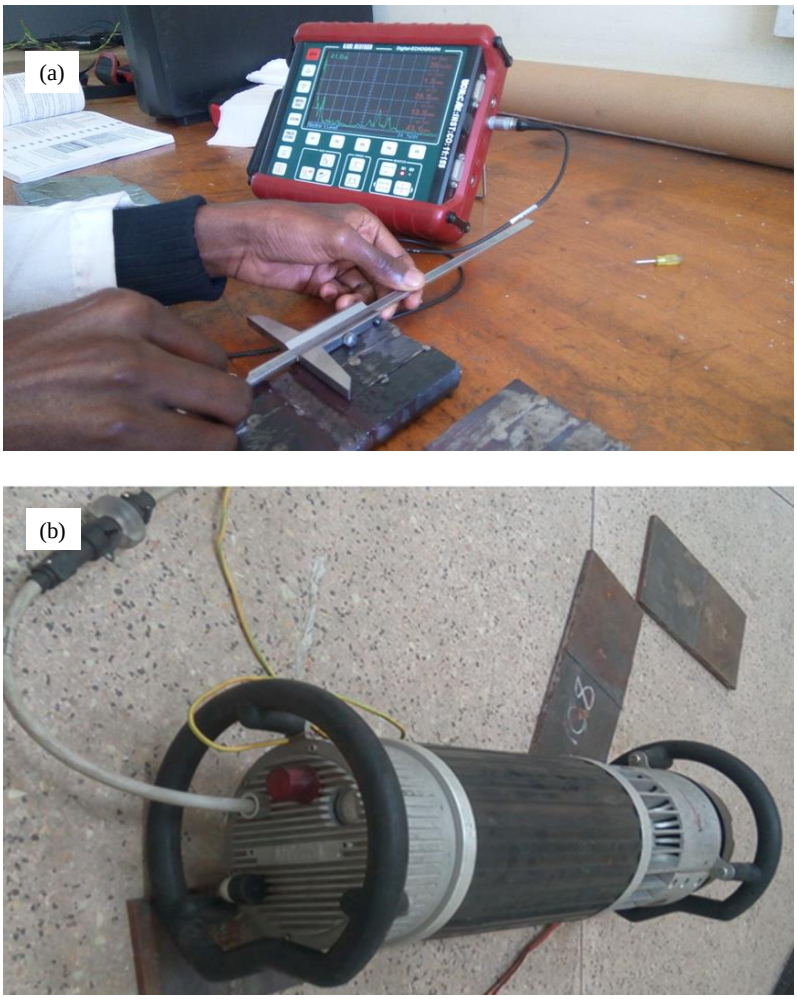

Figure 3.8: (a) Karl Deutsch Digital Echograph 1090 used in ultrasonic inspection and (b) Portable X-Ray tube YXLON Y SMART300HP used in radiographic inspection

3.8 Hardness test

Samples for hardness tests were sectioned from welded bars before and after PWHT. There was need to reveal the fusion boundary between weld metal and HAZ so that it can be used as reference during hardness measurements. To achieve this, a surface grinder was used to grind the surface transverse to weld direction under copious amount of coolant. Fine grinding was then carried out using silicon carbide papers of increasing grit size (180, 320, 400, 600 and 800) mounted on a flat surface. A rotary polishing machine and 1 micron diamond paste was then

used to polish the specimens to mirror finish. 100ml of Nital etchant was then prepared by adding 2 ml of nitric acid to 98ml of ethanol at ambient temperature. The samples were etched by dipping them in a beaker of nital for 10 seconds to reveal the fusion boundary.

Hardness tests were carried out on a Vicker's hardness tester model LECO LV800AT, shown in Figure 3.9, located at University of Nairobi metallurgy laboratory. The Machine is fitted with a diamond indenter. Indentation load was set to 98.07 N and loading time was set to 15 seconds. The test specimen was placed on the stage of the testing machine and focusing (by manipulating the Z-adjuster) was carried out to bring a sharp image of microstructure and fusion line. Hardness tests were carried out at intervals of 0.6 mm (by manipulating X-adjuster), Figure 3.10, on either side of the fusion line (FL) according to ASTM E92 Standard. This was continued until there was no significant change in value of hardness. The generated data was used to plot a hardness profile.

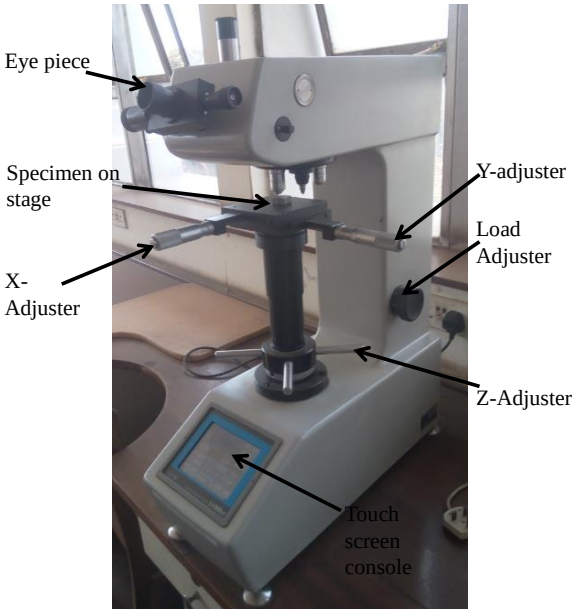

Figure 3.9: LECO LV800AT hardness tester

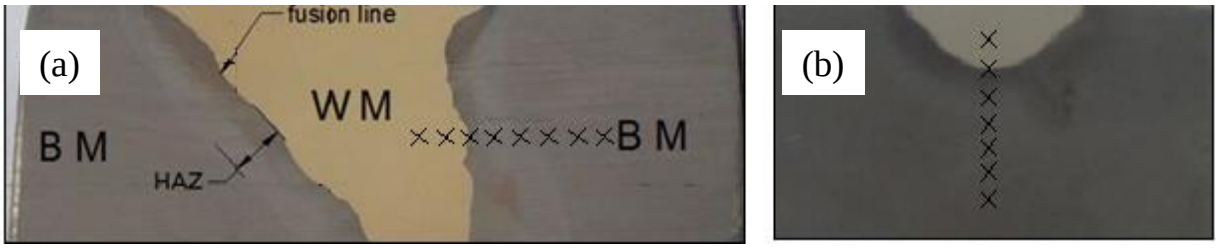

Figure 3.10: (a) Multi-pass and (b) single-pass weldment showing the fusion line (FL).The FL was used as reference line for hardness measurements at positions X

3.9 Tensile tests

Tensile tests were performed on an INSTRON universal hydraulic tensile testing machine, Figure 3.11 (a) located at the Masinde Muliro University of Science and Technology.

Standard specimen for tensile strength were extracted and tested according to ISO 6892-1 standard tensile test on round metallic specimen at room temperature. Tensile tests were performed on transversely welded tensile test specimens with heterogeneous sections that included weld metal, HAZ and base metal. The dimensions of the standard specimen used for tensile testing are given in Figure 3.12. Gauge length was marked on specimens before carrying out the tensile test. Four specimens were used for each PWHT condition giving four data points from which an average value was obtained. After breaking the tensile test specimens, the two pieces were reassembled and the new gauge length obtained. The % elongation (or ductility) was calculated.

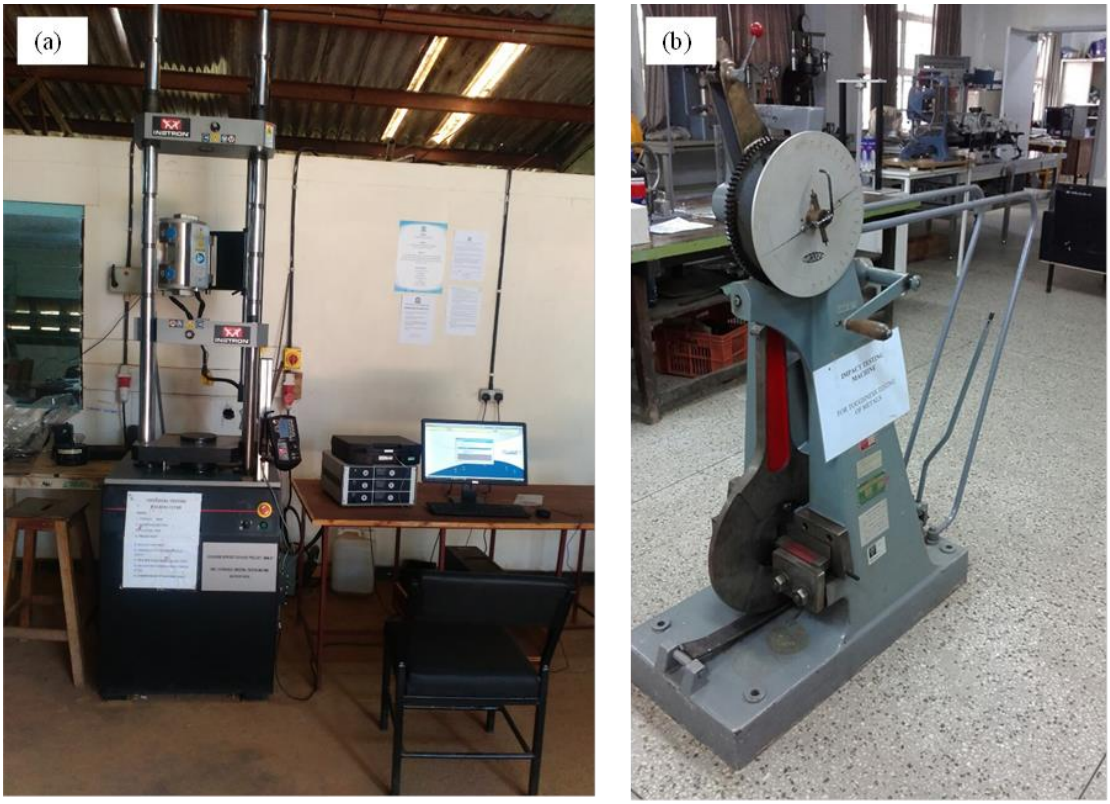

Figure 3.11: (a) INSTRON universal hydraulic tensile testing machine and (b) Charpy V-Notch impact tester

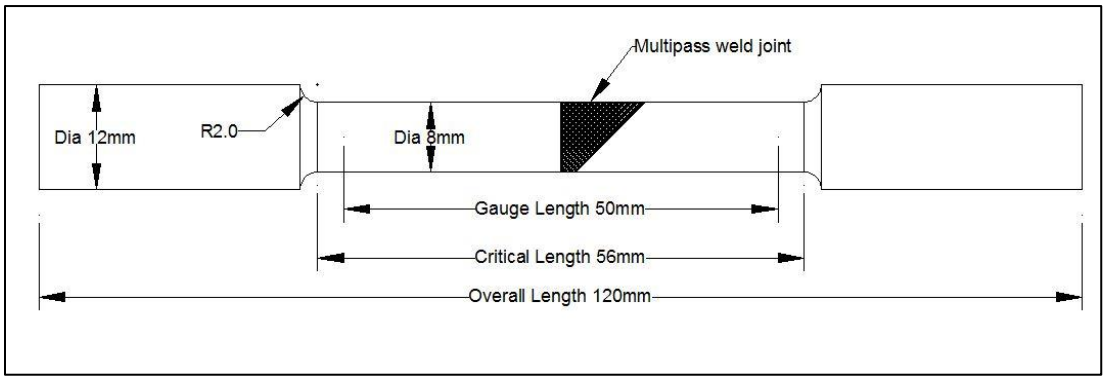

Figure 3.12: Standard transverse weld tensile test specimen

3.10 Impact tests

Impact test specimens were extracted from welded samples and machined by shaping and surface grinding to square sections of 10 mm X 10 mm X 80 mm with the weld joint located approximately midway along the length. Nital was applied on the specimens near the weld joint in order to reveal the fusion boundary. V-notches were located in the hardest region of the HAZ as shown in Figure 3.13.

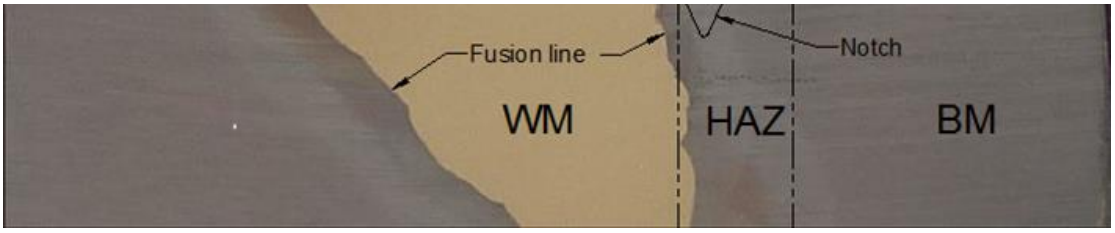

Figure 3.13: Notch location in the hardest region of HAZ

With the notch as reference, the samples were then sized to 10mm X 10mm X 55mm in accordance to ASTM E-23 or ISO 148-1. Room temperature Impact testing was performed on notched specimens using a conventional Torsee's Charpy impact testing machine, Figure 3.11 (b), located at Jomo Kenyatta University of agriculture and Technology. The technical parameters of the impact tester were as follows: hammer weight 25.71kg, length of hammer arm 0.75m and hammer lift angle 142.5˚. Four impact specimens were used for each PWHT condition giving four data points from which an average value was obtained.

3.11 **Microstructure Characterization**

Microscopy specimens were extracted from welded bars before and after PWHT. The surfaces were ground and then polished. Fine grinding was carried out progressively using finer abrasives of silicon carbide papers from 180 grit, 320, 400, 600, 800 then polishing was carried out with

diamond paste at 6 micron and finally 1 micron. The surfaces were cleaned then etched with Nital (2ml of nitric acid in 98ml of absolute alcohol) for the HAZ and BM microstructure according to ASTM E407-07. Villella's reagent consisting of 95 ml of ethyl alcohol, 5 ml of hydrochloric acid, and 1 g of picric acid was used for the austenitic weld metal. Microstructure analysis through optical microscopy was carried out on etched specimens. The Olympus BX41M-LED optical microscope, Figure 3.14, located in Jomo Kenyatta University of Agriculture and Technology metallurgical laboratory was used to obtain digital images of the micrographs. Besides the scale bar, the digital image display for this microscope is equipped with X and Y scales graduated in micrometers. Distances from fusion line to any feature on the image can be measured accurately on the image display.

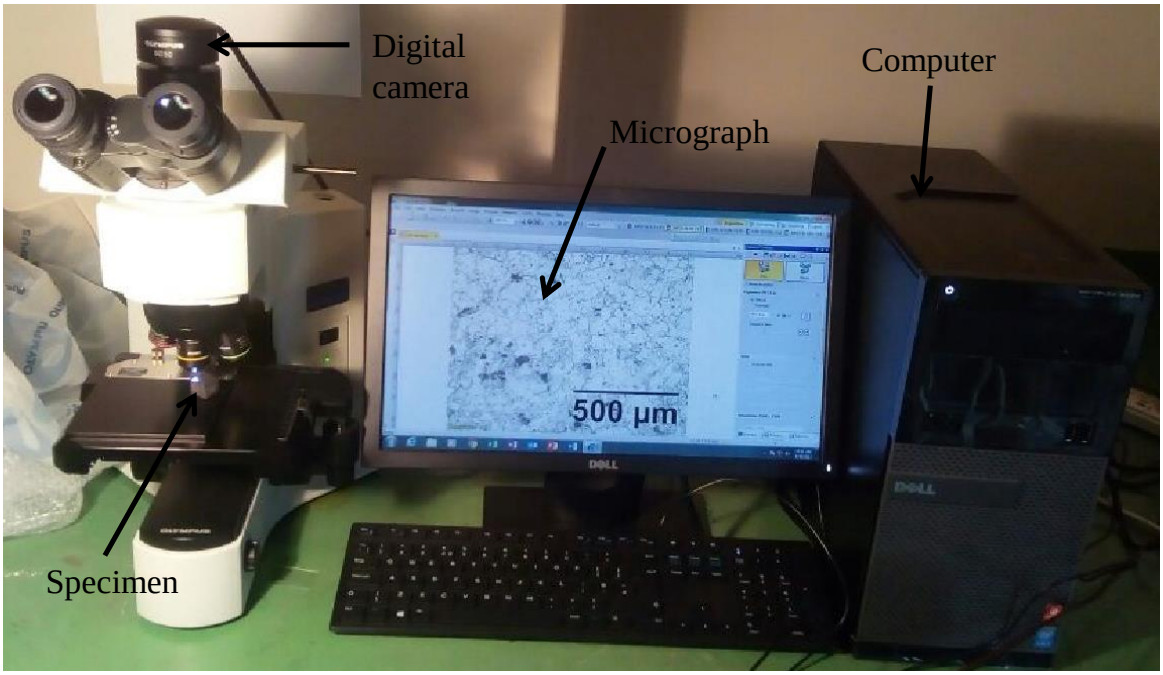

Figure 3.14: Olympus BX41M-LED Optical Metallurgical laboratory microscope

CHAPTER FOUR

RESULTS

4.1 Introduction

The peak temperature and cooling rate at different locations of HAZ produced differing microstructure across the weldment. Generally, PWHT tended to temper the hardness of microstructure leading to improvement in impact properties. Detailed results for this study are presented in sections 4.2 to 4.7.

4.2 Chemical composition and properties of test materials.

A sample of EN24T steel and a multi-pass welded joint were tested at four locations to determine the chemical compositions. The average results (table 4.1) show that Carbon and Molybdenum content of the weld metal is significantly lower than that of EN24Tsteel. The composition of Nickel, Chromium and Vanadium is significantly higher in the weld metal than in EN24T Steel. Additionally, small amount of Copper and traces of Antimony are found in EN24T steel and weld metal.

Table 4.1: Chemical composition of EN24 steel and weld metal AWS A5.4 E312-17

	Chemical composition (wt. %)											
Material	C	Ni	Cr	V	Mo	Si	Mn	S	P	Cu	Sb	Fe
EN24 Steel	0.43	1.52	0.95	0.006	0.23	0.18	0.53	0.005	0.008	0.068	<0.002	Bal.
A5.4 E312-17	0.143	8.57	25.47	0.059	0.040	0.603	0.88	0.005	0.004	0.040	<0.002	Bal.

The results of mechanical properties of EN24T, EN24A steel and the weld metal are shown in Table 4.2. Three specimens were tested for each property and the average values and standard Deviations were calculated. The results show that annealing of EN24T steel leads to a considerable increase in toughness (168%). The hardness of weld metal is approximately equal to the hardness of EN24A steel. The UTS and elongation of AWS A5.9ER312 welding material was not measured but it is cited by manufacturers as 752 MPa and 25% respectively and impact energy for austenitic weld metal cited as a minimum of 30J [8, 63].The measured value of impact energy of weld metal (76.6 J) indicate that it is tougher than EN24T steel.

Table 4.2: Properties of EN24 steel and austenitic weld metal AWS A5.4 E312-17

Test Material	Property	Test 1	Test 2	Test 3	Average	Standard Deviation
En24T Steel	UTS (Mpa)	979.0	1057.0	1010.0	1015.3	32.1
	% Elongation	14.0	13.0	13.0	13.3	0.5
	CVN Impact Energy (J)	40.7	38.4	40.7	39.9	1.1
	Hardness (HV10)	329.6	328.4	326.2	328.0	1.4
En24A Steel	UTS (Mpa)	1095.0	880.0	1051.0	1008.7	92.7
	% Elongation	14.0	15.0	15.0	14.7	0.5
	CVN Impact Energy (J)	110.1	112.9	110.1	111.0	1.3
	Hardness (HV10)	233.1	233.0	233.0	233.0	0.1
AWS A5.4 E312-17(Weld Metal)	CVN Impact Energy (J)	73.9	82.1	73.9	76.6	3.9
	Hardness (HV10)	235.0	235.7	237.1	235.9	0.9

4.3 Welding and NDT test

Welded bars of EN24T and EN24A steel were subjected to two radiographic tests and one Ultrasonic test. The first X-Ray and Ultrasonic tests on welded bars showed lack of root fusion a distance of between 1 and 2 mm from the bottom surface. These defects were removed during

subsequent machining that was carried out to extract test specimens. A second confirmatory X-ray radiograph (Figure 4.1a and 4.1 b) on extracted specimen, before machining to final size, showed acceptance level of more than 90% on all weld joints [see appendix A]. Slight warping was observed on unconstrained welded bars (Figure 4.1c). Warping was caused by weld metal shrinkage during solidification. Warping tendency was significantly reduced by constraining bars in a welding fixture before welding (Figure 3.7 in section 3.6.3).

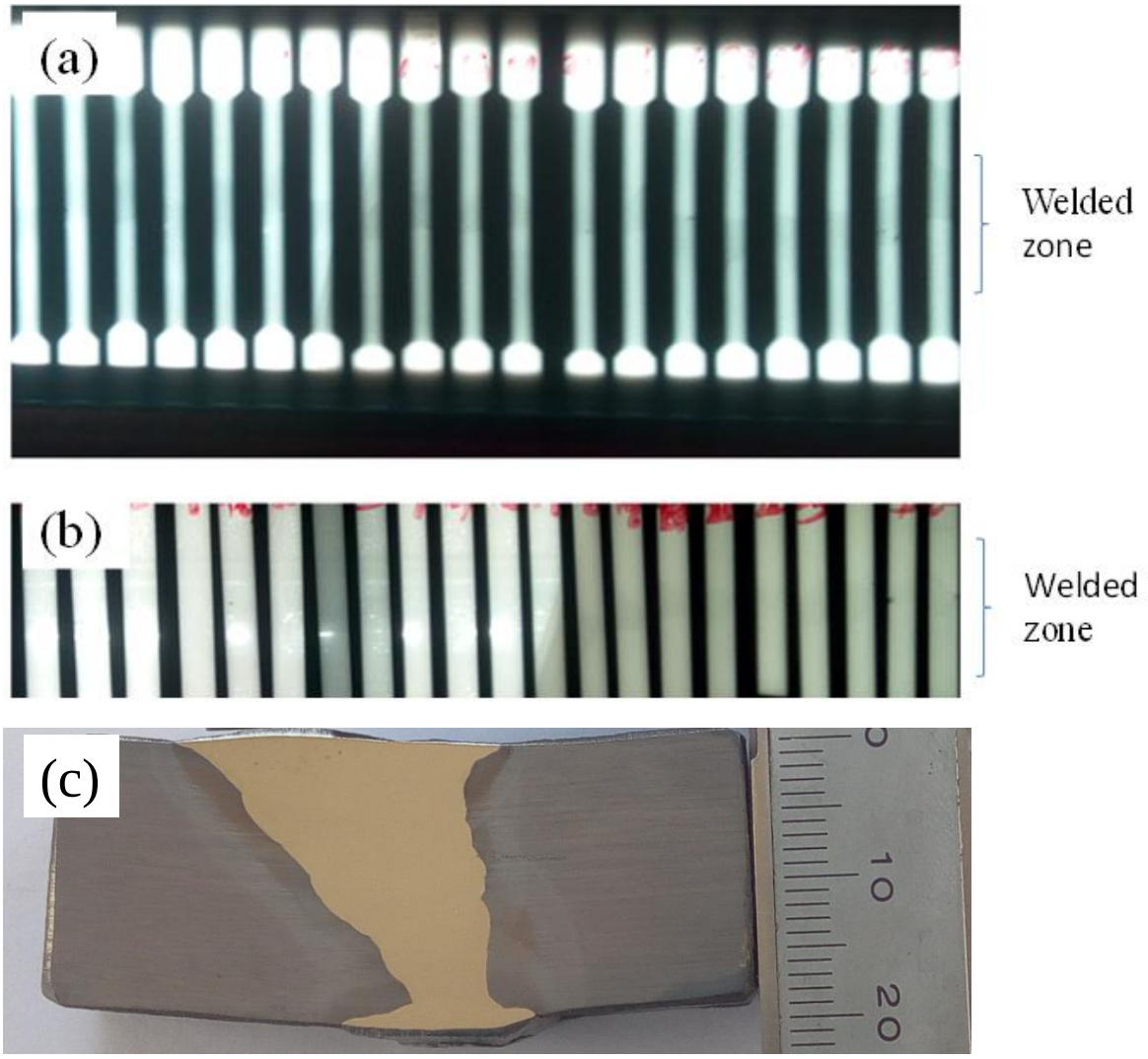

Figure 4.1 Radiographs of some multi-pass weld joints of (a) tensile test bars, (b) Impact energy test bars and (c) A macrograph for unconstrained welded joint

4.4 Microstructures

Base metal microstructure of EN24T steel before welding was found to consist of tempered martensite while EN24A steel consisted of pearlite colonies in a matrix of ferrite (Figure 4.2). Effect of PWHT on the CGHAZ in welded EN24T and EN24A steels are presented in Figures 4.3-4.6. In single pass welded EN24T steel, martensite with small patches of bainite before PWHT transformed to bainite and tempered martensite after PWHT at 350℃. Finally a mixture of ferrite and carbides was observed after PWHT at 620 and 675℃ (Figure 4.3). In single pass welded EN24A steel (Figure 4.4), the micrographs consisted of martensite before PWHT, tempered martensite/allotriomorphic ferrite after PWHT at 350℃ and ferrite/pockets of carbide precipitates in ferrite after PWHT at 620 and 675℃. Multi-pass welded EN24T (Figure 4.5) consisted of bainite before PWHT, mixture of bainite/ferrite/fine carbides after PWHT at 350 and 620℃. Lastly a mixture of ferrite and globular cementite is observed after PWHT at 675℃. Multi-pass welded EN24A (Figure 4.6) consisted of fine bainite before PWHT, course granulated bainite/retained austenite after PWHT at 350℃ and a mixture of ferrite/fine carbide precipitates after PWHT at 620 and 675℃. PWHT was found to have effects on the base metal microstructure in EN24T steel. The BM microstructure transformed from tempered martensite to a mixture globular cementite/ferrite/tempered martensite after PWHT at 675℃ (Figure 4.7). No effect was observed on the BM microstructure in EN24A steel (Figure 4.8). The weld metal (WM) structure comprising chiefly of skeletal delta ferrite in a plain austenite matrix was unaffected by PWHT (Figure 4.9). A fusion boundary of thickness between 20 and 40 microns was found to be separating the weld metal from the heat affected zone.

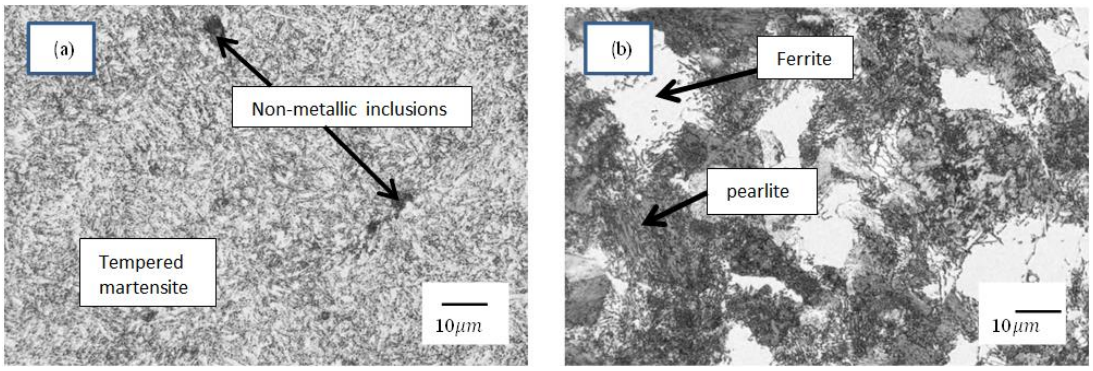

Figure 4.2: Micrographs for (a) EN24T steel and (b) EN24A steel base metals

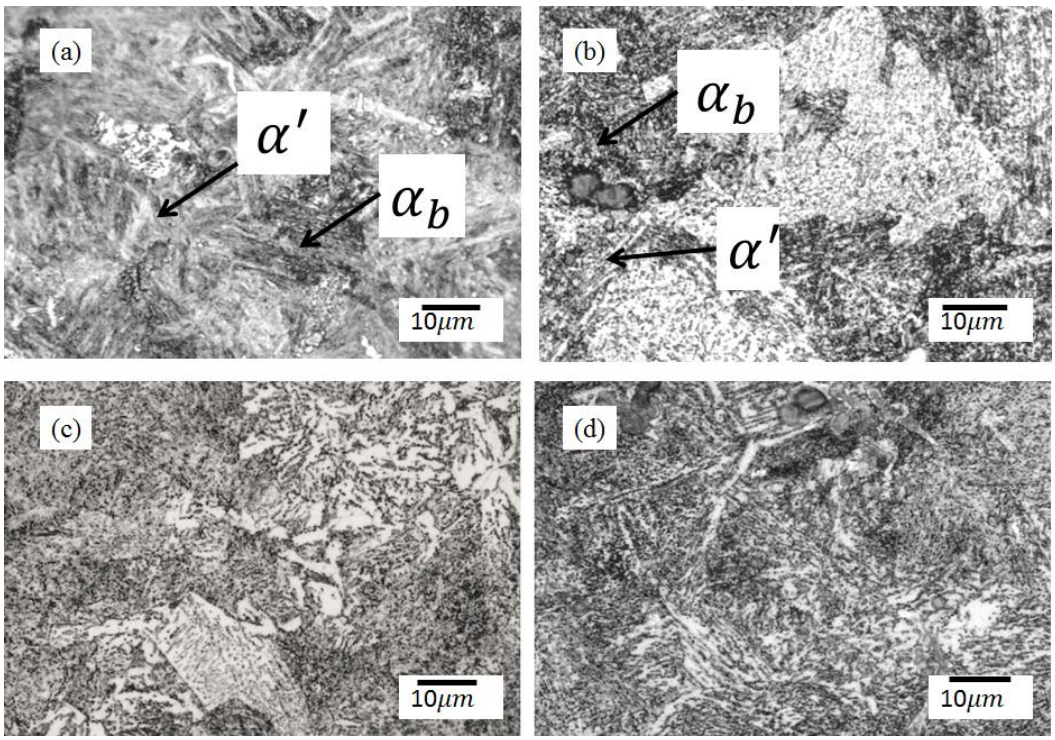

Figure 4.3: Micrographs for CGHAZ in single pass welded EN24T steel (a) before PWHT (b) PWHT at 350℃, (c) PWHT at 620℃, and (d) PWHT at 675℃.

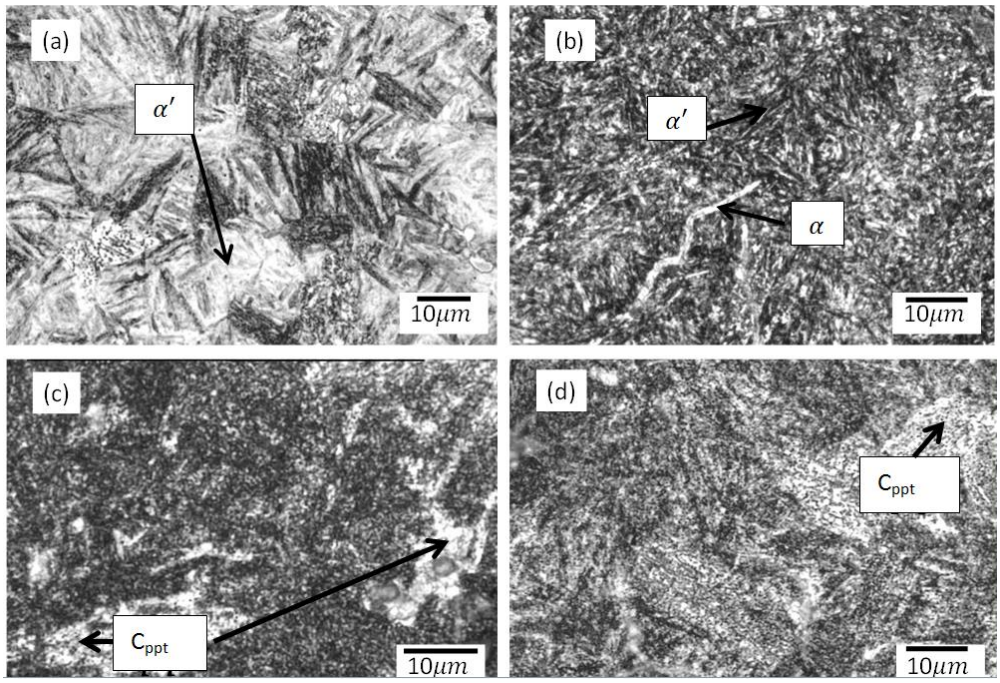

Figure 4.4: Micrographs for CGHAZ in single-pass welded EN24A steel (a) before PWHT (b) PWHT at 350℃, (c) PWHT at 620℃, and (d) PWHT at 675℃.

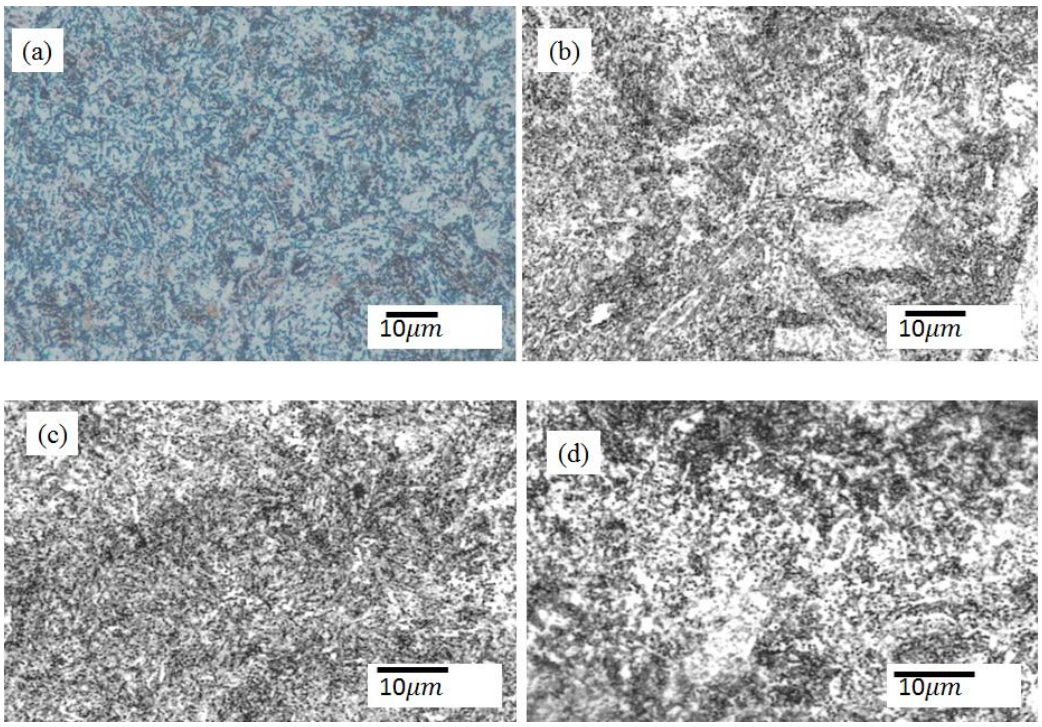

Figure 4.5: Micrographs for CGHAZ in multi-pass welded EN24T steel (a) before PWHT (b) PWHT at 350℃, (c) PWHT at 620℃, and (d) PWHT at 675℃

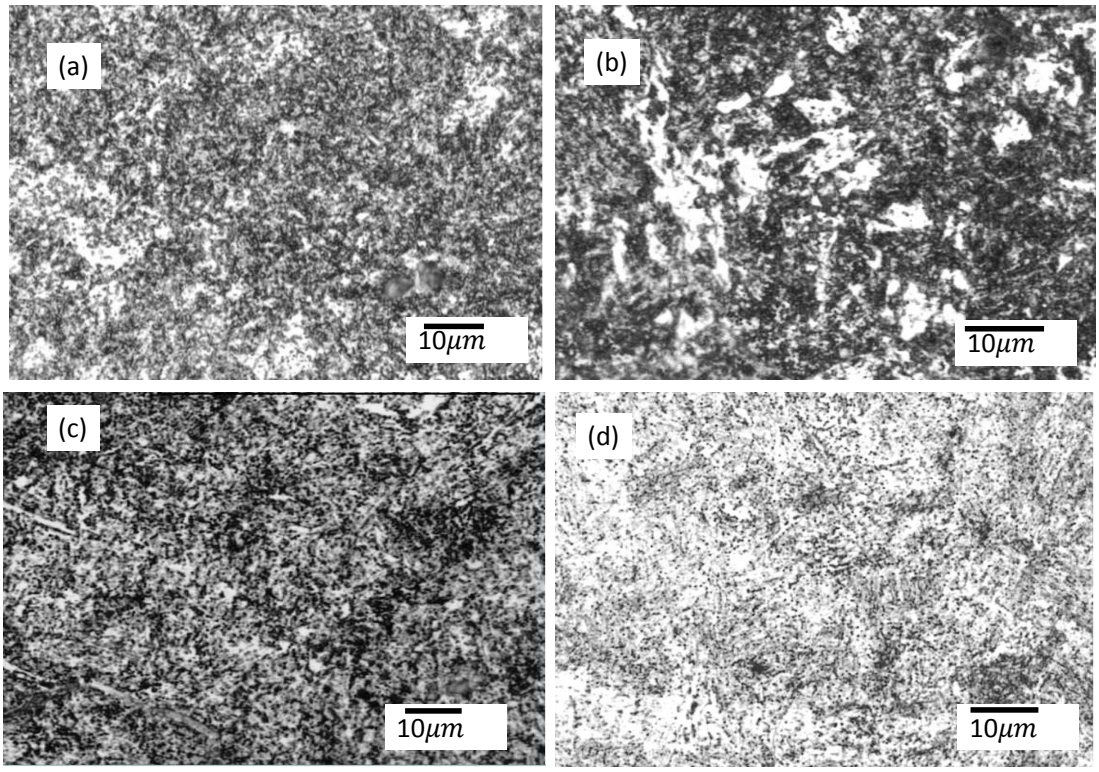

Figure 4.6: Micrographs for CGHAZ in multi-pass welded EN24A steel (a) before PWHT (b) PWHT at 350℃*, (c) PWHT at 620*℃*, and (d) PWHT at 675*℃*.*

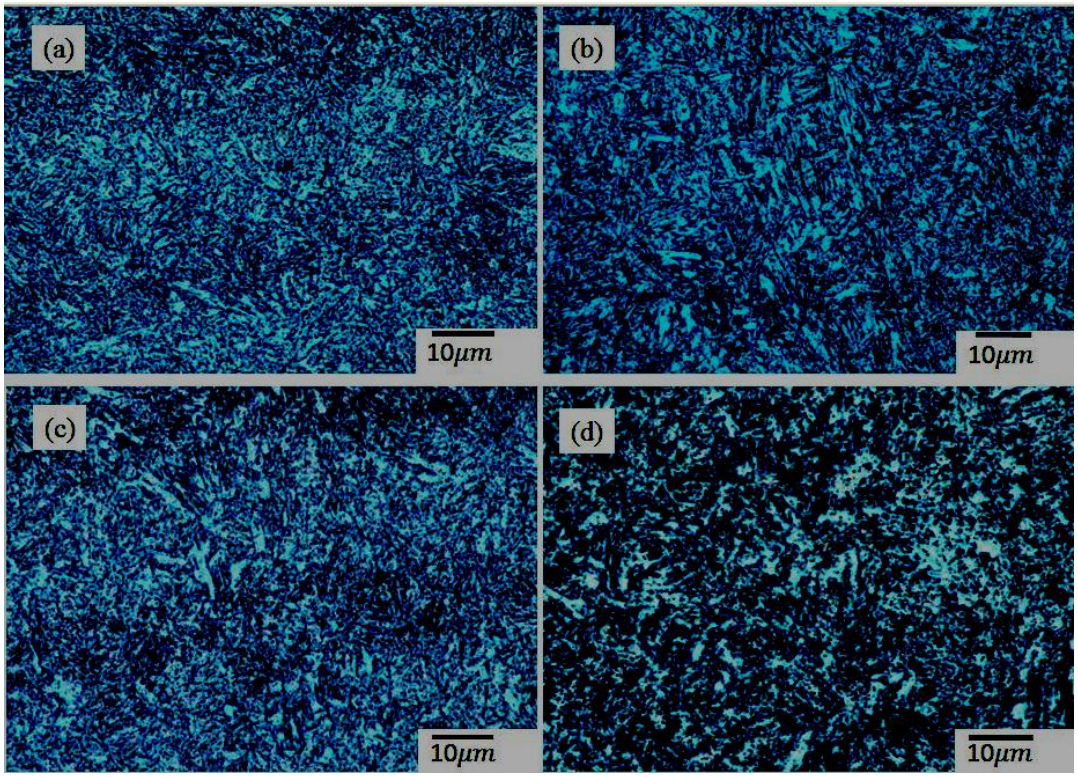

Figure 4.7: Base metal microstructure of multi-pass welded EN24T steel (a) before PWHT (b) PWHT at 350℃, (c) PWHT at 620℃, and (d) PWHT at 675℃

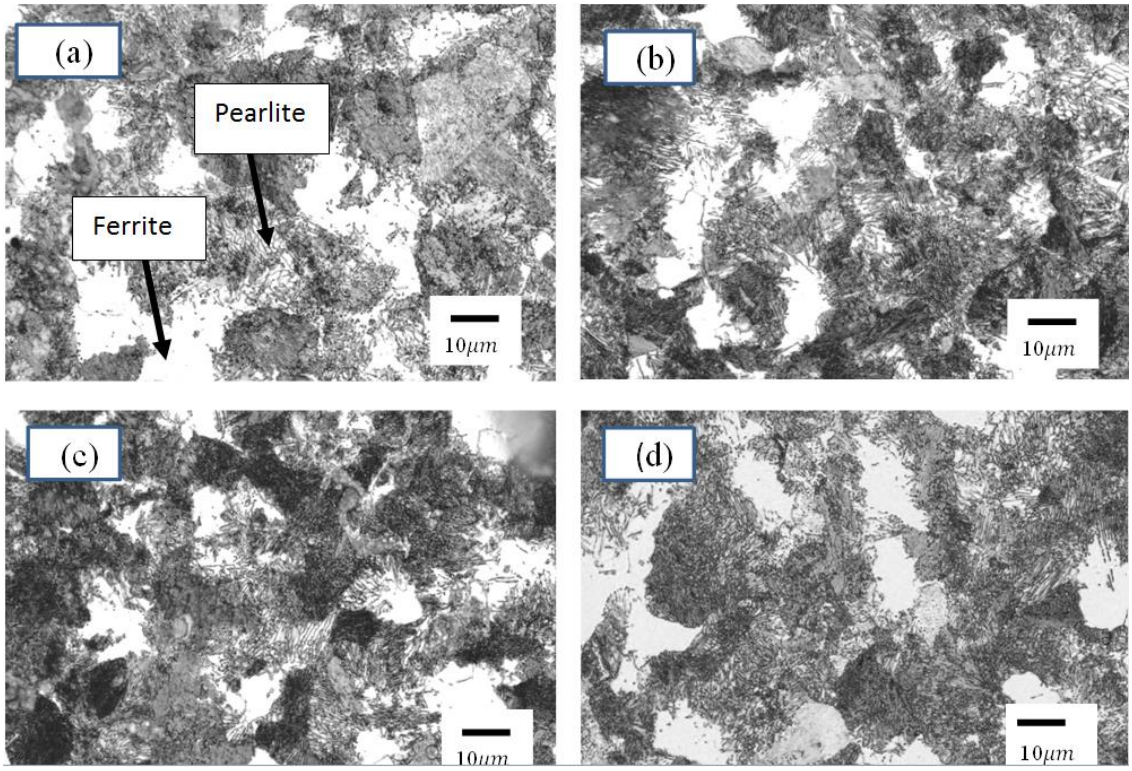

Figure 4.8: Base metal microstructure of multi-pass welded EN24A steel (a) before PWHT (b) PWHT at 350℃, (c) PWHT at 620℃, and (d) PWHT at 675℃.

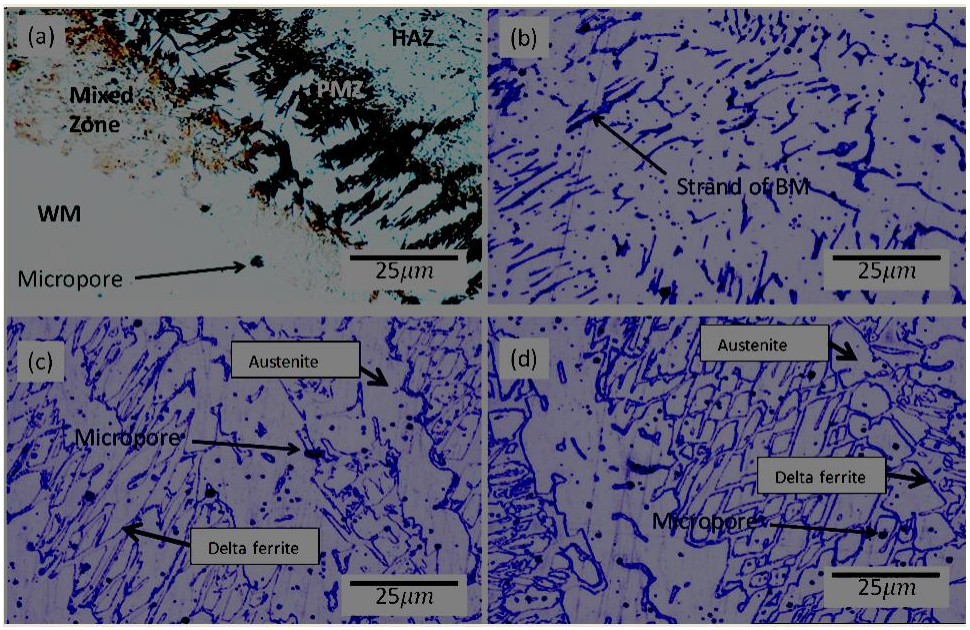

Figure 4.9: Weld metal microstructure (a) Partially melted zone (PMZ) with weld metal (WM) and HAZ on either side, (b) weld metal showing strands of EN24 steel in the weld metal matrix - close to mixed zone /WM interface, (c) body of weld metal before PWHT and (d) weld metal after PWHT at 675℃

4.5 Hardness Survey

Hardness values at various locations and PWHT are presented in Figure 4.10 to Figure 4.14. The hardest region in HAZ of EN24T and EN24A steel was found to be located at 0.6 mm from the fusion line. This region presented the lowest impact toughness and was therefore the most brittle. Generally, PWHT improved toughness values for this region. However, results depict an unusual hardness profile for multi-pass welded EN24A steel when it is subjected to PWHT at 350℃ (Figure 4.11b). Negligible difference in hardness in CGHAZ of EN24T-M was observed at PWHT temperatures 620℃ and 675℃ (Figure 4.12). Base metal hardness of EN24A steel is not affected in any significant way by PWHT, however, the hardness of EN24T steel reduces with

increase in PWHT temperature (Figure 4.13). After PWHT at 675℃ , the hardness of EN24T steel is higher than that of EN24A steel. Weld metal hardness survey reveal that PWHT has no effect on weld metal hardness (Figure 4.14).

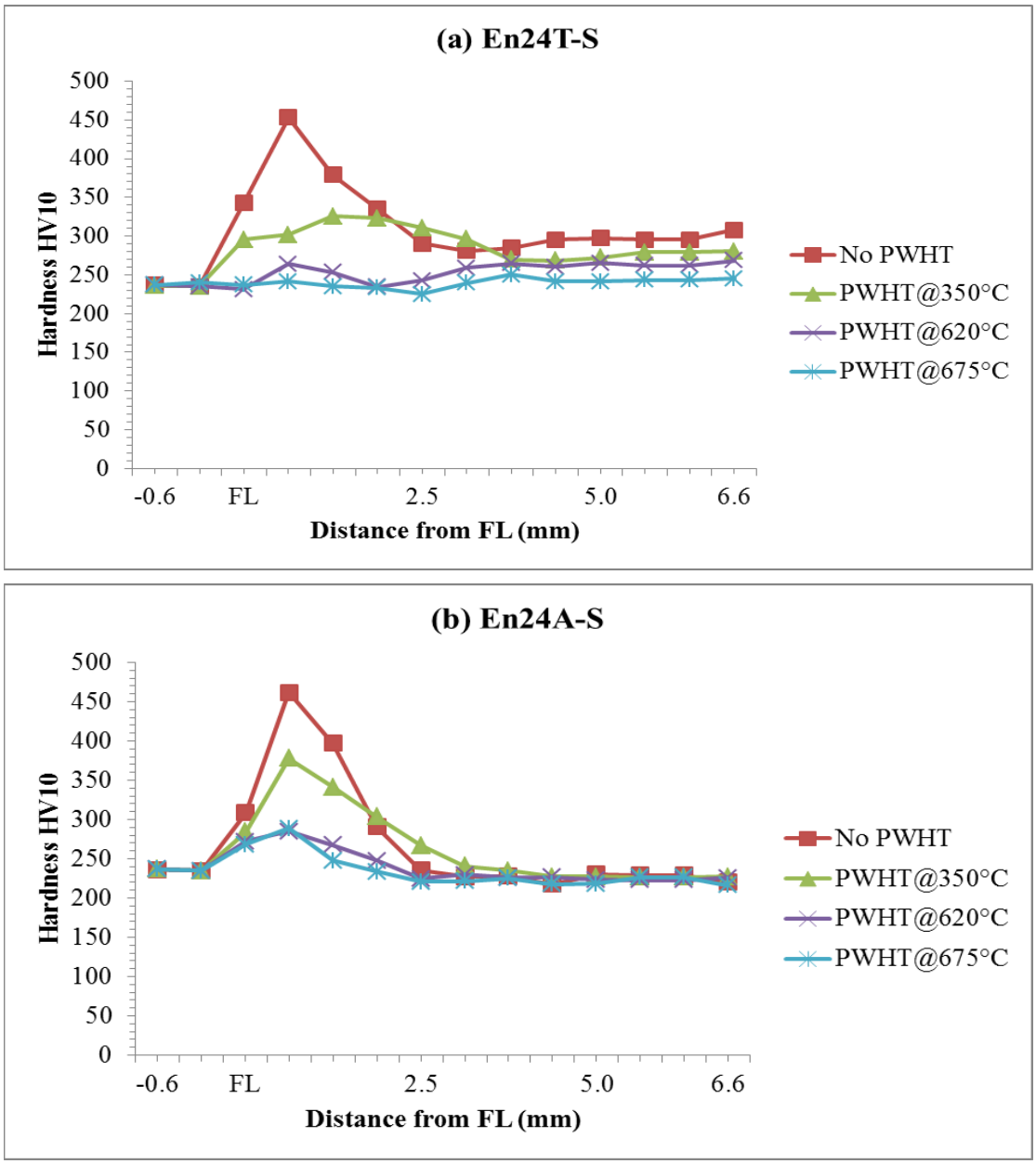

Figure 4.10: Effects of PWHT on the hardness profiles of single-pass welded (a) EN24T and (b) EN24A steel

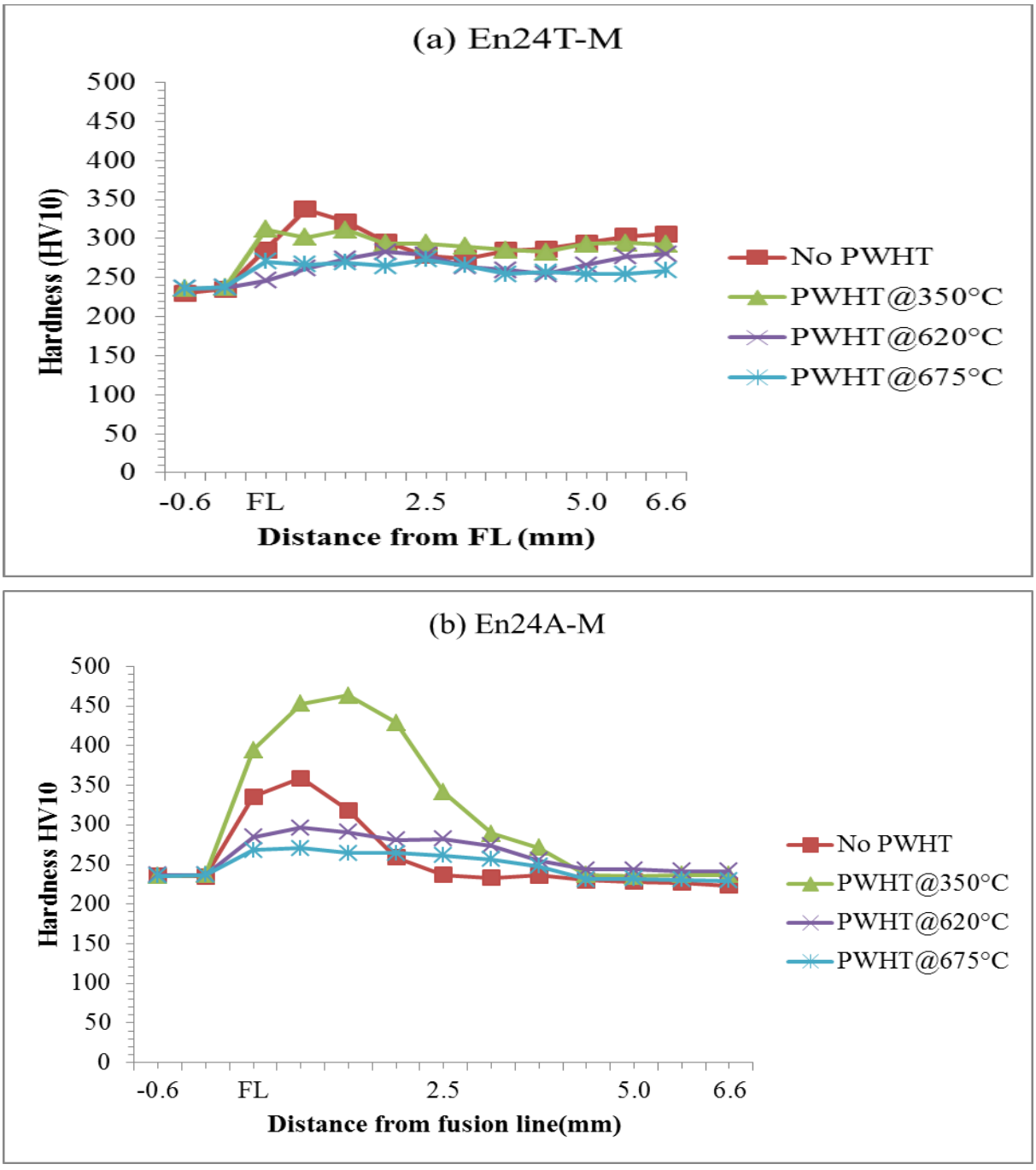

Figure 4.11: Effects of PWHT on the hardness profiles of multi-pass welded (a) EN24T and (b) EN24A steel

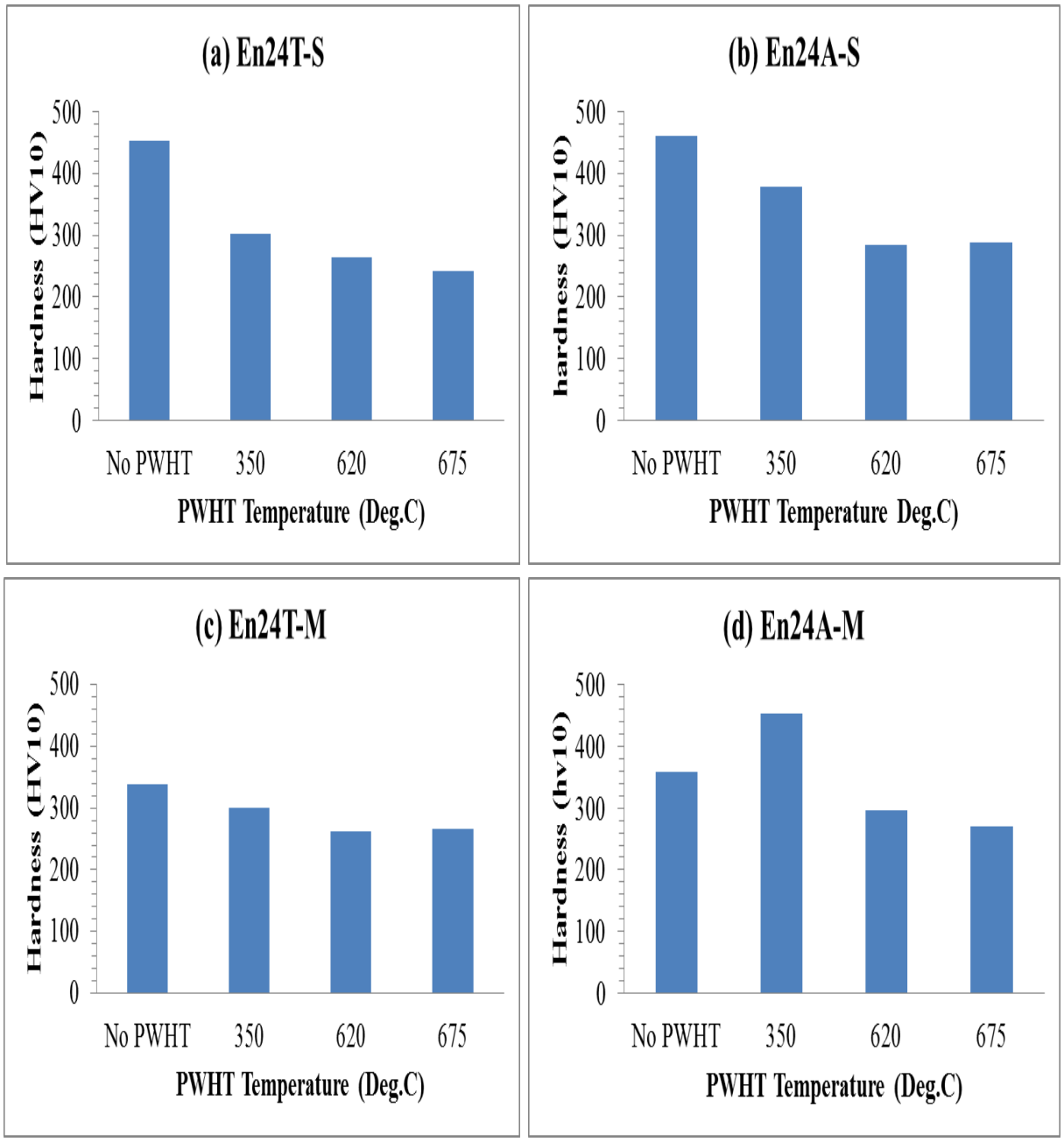

Figure 4.12: Effect of PWHT on hardness of CGHAZ

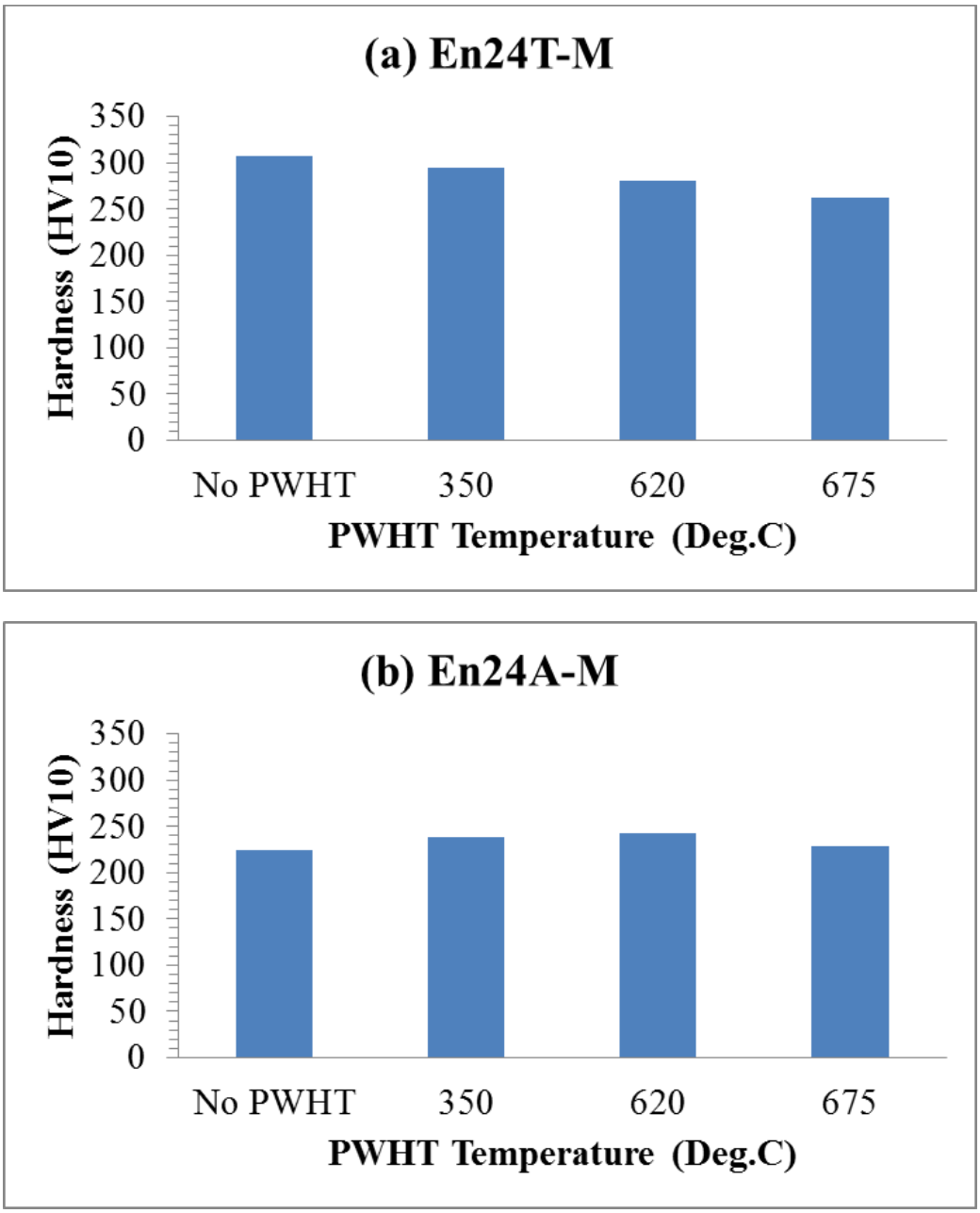

Figure 4.13: Effect of PWHT on hardness of base metal

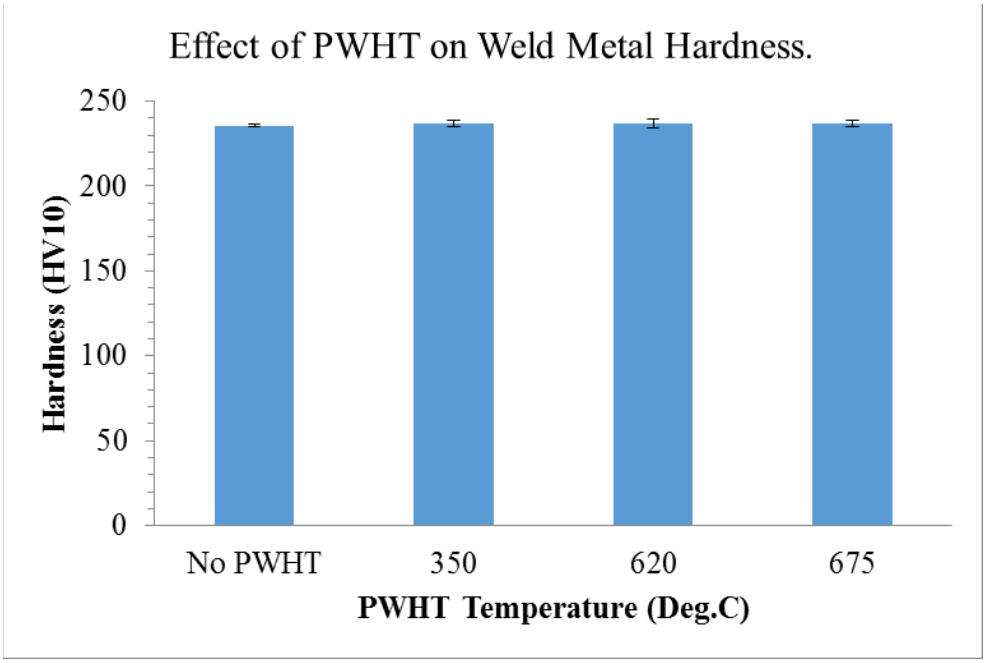

Figure 4.14: Effect of PWHT on hardness of weld metal

4.6 Impact energy tests

The notch on the impact specimen was located at the hardest region approximately 0.6mm from the fusion line of the welded joint (section 3.10). The results of impact test on the hardest region in welded EN24T and EN24A are shown in Figure 4.15. Four specimens were tested for each PWHT temperature and results compared.

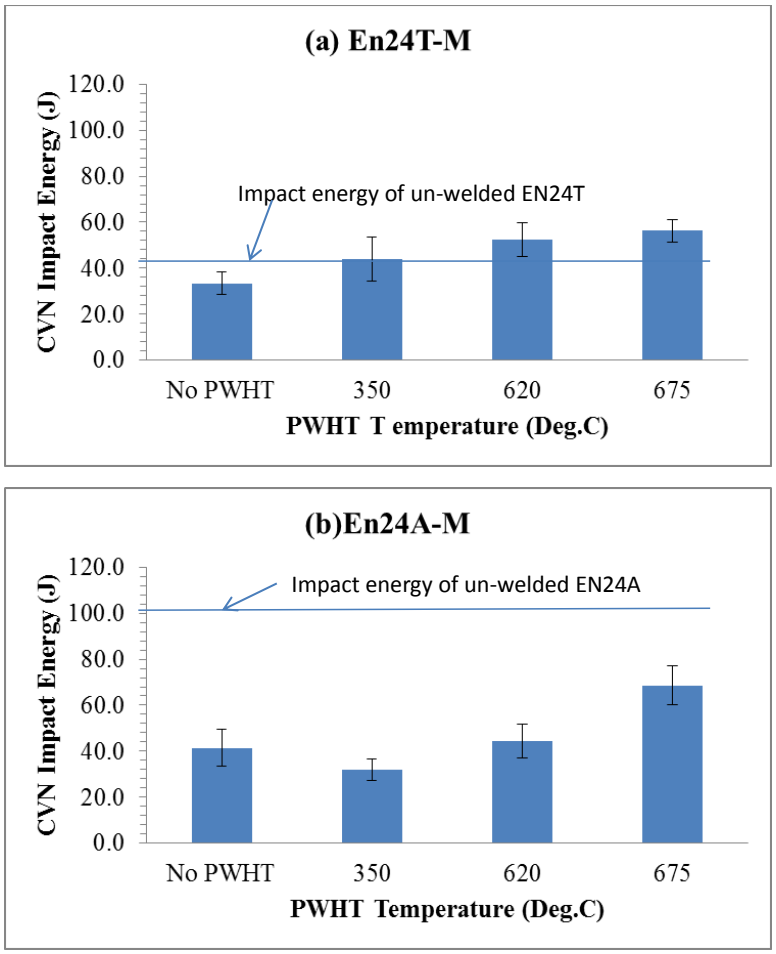

Figure 4.15: Results of impact test in CGHAZ (0.6mm from FL)

4.7 Tensile test

The results of transverse tensile test on multi-pass welded EN24T and EN24A steel are shown in Figures 4.16 and 4.17. Four specimens were tested for each PWHT temperature. Failure in all welded specimens was observed to occur on or near the fusion boundaries. The failure was sudden and with little or no necking-implying brittleness in the material at that location.

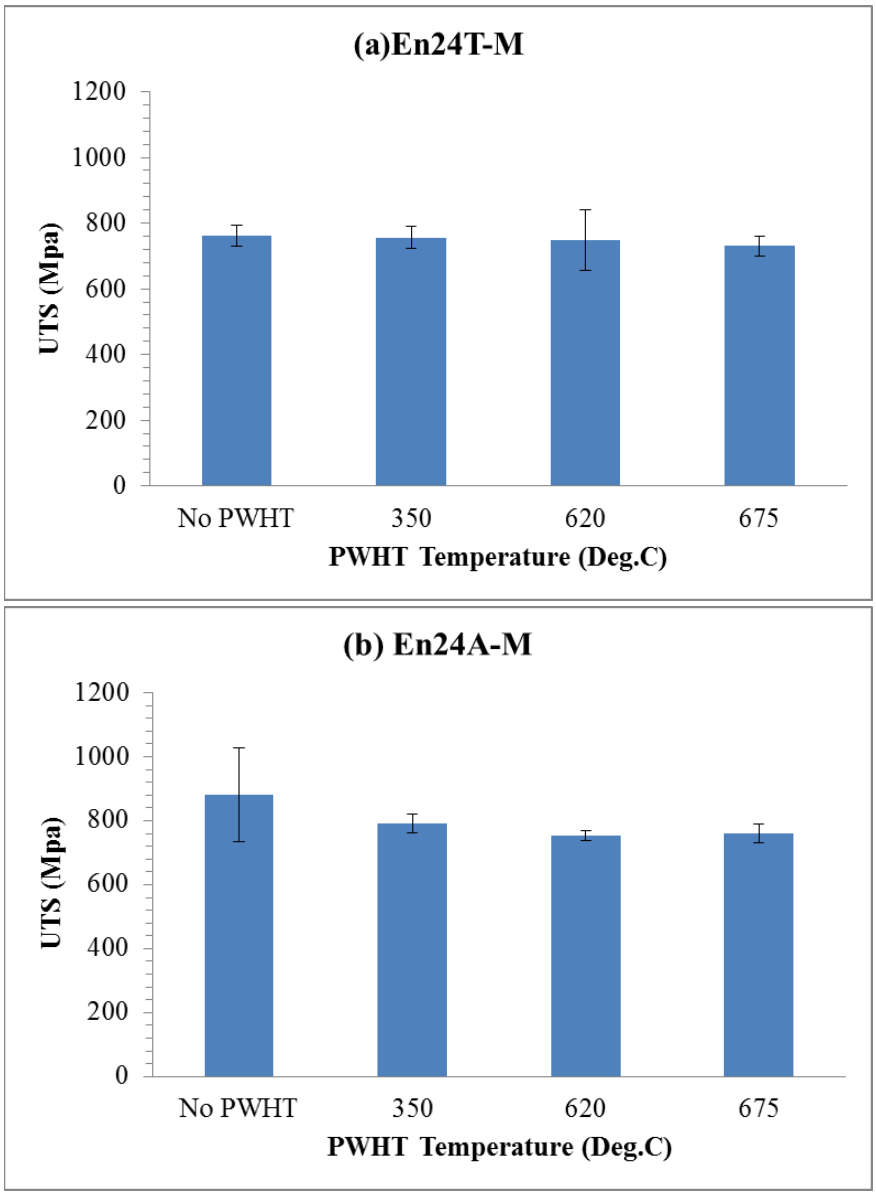

Figure 4.16: Effect of PWHT on tensile strength of welded EN24T and EN24A steel

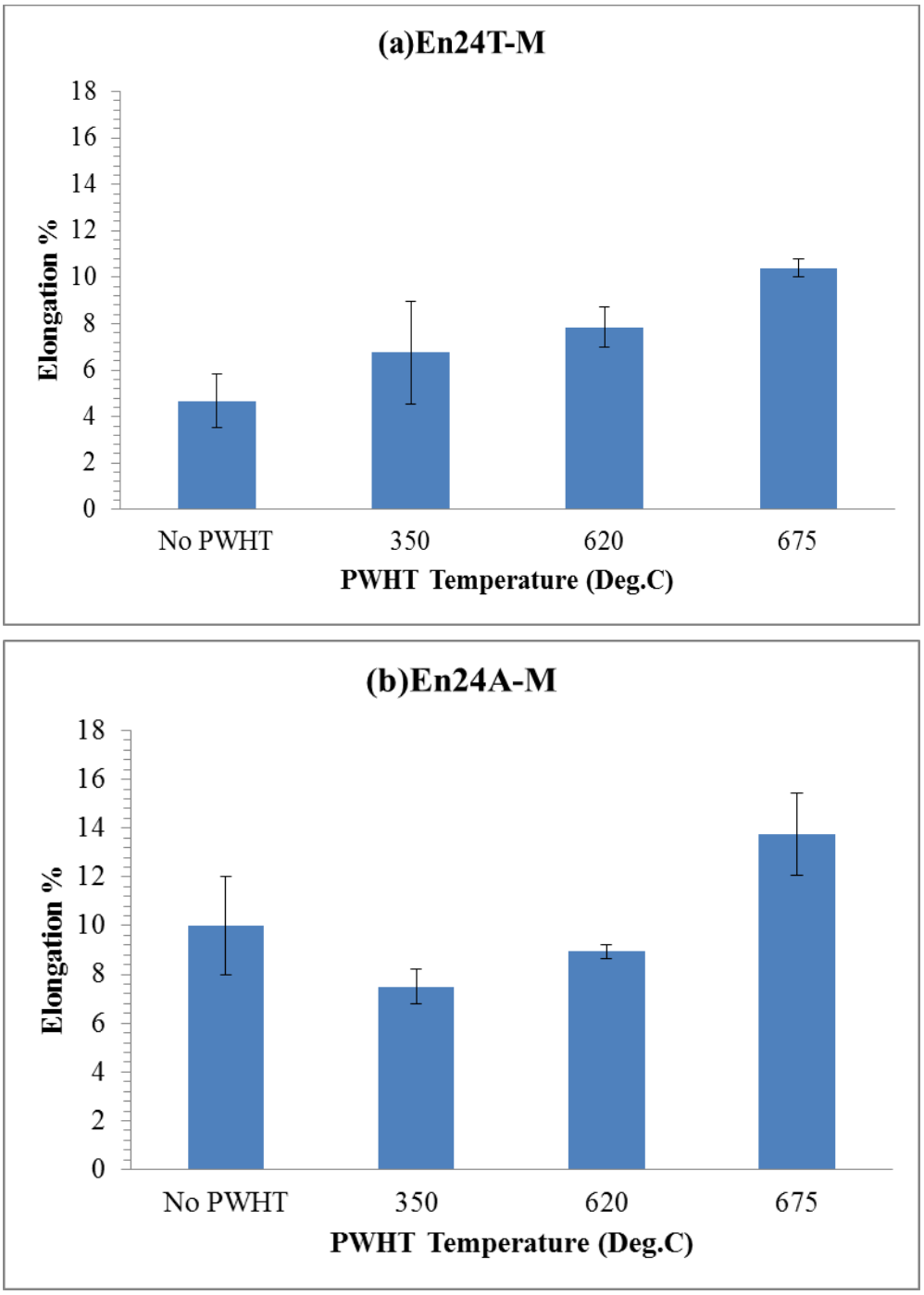

Figure 4.17: Effect of PWHT on elongation of welded EN24T and EN24A steel

CHAPTER FIVE

DISCUSSION

5.1Introduction

PWHT has been observed to cause some differences in microstructure and properties of EN24A and EN24T steel welded with austenitic filler materials. The detailed discussion is presented in sections 5.2 to 5.6.

5.2 Composition and properties of test materials.

The results of chemical composition (Table 4.1) show that amounts of major alloying elements in EN24T steel fall within the composition range cited by other researchers [9, 16, 18, 75]. However, the weight percentage of copper in the base metal was noted to be 0.0681%. Copper is normally added to steel in order to increase corrosion resistance and it is therefore likely to reduce corrosion in the HAZ of welded EN24 steel. Traces of antimony amounted to less than 0.002% (or equivalent to 20 ppm) in EN24T steel and in weld metal. The weight percentage of vanadium was found to be significantly lower at 0.0062% compared to 0.09% declared in EN24 steel product datasheet [9]. Alloy elements in this steel are responsible for low MS temperature [22]. Without them, the MS temperature for steel of equivalent carbon content would be slightly higher. Their presence is responsible for desirable characteristic of high hardness in tempered EN24 steel. All the alloying elements, and to lesser extent, nickel, confer this characteristic. Vanadium is a much stronger carbide former than chromium and molybdenum. It has a great influence on the hardness of tempered martensite [21]. It is known to improve hardenability even when added in low amounts. Effect of vanadium is considered to be due to the formation of an alloy carbide (V_4C_3 or VC), which replaces Fe_3C at high tempering temperatures and persists as a

fine dispersion up to the A1 temperature. However, the effect of vanadium in this steel is lessened due to its very low content. The hardness of tempered martensite in EN24T steel base metal (Figure 4.13) has been observed to reduce from 307 HV before PWHT to 262 HV after PWHT at 675℃. This insignificant reduction in hardness is attributable to retardation to softening conferred by the rest of the alloy elements despite the fact that their influence is not as strong as that of vanadium.

The major contributor of high 'as quenched' hardness in this steel is carbon (0.43%). Carbon increases strength significantly; however, high carbon content and high CE lowers weldability and for this reason EN24 steel is often preheated prior to welding to avoid fast quenching in the HAZ of thick plates [75]. Molybdenum is often added to EN24 steel in order to retard temper embrittlement. Molybdenum levels of 0.23% found in this steel are sufficient to retard embrittlement provided low levels of impurities - sulphur and phosphorus are maintained. From the results of chemical analysis, phosphorous and sulphur content is very low and can be described as trace amounts that exist in steel that are either difficult or expensive to remove completely. The low carbon content (0.143%) in the weld metal has profound effect on its ability to harden during heat treatment; even with high chromium and nickel content the hardenability of the weld metal is compromised. In fact high levels of chromium and nickel in the weld metal yield an austenite/ ferrite microstructure that is resistant to quench hardening. As in the base metal, the levels of sulphur and phosphorous in the weld metal are very low. Even if diffusion occurred across the fusion boundary, with such low level of impurities in both the base metal and the weld metal and also with Molybdenum level of 0.23 % in the base metal, the chances of temper embrittlement in EN24 steel would be low. However, Lim et al [51] reports that traces of impurity elements including sulphur, phosphorous and antimony of the order of a few parts per

million is postulated to cause temper embrittlement in EN24 steel. Therefore, from the results of chemical analysis it can be concluded that a possibility of temper embrittlement exists in EN24 steel when it is subjected to tempering at between 300 and 400℃.

The results of mechanical properties of tested materials (Table 4.2) indicate that the average physical properties of EN24T steel to be UTS 1015 MPa, hardness 328 HV10, elongation 13.3% and CVN impact energy 39.9J. These values are within the range of those cited in literature [9, 14, 16, 17].

5.3 Microstructures

The microstructure of EN24T steel consists of tempered martensite. Annealing process austenitizes the grains and when they cool down slowly to room temperature at cooling rates of the order of 0.02 - 0.006 ℃ /s [23], the microstructure transforms from tempered martensite to colonies of lamellar pearlite in a ferrite matrix. A similar microstructure was reported by Rajesh et al [16]. Therefore, the basic difference between EN24T and EN24A steel is in their microstructures. This is the initial microstructure prior to welding. The changes in the microstructure of the hardest region of the HAZ, base metal and weld metal and their response to PWHT are discussed in sections in 5.3.1 to 5.3.3. The microstructures of base and weld metal are included because they also relate to the tensile properties of welded EN24T and EN24A steels.

5.3.1 Effect of PWHT on the Microstructure of the hardest region

Optical microscopy on the hardest region of single-pass welded materials (Figure 4.3 and Figure 4.4) depicts a martensitic microstructure in both EN24T and EN24A steel before PWHT. The microstructure of this region is determined by the peak temperature attained during the welding cycle. Peak temperatures at various locations of weldment have been studied by researchers [12,

45] and the highest value in the HAZ is found in the immediate vicinity of the fusion line. The high peak temperature in this region activates grain growth leading to a coarse grained zone CGHAZ [86]. This region has typically the highest cooling rate than the rest of the regions in the HAZ. As can be observed in Figure 5.1, the cooling rate from 800 to 500℃ at the fusion line is lower than the cooling rate at a distance of 0.5 mm from the fusion line. From the CCT diagram for EN24 steel (section 2.1.2), the critical cooling rate for formation of martensite is 8.3℃ per second. This means that a cooling rate higher than this is likely to result in a microstructure comprising of martensite or a mixture of martensite and bainite [23].

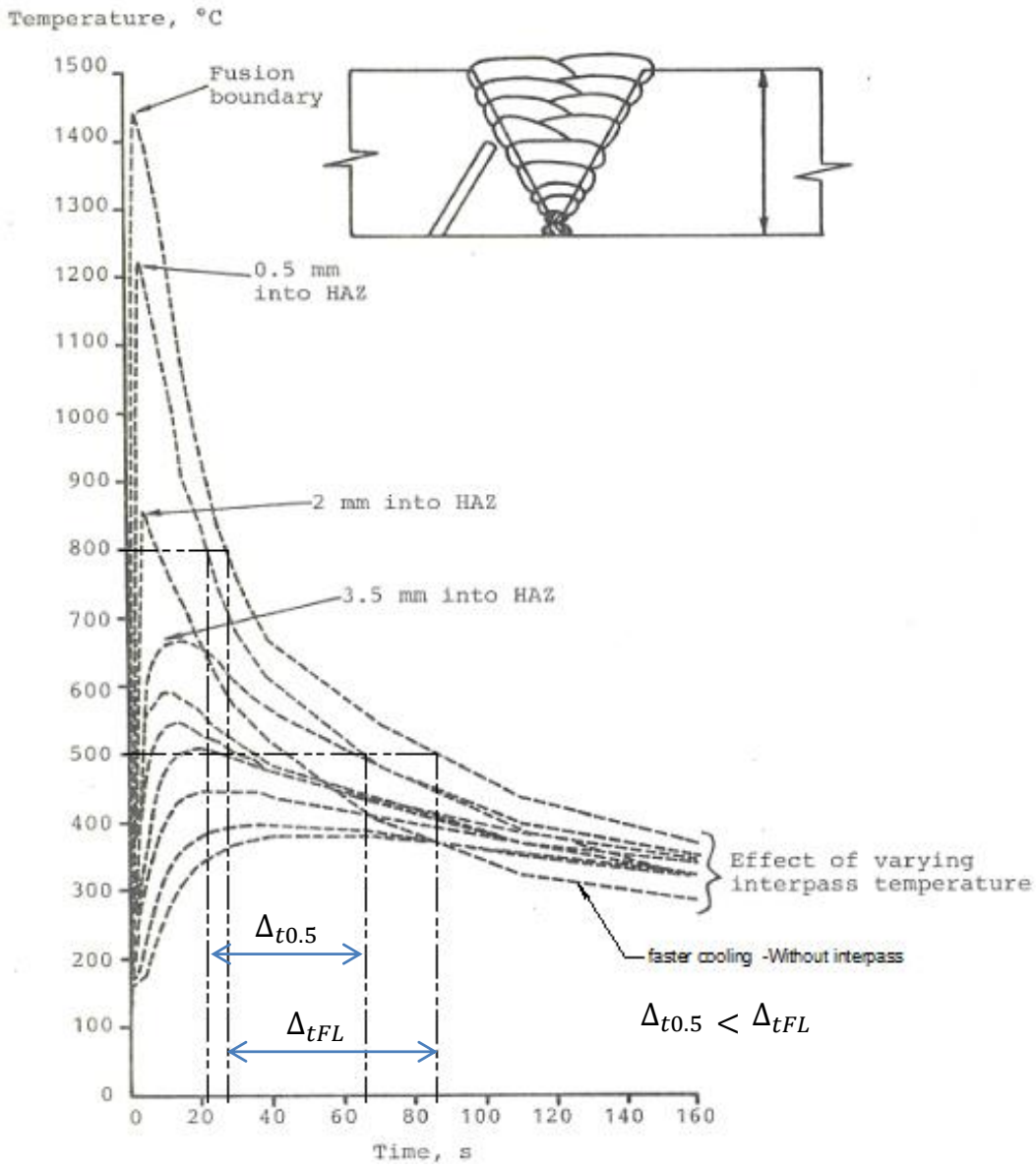

Figure 5.1: Typical HAZ thermal cycles for 5kJ/ mm heat input on multi-pass welded 40 mm thick steel plate [12]

In single pass welded EN24T steel (Figure 4.3), the microstructure of the hardest region depicts a transformation from martensite when no PWHT is applied to tempered martensite and bainite after PWHT at 350℃. Bainite forms on specific crystallographic planes of austenite and has characteristic straight edges separating it with martensite [35]. In comparison, the microstructure

for EN24A steel (Figure 4.4) depicts martensite when no PWHT is applied and tempered martensite after PWHT at 350℃. PWHT at 620℃ and 675 ℃ results in increasing levels of fine carbide precipitates in ferrite. These micrographs clearly shows the differences in CGHAZ microstructure brought about by the differences in the base metal microstructure prior to welding and how they evolve with PWHT. This is particularly important during welding of thin EN24 steel sheets where only single pass welding will suffice.

In multi-pass welding, as shown in Figures 4.5 and 4.6, the microstructure of the CGHAZ before any PWHT is bainitic in both EN24T and EN24A steels. This change of microstructure occurs because during multi-pass welding reheat zones are created [56] and this recrystallizes the hardest region. The original bainite in the CGHAZ of multi-pass welded EN24T steel appears tempered by the subsequent PWHT at 350℃, and that for EN24A steel appears enhanced. It is suspected TME in the CGHAZ of multi-pass welded EN24A may be responsible for the observed microstructural changes. TME can be characterized using electron diffraction with transmission electron microscope (TEM) or with X-ray diffraction [34]. This is supported by the hardness differences for EN24T-M350 which is 301 HV10 compared to 453 HV10 for EN24A-M350. PWHT at higher temperature produces cementite particles in ferrite for both multi-pass welded EN24A and EN24T steels. Similar microstructure has been reported by Grange et al [21] and this is postulated to be caused by diffusion of carbon due to high temperature.

5.3.2 Effect of PWHT on the Microstructure of base metal

The tempered martensite microstructure of EN24T steel is unaffected by PWHT at 350℃ and 620℃ (figure 4.7 b and c). However, a bushy microstructure comprising globular cementite, ferrite and tempered martensite is observed when PWHT temperature is raised to 675℃ (Figure

4.7 d). The high tempering temperature is considered to be the driving force that causes diffusion of carbon from martensite [32] during post weld heat treatment. Prabhavalkar et al [45] found that tempering the steel at 580-650℃ transformed the tempered martensite into lower bainite with numerous carbide precipitates. The microstructure of base metal in EN24A steel does not change with PWHT since the temperatures involved are below the austenitization range. It is therefore concluded that Hardness of as bought EN24T steel reduced with increase in PWHT temperature but that of EN24A steel was not affected by PWHT due to changes in its microstructure.

5.3.3 Microstructure of weld metal

The microstructure of the weld metal, Figure 4.9(c) and (d), is composed of large skeletal delta ferrite network in plain matrix of austenite grains. Suspected strands of melted but unmixed base metal were found to be washed into the weld pool. A similar observation was reported by Savage et al [89]. Alloying and impurity elements appear to segregate into inter- dendritic spaces. The low carbon content of the austenitic filler material and high chromium and nickel in the weld metal increases the ferrite and austenite phases significantly [8].The low carbon content is designed to overcome any possibility of carbide precipitation [8]. This explains why the microstructure of austenitic weld metal is unaffected by post weld heat treatment.

5.4 Hardness Survey

Hardness varies across the weldment due to differences in the peak temperature experienced at its different locations during the welding cycle. The hardest region is observed to be located in the HAZ at approximately 0.6mm from the fusion line. Peak hardness of between 450 and 470 HV10 are obtained after single pass welding in both EN24A and EN24T steels and also in multi-

pass welded EN24A steel after PWHT at 350℃. The peak hardness in EN24A-M350 is displaced towards the FGHAZ. A similar trend was reported by Pang et al [116] when they investigated hardness gradients in HAZ of welded Q & T steels. The peak HAZ hardness was found to be displaced from the CGHAZ to the FGHAZ. The origin of this phenomenon is considered to be an austenite grain size hardening effect, together with a bainitic hardenability that is high enough to cause the formation of bainitic ferrite over the range of cooling rates and austenite grain sizes inherent in arc welding process.

5.4.1 Effect of PWHT on hardness of CGHAZ

PWHT achieves a tempering effect on the microstructure of the weldment. The trends in the peak hardness of CGHAZ (Figure 4.12) depict a reduction in hardness as the PWHT temperature is increased. The microstructure change from martensite to bainite and to carbide precipitates in ferrite is accompanied by a reduction in hardness. This effect is similar to tempering a quench hardened EN24 steel at increasing tempering temperatures [6, 13, 45]. The hardness of EN24A-M350 is anomalous as it differs significantly from the rest. The reason for this could be due to suspected tempered martensite embrittlement. The optical microstructure (Figure 4.6) reveals a coarse bainitic structure and retained austenite different from the rest but cannot be used to ascertain whether it is the cause of embrittlement. This phenomenon can be investigated through a detailed Transmission Electron Microscopy or Scanning Electron Microscopy. Lim et al [51] has reported high phosphorous content segregated at pre-austenite grain boundaries to cause embrittlement in AISI4340 Steel tempered at 400℃. Other researchers [30, 49] attribute it to intra lath cementite and decomposition of retained austenite which occur during tempering at 400℃.

5.4.2 Effect of PWHT on weld metal hardness

Just like its microstructure, the hardness of the weld metal remains the same at all PWHT temperatures in this study. This is attributed to the highly Austenitic/ Ferritic structure of the weld pool brought about by very high Cr and Ni and relatively low carbon content (0.143%) of the weld metal [8]. The carbon content of the weld metal is in the range of mild steels [1].The weld metal hardness is unaffected by PWHT due to the existence of this microstructure [8].

5.4.3 Effect of PWHT on Base Metal hardness

EN24T steel base metal hardness reduces with increase in PWHT temperature. However, the hardness of EN24A steel remained unchanged as depicted in Figure 4.13. This is attributed to the base metal microstructure prior to PWHT. The hardness of EN24T steel reduces because PWHT tends to temper the material further. The hardness of EN24A steel is unchanged since PWHT, usually carried out below the eutectoid temperature, has no effect on an annealed microstructure.

5.5 Impact tests

Compared to un-welded EN24T and EN24A steel (Table 4.2 and Figure 4.15), the welding process lowered the CVN impact energy of the CGHAZ by 19.3% and 62.3% respectively in specimens which were not subjected to PWHT. This was as a result of formation of hard and brittle microstructures in the region. There was almost a linear increase in impact energy of CGHAZ in multi-pass welded EN24T steel as the PWHT temperature was increased. This is attributed to the tempering effect of PWHT on the microstructure. It is observed CGHAZ in EN24A steel is most brittle after PWHT at 350℃. Apart from a dipping of toughness in the CGHAZ of EN24A steel at 350℃, higher PWHT temperature caused an increase in CGHAZ toughness that was more pronounced in EN24A steel and gradual in EN24T. No dipping of

toughness was observed in EN24T steel at 350℃. A similar dipping in toughness is observed when quench hardened EN24 steel is tempered at between 350℃ and 400℃ [13].This phenomenon can be attributed to presence of retained austenite [49, 50] and residual impurities at the grain boundaries as a result of segregation during austenization [52]. Therefore, it is suspected that TME resulting from austenization of EN24T steel and subsequent microstructural changes during annealing brought about the two different responses to PWHT at 350℃. At the highest PWHT temperature of 675℃ the tempered microstructure of EN24A steel (Figure 4.6) is tougher than that of EN24T steel (Figure 4.5) by 22%. The trend of toughness increase with PWHT depicts better results in annealed EN24 steel provided PWHT at 350℃ is avoided.

5.6 Tensile test

Preliminary mechanical tests were carried out on EN24T, EN24A steel and weld metal and the results are recorded in Table 4.2. Results of tensile tests on welded and post heat treated EN24T and EN24A steels are presented in Figure 4.16. Considerable necking was observed on EN24T and EN24A steel specimens during tensile test and both failed in a ductile manner. However, all welded specimens were observed to fail suddenly, with little necking, at regions close to the fusion boundaries. The results show that PWHT had no significant effect on the UTS of welded EN24T and EN24A steels. Olabi et al [119] reported a similar observation when they investigated the effect of PWHT on UTS and toughness of structural steels. EN24T-M0, EN24T-M350, EN24T-M620, EN24T-M675, EN24A-M620 and EN24A-M675 specimens recorded UTS in the range 741 MPa to 762 MPa. These values are close to the UTS of the austenitic weld metal declared by the filler rod manufacturer as 752 MPa [8, 63] which is low compared to that of EN24A and EN24T steel (Table 4.2). Therefore, it can be deduced that the weaker weld metal significantly influenced the unchanging results of tensile test. This is further supported by the

fact that the weld metal microstructure (Figure 4.9) and hardness of weld metal (Figure 4.14) show no change with PWHT. Additionally, the UTS of weld metal can be correlated with hardness [109]. Therefore, it is not expected to change with PWHT.

Generally, the microstructure and hardness of weld metal and base metal in EN24A steel are not affected by PWHT and the same is expected of their strength [109]. However, ductility changes in EN24T steel base material occur if PWHT is carried out at temperatures higher than the last tempering temperature [13] encountered during its production. This is supported by the microstructure changes in EN24T steel during PWHT at 675℃ (Figure 4.7). The optical micrographs show that the tempering temperature of EN24T steel may have been lower than 675℃ since no change of microstructure occurred at lower PWHT temperatures. EN24A steel cannot experience ductility changes with PWHT since its initial microstructure is a mixture of perlite and ferrite and this microstructure was not altered by PWHT (Figure 4.8). Therefore, it can be inferred that the changes in ductility with PWHT of welded EN24T and EN24A steel can be largely but not solely attributed to the tempering effect in the HAZ. This is because major changes in HAZ hardness and HAZ microstructure occurs with PWHT and only minimal changes occur in the base material and weld materials.

Results for elongation of the welded materials (Figure 4.17) show the ductility of EN24A-M620 to be 8.9% while that of EN24T-M620 specimens was 7.9%.This represents an increase of 13.8%. Highest ductility, 13.75%, was observed on EN24A-675. Lowest ductility, 4.7%, was observed on EN24T-M0. Its ductility more than doubled after a PWHT at 675℃.

CHAPTER SIX

CONCLUSIONS AND RECOMMENDATIONS

6.1 CONCLUSIONS

1. It was concluded that the hardest location in as welded specimens was in the HAZ at approximately 0.6 mm from the fusion line. Multi-pass welding was found to temper the previous HAZ and tended to increase the band of the hardest region from CGHAZ to the Fine Grained HAZ. PWHT at 620℃ and 675℃ was found to temper all specimens to hardness below 300HV and a minimum difference in hardness levels between base metal and HAZ was found during PWHT at 675℃.

2. The CGHAZ of single-pass welded specimens of EN24A and EN24T steel presented a martensitic structure before PWHT. The CGHAZ microstructure of all specimens that were subjected to PWHT at 620℃ and 675℃ mainly comprised of carbide precipitates in ferrite. Multi-pass welded specimens exhibited bainitic microstructure in the CGHAZ before PWHT.

3. Suspected embrittlement in the CGHAZ may be responsible for high hardness and low impact energy on multi-pass welded EN24A steel subjected to PWHT at 350℃. The same was not suspected in the CGHAZ of multi-pass welded EN24T steel specimens under same PWHT condition. At PWHT temperature of 675℃ the room temperature - impact energy of CGHAZ in EN24A steel was higher than that of EN24T steel by 22%

4. All Tensile test specimens failed with a brittle fracture near the fusion line. Generally, PWHT had negligible effect on the UTS of all specimens but elongation was found to increase with PWHT temperature partially due to tempering effect on the CGHAZ.

6.2 RECOMMENDATIONS FOR FUTURE WORK

- Work on SEM of the HAZ is recommended to be carried out after PWHT at 350℃ to find out if tendencies for impurities to segregate at the grain boundaries in EN24A are different from those of EN24T steel.
- Fractography of the fracture surface after impact test is recommended in order to conclusively determine the mechanism of failure in EN24A and EN24T steel after PWHT at 350℃. Fractography will determine whether failure is caused by TME or hydrogen cracking.
- The CGHAZ of EN24A and EN24T steel should be generated through simulation work on the Gleeble simulator by simulating the peak temperature and CGHAZ cooling rate. With the whole specimen having a uniform CGHAZ microstructure it will be easier to compare effects of PWHT on its microstructure and mechanical properties.
- It is recommended that further work be carried out on effect of PWHT on fatigue strength of EN24A and EN24T steels welded with austenitic electrodes because this is an important mechanical property especially for shaft power transmission.

REFERENCES

1. S. Kou, Welding Metallurgy - John Willey &Sons, Inc., Publication (2003).
2. G.E. Linnert, Welding Metallurgy-Carbon and Alloy Steels, Volume I Fundamentals-American Welding Society (AWS) (1994).
3. R.S. Funderburk, Key Concepts in Welding Engineering-Fundamentals of Preheat. Welding Innovation 14(2) (1997).
4. Brazing and Soldering, ASM Handbook Welding, 6(1993) 1647-1656.
5. AISI 4340 Steel, www.astmsteel.com/product/4340-steel, Date accessed 7th April 2015.
6. H.W. Mishler, R.E. Monroe and P.J. Rieppel, Welding of High Strength Steels for Aircraft and Missile Applications, Defense Metals Information Report No.118 (1959) Battelle Memorial Institute Columbus 1, Ohio.
7. G.M. Reddy, T. Mohandas, G.R.N. Togore, Weldability Studies of High Strength Low Alloy Steel Using Austenitic Fillers, Journal of Material Processing Technology, 49 (1995) 213-228
8. Product Datasheet Afrox 312 welding rods: website www.afrox.co
9. Product Datasheet, Kensmetal Industries Limited, (2015).
10. B.K. Srivastava, S.P. Tewari and J. Prakash, A review on effect of preheating and/or post weld heat treatment (PWHT) on mechanical behavior of ferrous metals. International Journal of Engineering Science and Technology, 2(40) (2010) 625-631.
11. A.C. Davies, The Science and Practice of Welding Vol.2-The Practice of Welding. Cambridge University Press (2002).

12. M.J. George, Technical Steel Research, Measurement of toughness in HAZ of welded structural steel, Commission of European Communities, 1985.
13. J. Woolman, and R.A. Mottram, The mechanical and physical properties of the British standard En steels from EN21 to EN39,Pergamon press, (1966) 72-110.
14. Special Steels Product Information EN24 Steel, http://www.specialsteels.co.za, Date accessed 7th April 2015.
15. Macsteel: Special Steels Catalogue 81(EN24 steel), http://www.macsteel.co.za, Date accessed 7th April 2015.
16. K.K. Rajesh, Y. Prashant and G.S. Sunjay, Structural and Wear Characterization of Heat Treated EN24 Steel, ISIJ International, 52(7) (2012) 1370-1376.
17. S. Hari and K. Pradeep, Mathematical Model of Tool Life and Surface Roughness for Turning Operation through response Surface Methodology. Journal of Scientific and Industrial Research, 66(2007) 220-226.
18. Y.M. Shivaprakash, B.M. Gurumurthy, M.C. Gowrishankar and A. Kini, Comparative Studies on Mechanical Properties of AISI 4340 High Strength Alloy Steel under Time-Quenched and Austempered Conditions ,IJRET, 4(2)(2015) 530-535.
19. Atlas Specialty Metals 2006, www.atlasmetals.com.au.Date accessed May 2015.
20. V.B. Nosov and S.A. Yurasov, Calculation of hardenability of structural steels from their chemical composition. Metal science and heat treatment, 37(1-2) (1995) 16-21.

21. R.A. Grange, C.R. Hribal and L.F. Porter, Hardness of tempered martensite in carbon and low alloy steels, Metallurgical Transactions A, 8A(1977) 1775-1785.
22. J.F. Wallace, A review of Welding Cast Steels and its Effect on Fatigue and Toughness Properties. Steel founders' society of America, (1979) printed in USA.
23. W.D. Callister and J.R. Callister's Material Science and Engineering. Adapted by R. Balasubramaniam, Wiley India Pvt Ltd, (2009) 256.
24. http://www.azom.com/article.aspx?ArticleID=6772. Date accessed 7th April 2015
25. West Yorkshire Steel, EN24 Alloy Steel, http://www.westyorksteel.com, Date accessed 7th April 2015.
26. Heat treating, ASM handbook, vol.4, (1991).
27. L.D. Jaffe and B. Swartz, Time-Temperature Relations in Tempering Steel, Watertown Arsenal Laboratory Report No.WAL.310/21,1944.
28. E.B. William, Heat Treatment Selection, and Application of Tool Steels, 2nd Edition, Hanser Publishers, Munich 2009.
29. L. Chen, C.M. Brackman, B.M. Korevaar, E.J. mettemeijer, The Tempering of Iron-Carbon Martensite; Dilatometric and Calorimetric Analysis, Metallurgical transactions A, 19A (1988) 2416-2426.
30. H.K.D.H. Bhadeshia and D.V. Edmonds Tempered Martensite Embrittlement: Role of Retained Austenite and Cementite. Metals science, 1979, pp325-334.

31. H. K. D. H. Bhadeshia, Carbon Content of Retained Austenite in Quenched Steels. Metal science, 17(3) (1983) 151-152.
32. H.K.D.H. Bhadeshia, Bainite in steels, 2nd edition, 2001.
33. H.K.D.H. Bhadeshia, J.W. Christian, Bainite in Steels, Metallurgical Transactions A, 21A (1990) 767-797.
34. E. Keehan, L. Karlson, M. Thuvander, E.L. Bergquist, Microstructural Characterization of as Deposited and Reheated Weld Metal-High Strength Steel Weld Metals, ESAB AB ,IIW Doc.IX2187-06,Gothenburg,Sweeden
35. H.K.D.H. Bhadeshia, Interpretation of the microstructure of steels, http://www.msm.cam.ac.uk/phase-trans/. Date accessed June 2016.
36. N. Saeidi, A. Ekrami. Comparisons of Mechanical Properties of Martensite/Ferrite and Bainite/Ferrite in Dual Phase 4340 Steel. Material Science and Engineering A, 523 (2009) 125-129.
37. G. Krauss, Martensite in Steel: Strength and Structure, Materials and Engineering, A273-275 (1999) 40-57.
38. B. Hutchinson, J. Hagstrom, O. Karlsson, D. Lindell, M. Tornberg, F. Limberg, M Thuvander, Microstructure and Hardness of as Quenched Martensites (0.1-0.5%C), Acta Materialia, 59 (2011) 5845-5858.
39. G. Krauss, A.R. Marder, The Morphology of Martensite in Iron Alloys, Metallurgical Transactions A, 2 (1971) 2243-2357.
40. S. Morito, H. Tanaka, R. Konishi, T. Furuhara, T. Maki, The Morphology and Crystallography of Lath Martensite In Fe-C Alloys, Acta Materialia, 51 (2003) 1789–1799.

41. S. Morito, H. Saito, T. Ogawa, T. Furuhara, T. Maki, Effect of Austenite Grain Size on the Morphology and Crystallography of Lath Martensite in Low Carbon Steels. ISIJ International 45(1) (2005) 91-94.
42. J.P. Naylor, The influence of Lath Morphology on the Yield Stress and Transition Temperature of Martensitic-Bainitic Steels, Metallurgical Transactions A, (1979) 861-873.
43. S. Morito, H. Yoshida, T. Maki, X. Huang, Effect of block size on strength of lath martensite in low Carbon steels, Materials Science and Engineering A, 438-440(2006) 237-240.
44. H. Kitahara, R. Ueji, N. Tsuji, Y. Minamino, Crystallographic features of lath Martensite in Low-Carbon Steel, Acta Materialia, 54 (2006), 1279–1288.
45. M.S. Prabhavalkar, V.V. Idane, S.M. Gurav, S.G. Dhanawade, Influence of Tempering Temperature on Mechanical Properties and Microstructure of EN 24 Steel. International Conference on Recent Advances in Computer Science, Engineering and Technology, pp 96-101.
46. W-S. Lee and T-T.Su, Mechanical Properties and Microstructural Features in AISI 4340 High-Strength Alloy Steel under Quenched and Tempered Conditions, Journal of Materials and Processing Technology, 87(1999) 198-206.
47. E.R. Parker and V. F. Zackay, Microstructural Features affecting Fracture Toughness of High Tensile Steels. Engineering Fracture Mechanics, 7(1975) 371-375.
48. N.A. Eliaz, B. Shachar, B. Tal and D. Eliezer, Characteristics of Hydrogen Embrittlement, Stress Corrosion Cracking and Tempered Martensite

Embrittlement in High Strength Steels, Engineering Failure Analysis, 9(2002) 167-184.

49. B.C. Kim, S. Lee, D.Y. lee and N.J. Kim, In-situ Fracture observations on Tempered Martensite Embrittlement in AISI 4340 Steel. Metallurgical transactions A, 22A (1991) 1889-1892.
50. N. Bailey, Weldability of Steel, Woodhead Publishing Ltd 1994.
51. N.S. Lim, C.W. Bang, S. Das, H.W. Jin, R. Ayer and C.G. Park., Influence of tempering temperature on both the microstructural evolution and elemental distribution in AISI 4340 steels, Metallurgical Materials International,18(1) (2012) 87-94.
52. R.M. Horn and R.O. Ritchie, Mechanisms of Tempered Martensite Embrittlement in Low Alloy Steels, Metallurgical transactions A, (1978)1039-1053.
53. N. Yurioka, Progress in Welding and Joining Technology and its Future Prospects. Nippon steel technical report no.65, (1995).
54. S.A. David, J.M. Vitek, S. Babu, and T. DebRoy, Advances in Welding Science, Oak ridge laboratory report, Department of Material Science and Engineering, Pennsylvania State University.
55. M.A. Yassin, S.M.S. Khairul, I. Mahadzir and A.K. Basim, History of Elements and Welding Processes. Australian Journal of Basic and Applied Sciences 8(13) (2014) 296-315.
56. J.C. Lippold, Welding Metallurgy and Weldability, John Wiley and Sons Printed in USA

57. J. M. Greitman, Welding through the ages, American Welding Society (2013).
58. E. P. De Garmo, J.T. Black and R. Koshser, Materials and Processes in Manufacturing 7th ed.1988, pp880-962.
59. P. Cico, D. Kalincova and M. Kotus, Influence of Welding Method on Micro Structural creation of Welded Joints .Res.Agri.Eng.,57 (2011) 50-56.
60. W. Omer, R. Blodgett , F.B. Scott , K.M. Duane and Q. Marie, Fabricators' and Erectors' Guide to Welded Steel Construction, The James F. Lincoln Arc Welding Foundation (1999).
61. Structural welding code-Steel, American Welding Society AWS D 1.1(2008) 58 -66.
62. Preheat and inter-pass temperature control, American Association of State Highway and Transportation Officials (AASHTO)/AWS D1.5M/D1.5 (2008) Bridge Welding code c-12.14 pp 387.
63. Alloy description and application 312 welding wire and rod www.weldingwire.com
64. R.S. Funderburk, Key Concepts in Welding Engineering-Heat Input, Welding innovation, XVI (1) (1999).
65. Guidelines for Weldability Tests for Normal and High Strength Steels (2015), Lyods Register Materials and Qualification Procedure for Ships, Book A, Procedure 0-3.
66. H. Granjon, Fundamentals of welding metallurgy, Woodhead publishing company, 2001, pp 41.

67. G. Spanos, R. Fonda, R.A. Vandermeer, A. Matuszeski, "Microstructural changes in HSLA-100 steel thermally cycled to simulate the heat-affected zone during welding," Materials Transactions A, 26A (1995) 3277–3293.
68. O. Grong and D.K Matlock, Microstructural Development in Mild and Low Alloy Steels. International Metals Reviews, 31(1) (1986) 27-48.
69. M.F. Ashby and K.E. Easterling, A First Report on diagrams for grain growth in welds, Acta Metall, 30 (1982) 1969-1982.
70. H. Okabayashi, R. Kume, Effects of pre- and post-heating on weld cracking of 9Cr-1Mo-Nb-V Steel, Transactions of Japan welding society, 1998, pp. 63-68.
71. R.S. Funderburk, Key Concepts in Welding Engineering -Post Weld Heat Treatment. Welding Innovation, XV (2) (1998) 2.
72. V.A. Troitsky, A.A. Trushchenko and I.P. Belokur, Quality Control of Welding. Lectures for welding specialists, EO Paton institute of electric welding of Ukranian SSR Academy of sciences, (1983), pp 9-22.
73. R.W. Hinton and R.K Wiswesser, Estimating Welding Preheat Requirements for Unknown Grades of Carbon and Low Alloy Steels. Welding Research Journal, 87 (2008) 273-278.
74. J. F. Wallace, Steel Castings Handbook Supplement 6: Repair Welding and Fabrication of Carbon and Low Alloy Steel Castings, Steel Founders' Society of America, (1980) pp. 87.
75. Metallography and Microstructures, ASM Handbook vol.9, Eighth printing, (1998) 1260-1281.

76. A. Khaleel and J.Krishnan, Post-Weld Heat Treatment- Case Studies. Bhabha Atomic Research Centre Newsletter (2002), pp 111-115.

77. J. W. Mc Enerney, Recommended practices for local post weld heat treatment. WRC Bulletin 452 (2000).

78. G.M. Evans, and N. Bailey, Metallurgy of basic weld metal, Woodhead Publishing Limited, 1997, pp 108-126.

79. A.J. Williams, P.J. Rieppel and C.B. Voldrich, Literature Survey on Weld Metal Cracking, Wright Air Development Centre (WADC) Technical Report No 52-143(1952).

80. Design, Fabrication and Inspection of Welded Joints, Lyods Register Rules for Classification and Construction Materials and Welding: (2000) Published by www.gl-group.com.

81. ISO 10675: Non–destructive testing of welds-Acceptable levels for radiographic testing.

82. H. Zhang and J. Senkara, Resistance Welding, Fundamentals and Applications, Published in 2006 by Taylor & Francis Group, LLC

83. Ali Emamian, Ardalan Emamian, A. H. Kowkabi, Effects of Filler-wire Composition along with different Pre- and Post-Heat Treatment on Mechanical Properties of AISI 4130 Welded by the GTAW Process, Materials Sciences and Applications, 1(2010) 135-140.

84. M. Srangwood, The prediction and assessment of weld metal microstructures. PhD Thesis, King's college,Cambridge,1987

85. M. Eroglu , M. Aksoy and N. Orhan, Effect of coarse initial grain size on microstructure and mechanical properties of weld metal and HAZ of a low carbon steel, Materials Science and Engineering, A269 (1999) 59–66.

86. J. J. J. Zayman and G.T. van Rooyen, The Toughness of Heat Affected Zone of welds in 11.5 % Chromium Steels. Proceedings of the 1st International Chromium Steels and Alloys Congress, Cape Town, 2 (1992) 137-142.

87. J.H. Chen, T.D. Xia and C. Yan, Study on Impact Toughness of C-Mn ,multilayer weld metal at -60℃ , Welding research supplement, (1993) 19s -27s.

88. S. S. Strunck and R.D. Stout, Heat Treatment Effects in Multi-pass Weldments of a High-Strength Steel, Welding Research Supplement, (1972) 508s - 520s.

89. W.F. Savage, E.F. Nippes and E.S. Szekeres, Study of Weld Interface Phenomena in a low alloy steel. Welding Research Supplement, (1976) 260s-268s.

90. J.W. Brooks, M.H. Loretto and R.E. Smallman, In Situ Observations of the formation of Martensite in Stainless Steel, Acta Metallurgica, 27(1979) 1829-1838.

91. R. Loots and G.T. Rooyen, A Comparison of Reheat Cracking susceptibility of a service exposed high temperature alloy steel with that of a new material. The journal of South African institute of mining and metallurgy (2004) 627-632.

92. N. Tammasophon, W. Homhrajai and G. Lothongkum, Effect of Post Weld Heat Treatment on Microstructures and Hardness of TIG Weldments between P22 and P91 Steels with Inconel 625 Filler Metal, Journal of Metals, Materials and Minerals, 21(1) (2011) 93-99.

93. J. Cormu, Fundamentals of Fusion Welding, Springer-Verlag Berlin Heidelberg 1988

94. W.W. Gerberich, T. Livne, X-F Chen, M.Kaczorwski, Crack Growth from Internal Hydrogen-Temperature and Microstructural Effects in 4340 Steel. Metallurgical transactions A, 19A (1988) 1319-1334.

95. N. Bailey, Weldability of ferritic steels, Woodhead Publishing Ltd 1994.

96. A.J. Kinsey, Welding of Structural Steels without Preheat, Supplement to the Welding Journal, (2000) 79s-88s.

97. G. Neville, Why do welds crack?, TWI Bulletin, 1991.

98. P. Bernasovsky, Failure Analysis of Welded Components-Importance of Technical Practice, Proceedings of IIW International Congress in Central and East European Region Slovakia, High Tatras, Stara Lesna, 14-16 Oct.,2009.

99. A.V. Adedayo, S.A. Ibitoye and A.O. Oyetoyan, Annealing Heat Treatment Effects on Steel Welds, Journal of Minerals and Material Characterization and Engineering 9(6)(2010) 547-556.

100. D.P. Singh, S. Mithlesh, and J.S. Gill, Effect of Post Weld Heat Treatment on the Impact Toughness and Microstructure Property of P- 91 steel weldment. IJRMET 3(2) (2013) 216-219.

101. ISO 1143:2010 Metallic materials -- Rotating bar bending fatigue testing.

102. K.J. Kirkhope, R. Bell, L. Caron, R.C. Basu and K.T Ma., Weld detail fatigue life improvement techniques part 1 review, Marine Structures, 12(1999) 447-474.

103. M.A.S. Torres and H.J.C. Voorwald, An evaluation of shot peening, residual stress and stress relaxation on the fatigue life of AISI 4340 steel. International journal of fatigue, 24 (2002) 877-886.

104. T. Okawa, T. Nose, H. Shimanuki and T.Suzuki, Fatigue life prediction of welded structures based on crack growth analysis. Nippon steel Technical Report No.102 (2013).

105. H.K.D.H. Bhadeshia, Developments in Martensitic and Bainitic Steel: Role of Shape Deformation, Materials Science and Engineering, A 378(2004) 34-39.

106. O.W. Blodgett, and D.K. Miller, Welded connections-structure Engineering Handbook. CRC Press LCC (1999).

107. AWS B 4.0:2007, An American national standard: Standard methods for mechanical testing of welds.

108. S. Gibson, Practical Welding, Macmillan Publishers Limited and Stuart Gibson 1994.

109. J. Pavlina and C.J. Van Tyne, Correlation of Yield Strength and Tensile with Hardness for Steels, JMEPEG, (2008)17:888-893.

110. P. Zhang, S.X. Li, Z.F. Zhang, General Relationship between Strength and Hardness, Materials Science and Engineering, A 529 (2011) 62– 73.

111. M. Gasko, G. Rosenberg, Correlation between Hardness and Tensile strength in Ultra-High Strength Dual Phase Steels, Short Communication, Materials Engineering,18 (2011) 155-159.

112. ASTM E23-05: Standard Test Methods for Notched Bar Impact Testing of Materials.

113. A. Calic, Effect of Cooling Rate on Hardness and Microstructure of AISI 1020, AISI 1040 and AISI 1060 steels. Int. J. of Physical Sciences, 4(9) (2009) 514-518.

114. B. Zakaria and D.T.B Chemseddine, Effect of Welding on Microstructure and Mechanical Properties of industrial Low Carbon Steel. Engineering Journal, 2(2010) 502-506.

115. J.E. Ramirez, S. Mishael and R. Shockley, Properties and Sulphide Stress Cracking Resistance of CGHAZ in V Micro-alloyed X60 Steel Pipe, Welding Journal, (2005) 113s-123s.

116. W. Pang, N. Ahmed and D. Dunne, Hardness and microstructural gradients in the heat affected zone of welded low-carbon quenched and tempered steels. Australasian Welding Journal – Volume 56, Second Quarter, (2011) 36-48.

117. I. M. Momo, O.J. Akinribide, J. Ayanleke, J. Olowonubi, G.O. Olorunfemi and T. Oshodin, Investigating the Mechanical Properties of Post Weld Heat Treated 0.33%C –Low Alloy Steel, Int. Journal of Science and Technology, 2(6) (2013) 433-437.

118. S. Ravi, V. Balasubramanian, S. Babu, S. Nemat, Nasser Influences of MMR, PWHT and notch location on fatigue life of HSLA steel welds, Engineering Failure Analysis, 11 (2004) 619–634.

119. A.G. Olabi and M.S.J. Hasmi, The Effect of Post Weld Heat Treatment on Mechanical Properties and Residual Stresses mapping in Welded Structural Steel, Journal of materials processing technology, 55(1995) 117-122.

120. K.H. Lee, J.H. Myung M-C Kim and B.S. Lee, Effects of Tempering and Post Weld Heat Treatment on Microstructure and Mechanical Properties of SA 508 GR. 4N steel. Nuclear Engineering and Technology, 46(3) (2014) 413-422.

121. B. Silwal, L. LI, A. Deecuster and B. Griffiths, Effect of Post Weld Heat Treatment on the Toughness of Heat Affected Zone for Grade 91 Steel. Welding Research, 92(2013) 80s-87s.

122. R. Roberti, G. Cornacchia, and M. Faccoli, Effect of Increasing Post Weld Heat Treatment Temperature on the Fracture Toughness of an ASME SA-542M Steel. Italia, 1-3 Marzo (2012) 137-143.

123. G.M. Evans, Effect of stress relieving on the microstructure and properties of C-Mn all-weld metal deposits, Welding journal, 65(12) (1986) 326s-334s.

124. B.E Peddle and C.A Pickles, Carbide and Hardness Development in the Heat Affected Zone of Tempered and Post Weld Heat Treated 2.25Cr-1Mo Steel Weldment, Journal of Material Engineering and Performance, 9 (5) (2000) 477-488.

125. P. Campbell, Basic Fixture Design, Industrial press, 1994, pp 7-17.

APPENDICES

Appendix A (Results of X-Ray Test)

X-RAY REPORT-WELDED COUPONS

KENYA INDUSTRIAL RESEARCH & DEVELOPMENT INSTITUTE

(KIRDI) ATTN: Eng. K. Mutonga

TESTED ACCORDING TO ASME SEC IX & ASME V ON

NON-DESTRUCTIVE TESTING.

BS201635528- SQUARE WELDED COUPONS

S/No.	COUPON NO.	TEST SECTION	EVALUATION REPORT	COMMENTS(REMARKS)
1	1	Weld	Slight Slag Inclusion	Acceptable
2	2	Weld	Slight Slag Inclusion	Acceptable
3	3	Weld	Lack of Fusion-8mm long	Not Acceptable
4	4	Weld	Very Slight Slag Inclusion	Acceptable
5	5	Weld	Homogeneous Weld	Acceptable
6	6	Weld	Slag Inclusion-2mm Dia.	Acceptable
7	7	Weld	Lack of Fusion	Not Acceptable
8	8	Weld	Slight Slag Inclusion	Acceptable
9	9	Weld	Homogeneous Weld	Acceptable
10	10	Weld	Very Slight Slag Inclusion	Acceptable
11	11	Weld	Homogeneous Weld	Acceptable
12	12	Weld	Homogeneous Weld	Acceptable
13	13	Weld	Homogeneous Weld	Acceptable
14	14	Weld	Homogeneous Weld	Acceptable
15	15	Weld	Very Slight Slag Inclusion	Acceptable

KENYA BUREAU OF STANDARDS
P. O. Box 54974
NAIROBI

16	16	Weld	Homogeneous Weld	Acceptable
17	17	Weld	Homogeneous Weld	Acceptable
18	18	Weld	Homogeneous Weld	Acceptable
19	19	Weld	Homogeneous Weld	Acceptable
20	20	Weld	Homogeneous Weld	Acceptable
21	21	Weld	Homogeneous Weld	Acceptable
22	22	Weld	Very Slight Slag Inclusion	Acceptable
23	23	Weld	Homogeneous Weld	Acceptable
24	24	Weld	Slight Slag Inclusion-2mm Dia.	Acceptable
25	25	Weld	Slag Inclusion-3mm Dia.	Acceptable
26	26	Weld	Slag Inclusion-2mm Dia.	Acceptable

EVALUATED BY: NATHAN M. WAKALO & DEDAN KARIUKI **DATE: 01-12-2016**

NWakalo 2/12/2016

SIGN: ----------

KENYA BUREAU OF STANDARDS
P. O. Box 54974
NAIROBI

Round Specimens

DUMBELLS-BS201635531

S/No.	COUPON No.	TEST SECTION	EVALUATION REPORT	COMMENTS/REMARKS
1	1	Weld	Homogeneous Weld	Acceptable
2	2	Weld	Homogeneous Weld	Acceptable
3	3	Weld	Homogeneous Weld	Acceptable
4	4	Weld	Homogeneous Weld	Acceptable
5	5	Weld	Homogeneous Weld	Acceptable
6	6	Weld	Homogeneous Weld	Acceptable
7	7	Weld	Homogeneous Weld	Acceptable
8	8	Weld	Homogeneous Weld	Acceptable
9	9	Weld	Homogeneous Weld	Acceptable
10	10	Weld	Slight Slag Inclusion	Acceptable
11	11	Weld	Slight Slag Inclusion	Acceptable
12	12	Weld	Homogeneous weld	Acceptable
13	13	Weld	Homogeneous weld	Acceptable
14	14	Weld	Homogeneous weld	Acceptable
15	15	Weld	Homogeneous weld	Acceptable
16	16	Weld	Homogeneous weld	Acceptable
17	17	Weld	Lack of Fusion	Not Acceptable
18	18	Weld	Homogeneous Weld	Acceptable
19	19	Weld	Homogeneous Weld	Acceptable
20	20	Weld	Slight Slag Inclusion	Acceptable
21	21	Weld	Homogeneous Weld	Acceptable
22	22	Weld	Lack of fusion	Not Acceptable
23	23	Weld	Homogeneous Weld	Acceptable
24	24	Weld	Homogeneous weld	Acceptable
25	25	Weld	Homogeneous Weld	Acceptable
26	26	Weld	Slag Inclusion &Lack of Fusion	Not Acceptable

EVALUATED BY: NATHAN M. WAKALO & DEDAN KARIUKI DATE: 01-12-201

SIGN: ----------

NWakalo 2/12/2016

KENYA BUREAU OF STANDARDS
P. O. Box 54974
NAIROBI

Appendix B (Data for Hardness Profiles)

Distance from FL (mm)	-0.6	-0.3	FL	0.6	1.3	1.9	2.5	3.1	3.8	4.4	5.0	5.6	6.2	6.6	9.4
En24A-M0	236	235	336	359	319	259	237	233	236	230	228	227	227	223	224
En24A-M350	236	237	395	453	464	429	342	289	271	237	235	237	237	237	238
En24A-M620	237	237	285	296	291	281	282	274	255	244	244	242	242	242	242
En24A-M675	236	237	268	271	265	264	262	257	248	232	232	231	231	229	228
En24A-S0	236	235	308	462	397	291	235	227	228	218	230	229	229	220	225
En24A-S350	237	235	284	378	341	303	267	241	235	227	227	227	227	227	226
En24A-S620	237	235	272	285	268	248	225	230	226	226	224	223	223	226	226
En24A-S675	237	235	268	289	248	234	221	222	225	218	218	227	227	216	220
En24T-M0	230	235	285	338	322	296	279	275	285	287	295	303	303	306	307
En24T-M350	236	237	312	301	311	294	294	290	285	283	293	294	294	293	294
En24T-M620	236	237	246	262	274	283	279	264	260	254	266	277	277	280	280
En24T-M675	236	238	270	267	270	265	273	265	254	257	254	254	254	259	262
En24T-S0	237	235	343	453	379	335	291	281	285	296	297	295	295	308	310
En24T-S350	236	235	295	302	326	323	311	296	270	269	272	279	279	281	276
En24T-S620	237	235	231	264	254	235	243	259	265	260	265	262	262	269	266
En24T-S675	237	240	237	242	235	233	225	240	251	242	242	243	243	245	244

Appendix C (Results of Impact Tests)

	CVN Impact energy (J)					
Material -PWHT	Test 1	Test 2	Test 3	Test 4	Av.	Std.Dev
En24A-M0	36.0	53.1	36.0	40.7	41.4	8.1
En24A-M350	26.9	31.4	31.4	38.4	32.0	4.7
En24A-M620	38.4	53.1	48.1	38.4	44.5	7.3
En24A-M675	65.9	76.6	58.2	74.0	68.7	8.3
En24T-M0	30.8	40.7	30.8	30.8	33.3	5.0
En24T-M350	58.2	40.7	38.4	38.4	43.9	9.6
En24T-M620	63.4	48.1	50.5	48.1	52.5	7.3
En24T-M675	53.1	55.6	53.1	63.4	56.3	4.9

Appendix D (Results of Tensile Tests-UTS)

	UTS(Mpa)					
Material -PWHT	Test 1	Test 2	Test 3	Test 4	av.	Std. Dev
En24A-M0	784.0	809.0	1051.0	-- --	881.3	147.5
En24A-M350	812.0	770.0	-- --	-- --	791.0	29.7
En24A-M620	-- --	770.0	749.0	738.0	752.3	16.3
En24A-M675	722.0	781.0	753.0	784.0	760.0	28.9
En24T-M0	762.0	795.0	731.0	-- --	762.7	32.0
En24T-M350	791.0	777.0	738.0	717.0	755.8	34.2
En24T-M620	753.0	827.0	795.0	617.0	748.0	92.4
En24T-M675	715.0	765.0	744.0	-- --	741.3	25.1

Appendix E (Results of Tensile Tests-Elongation)

	% elongation					
Material-PWHT	Test 1	Test 2	Test 3	Test 4	Av.	Std.Dev
En24A-M0	12.0	10.0	8.0	-- --	10.0	2.0
En24A-M350	7.0	8.0	-- --	-- --	7.5	0.7
En24A-M620	-- --	9.2	8.6	9.0	8.9	0.3
En24A-M675	16.0	13.0	14.0	12.0	13.8	1.7
En24T-M0	6.0	4.0	4.0	-- --	4.7	1.2
En24T-M350	6.0	5.0	6.0	10.0	6.8	2.2
En24T-M620	8.0	7.4	9.0	7.0	7.9	0.9
En24T-M675	10.8	10.0	10.4	-- --	10.4	0.4